A Semi Quantitative Landslide Susceptibility Assessment using Logistic Regression Model and Rock Mass Classification System: Study in a Part of Uttarakhand Himalaya, India

Sashikant Sahoo

January, 2009

A Semi Quantitative Landslide Susceptibility Assessment

Using Logistic Regression Model & Rock Mass Classification System: Study in a part of Uttarakhand Himalaya, India

by

Sashikant Sahoo

Thesis submitted to the International Institute for Geo-information Science and Earth Observation in partial fulfilment of the requirements for the degree of Master of Science in Geo-information Science and Earth Observation, Specialisation: (Geo-Hazards)

THESIS ASSESSMENT BOARD

Dr. Cees J. van Westen, ITC (Chairman)
Prof. R.C. Lakhera, IIRS
Mr. I.C. Das, IIRS

Dr. P.K. Champati ray
SAARC, New Delhi
(External Examiner)

SUPERVISORS

ITC, The Netherlands

Dr. Cees J. van Westen
Associate Professor

IIRS, India

Prof. R.C. Lakhera
Head, Geosciences Division

Mr. I.C. Das
Scientist SE

ADVISOR
Dr. Robert hack
Associate Professor
ITC, The Netherlands

INTERNATIONAL INSTITUTE FOR GEO-INFORMATION SCIENCE AND EARTH OBSERVATION
ENSCHEDE, THE NETHERLANDS
&
INDIAN INSTITUTE OF REMOTE SENSING, NATIONAL REMOTE SENSING CENTER (NRSC), DEPARTMENT OF SPACE, DEHRADUN, INDIA

I certify that I might have conferred with others in preparing for this assignment, and drawn upon a range of sources in this work, the content of this thesis work is my original work.

Signed…………………………………

Disclaimer

Sashikant Sahoo.

Dedicated

To

Maa & Papa

Abstract

Landslide susceptibility assessment is necessary for development planning and disaster management activities in mountainous region. Various statistical methods have been applied in landslide mapping for more than two decades. In this present research, multivariate statistical analysis in the form of logistic regression was used to produce a landslide susceptibility map for a major communication road corridor (National Highway 108) in Uttarakhand Himalaya, India. Slope Stability Probability Classification (SSPC) system was also used for slope stability assessment along the road corridor. The result of slope stability assessment along the road corridor was further used for validation of the final susceptibility map of whole study region. The accuracy assessment has done by the ROC curve analysis.

In susceptibility mapping, the logistic regression model has been used to find the best fitting function to establish the relation between the dependent variable (presence or absence of landslides) and a set of independent variables such as lithology, slope angle, aspect, etc. Here, 41 landslides were mapped to prepare an inventory map as dependent variable, which takes the value 0 for the absence and 1 for the presence of slope failures. Lithology, slope angle, aspect, geomorphology, landuse land cover, drainage density, lineament density, weathering, proximity to road with anthropogenic (road / slope cut) were taken as independent variables for the analysis. Three training datasets were used in logistic regression model for susceptibility assessment. According to their accuracy, the best training dataset was used for final analysis. The influence of each parameter on landslide occurrence was assessed from the corresponding coefficient that results after the logistic regression analysis. Using the coefficients of each parameter, the spatial probability was calculated for each cell in the whole region. The final susceptibility map was prepared for whole study area with these spatial probabilities.

The Slope stability map was also prepared for the road corridor using the SSPC system. 32 homogenous locations were observed for slope stability assessment along the road corridor. Eight locations found high slope instability probability value higher than 0.6. The final probability map was validated with the result of slope stability map and 72 % accuracy observed finally. But the accuracy assessment was established by ROC curve analysis. The curve shows 83% area was perfectly classified with respect to landslide pixels. It was also observed, among the lithological parameters, slope gradient as well as lineament and drainage density has more significant contribution for slope failure. Using the final predicted map of spatial probability, the study area was classified into four classes of landslide susceptibility: very low, low, medium and high. The high susceptibility class occupied 5.78% and approximate 35% shows very low susceptible class in the study area, a part of Uttarakhand Himalaya, India.

Keywords: Landslide, Susceptibility, Slope stability, Logistic regression, SSPC, GIS.

Acknowledgements

It is with great pleasure for me to pay gratitude to people who have helped and encouraged me during the difficult and challenging time of this study, without whom I would have not come so far. First of all, I would acknowledge ITC and IIRS for giving me this opportunity to do this highly reputed international joint education programme.

Before thanking God, I would like to give all my gratitude to my supervisor Dr. Cees van Westen, who kept my confidence and spirit high throughout the 6 months of thesis work. I am indebted for his overall guidance. I highly appreciate his careful thoughts, invaluable comments, constructive suggestions and patience. Dear Sir it has been a great pleasure and a privilege for me to be your student.

I would like to express my sincere appreciation and thanks to Prof. R. C. Lakhera and Mr. I.C. Das for being my IIRS supervisors. Their suggestions for time to time made me stay focused in the right direction to achieve the objective of the study. Words are not enough to express the gratitude to Dr. Robert Hack for spending his valuable time and efforts in the field with me in Himalaya for a week.
I thank him for guiding me to learn the fundamentals of rock mass classification system and hope that I could do justice to the time that he had spent for me.

I thank to Dr. V.K. Dadhwal, Dean, IIRS for providing me all the necessary support during the entire course. I cannot forget to mention Dr. V. Hari Prasad, Programme Coordinator (Geo-Hazards Course), IIRS for the help extended in course of research, especially guiding me in proper aspect. I am also grateful to Drs. Michiel Damen, Programme Coordinator, ITC for his kind cooperation and providing all support at ITC. A special thanks to all faculty of Geosciences Division and Water Resource Division of IIRS and Faculty of Department of Applied Earth Science, ITC.

I am immensely thankful to Mr. Saibal Ghosh (GSI) and Mr. Tapas Martha (NRSC) for their critical reviews and effective suggestions which helped a lot for completion of this research. I thank Dr. John Mathew for his guidance and help during the research.

I extend my thank to each of my batchments and friend indeed, Amarinder, A. Pandey, M. K. Beg, A. Malik, Maity Da, Arun for being there to stand with me for all difficulties and funny moments at IIRS and ITC. Thanks are due to the all friends of Geoinformatics Division Rahul, Naveen, Jitu, Amitav, Shashi, Gaurav, Vijay, Alka, Navneet and Anurag for time spent with them throughout the whole course. The fun we had at IIRS and the 3 months in ITC can never be out of my memory.
A word of thanks to Shubharanjan, Jagannath, Ritwik, Sourav and Sidharth, for their help and sharing with me their knowledge about Earth Sciences. I also thankful to my seniors Chandan and Ambika for their support from beginning of this course. Special thanks and regards are extended to Das family who was a constant source & support here at Dehradun.

Finally the love of my life, my loving parents and sisters, thank you for your constant support and encouragement to complete this course. Your love and faith are my strengths without I would not have reached this far. No words to express my debt and my love for you. Bless me for success all time in future so that I am able to fulfil your dream.

Table of contents

List of figures

List of tables

Natural disasters are often perceived as being "Acts of God"

Annon

1. Introduction

1.1. Background of the research

Mass movements in mountainous terrain are natural degradational processes, and one of the most important landscape building factors (Van Westen, 1993). Landslides constitute the fragile landscape where habitation or other engineering structures cannot be developed or constructed. Landslides are one of the most common events in mountainous region because of their physiographic set-up and triggering factors. Increase in human population and rapid urbanisation has led to expansion of construction activities in hilly terrains and has resulted in frequent landslide events in recent times. In many developing countries, this type of problem is largely remarkable due to rapid non-sustainable development of natural resources. As a thumb rule, the losses due to the mass movements are estimated to be ¼ th of the total losses as compared to all natural hazard (Hansen, 1984).

Landslides have been the focus of research during the last quarter of the 20th Century in all over the world. There is still difficulty in defining the various mechanisms going on in the landslide phenomena. Landslides pose a serious geological hazard especially in rugged mountainous terrain like the Himalayas. Slope failure, one of the major causes of landslide initiation is an outcome of the interplay of physical processes. Till date, no technique in the world can accurately predict the occurrence of landslides. A certain degree of uncertainty always remains.

Landslide is a dynamic, naturally occurring phenomenon that occurs annually along the major communication routes, which are located in the folds of the Himalayas. One of the major triggering factors of landslide is rainfall in the higher reaches on the natural slopes. Such slopes, when steeply cut and left overhanging along the road corridor, they make the area more vulnerable to future instability.

According to EM-DAT: (Emergency Events Database) during recent period of 2008 natural hazards caused a lot of damage globally. Emergency Event Database for the same period shows that 35 landslides events killed as many as 3924 people and 3828660 people are affected. Estimated damage from these events are up to 4500,000 US Dollars (EM-DAT, 2008).

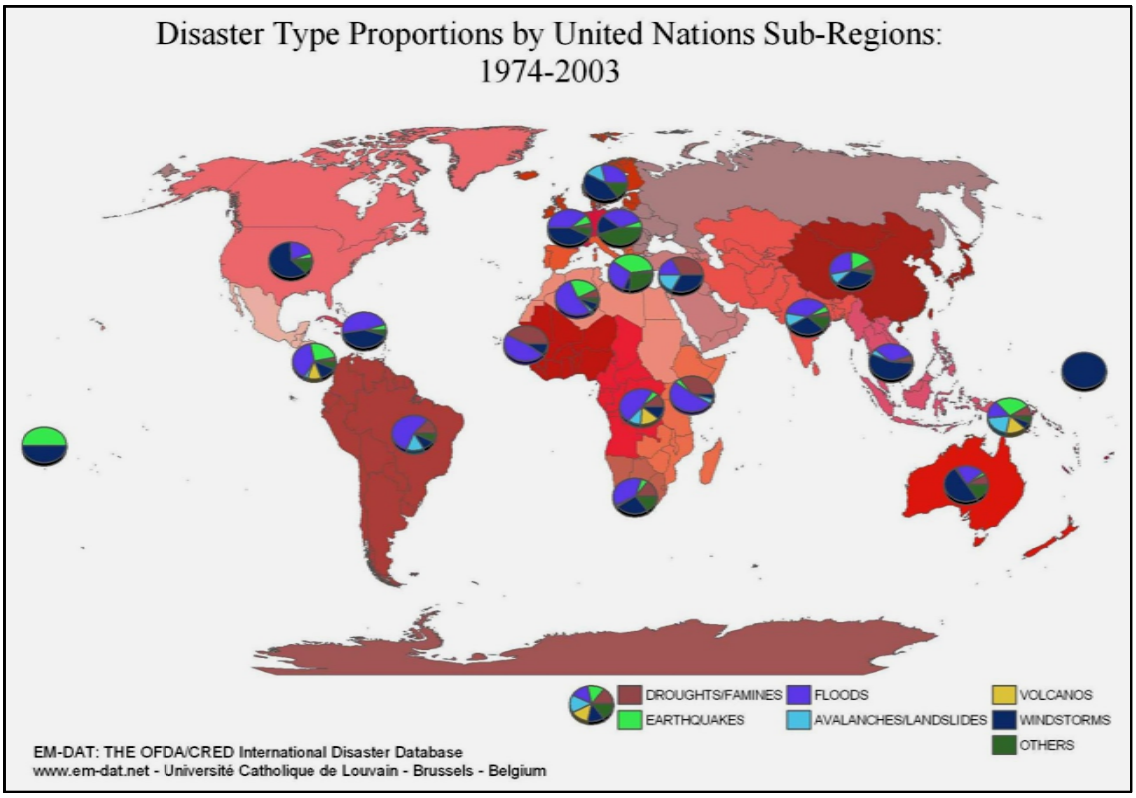

Figure 1-1: Emergency Events Database shows the Proportions of various disasters globally

Landslides are relatively rapid down slope movement of soil and rock, which takes place characteristically on one or more discrete bounding slip surfaces, which define the moving mass [(Hutchinson, 1988) cited in (Sekhar, 2006)]

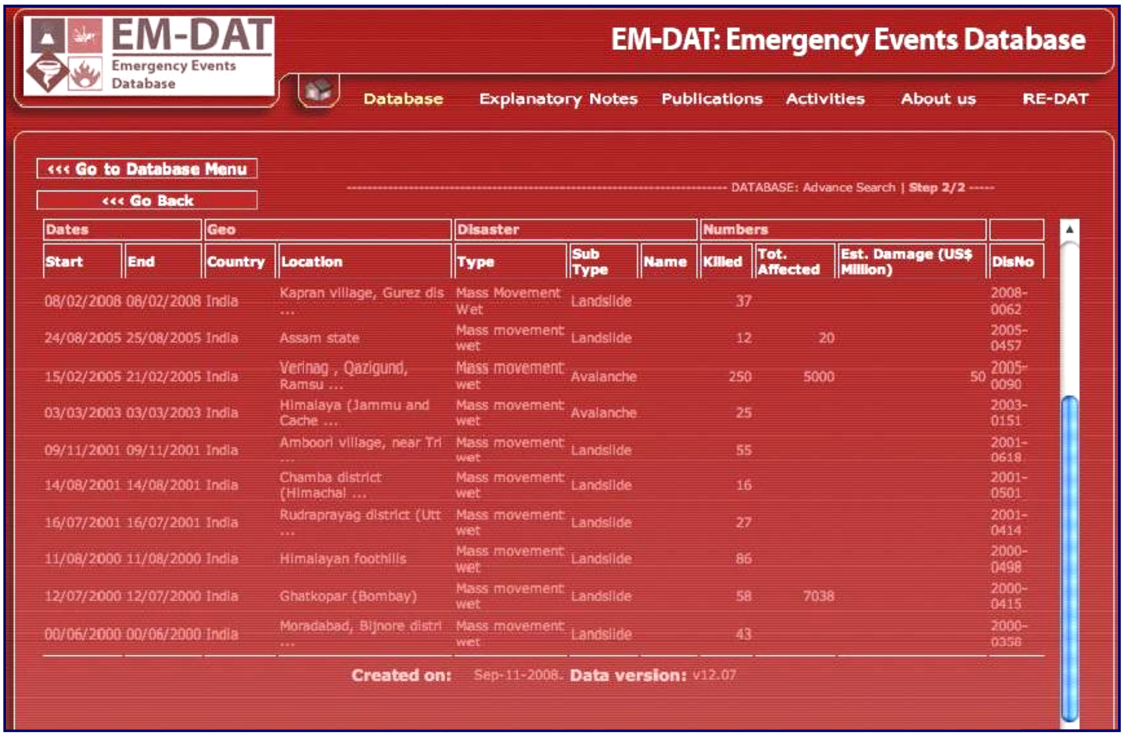

Dates		Geo		Disaster			Numbers			
Start	End	Country	Location	Type	Sub Type	Name	Killed	Tot. Affected	Est. Damage (US$ Million)	DisNo
08/02/2008	08/02/2008	India	Kapran village, Gurez dis ...	Mass Movement Wet	Landslide		37			2008-0062
24/08/2005	25/08/2005	India	Assam state	Mass movement wet	Landslide		12	20		2005-0457
15/02/2005	21/02/2005	India	Verinag , Qazigund, Ramsu ...	Mass movement wet	Avalanche		250	5000	50	2005-0090
03/03/2003	03/03/2003	India	Himalaya (Jammu and Cache ...	Mass movement wet	Avalanche		25			2003-0151
09/11/2001	09/11/2001	India	Amboori village, near Tri ...	Mass movement wet	Landslide		55			2001-0618
14/08/2001	14/08/2001	India	Chamba district (Himachal ...	Mass movement wet	Landslide		16			2001-0501
16/07/2001	16/07/2001	India	Rudraprayag district (Utt ...	Mass movement wet	Landslide		27			2001-0414
11/08/2000	11/08/2000	India	Himalayan foothills	Mass movement wet	Landslide		86			2000-0498
12/07/2000	12/07/2000	India	Ghatkopar (Bombay)	Mass movement wet	Landslide		58	7038		2000-0415
00/06/2000	00/06/2000	India	Moradabad, Bijnore distri ...	Mass movement wet	Landslide		43			2000-0358

Created on: Sep-11-2008. Data version: v12.07

Figure 1-2: Recent EM-DAT Facts and Figures of Landslide in India

Spatial probability i.e. susceptibility of landslide hazard, defined as the probability of occurrence of potentially damaging phenomena at a particular place, is a function of controlling environmental factors. The accuracy of a susceptibility map is very much dependent upon the proper combination of environmental factors that cause landslides. Hence, there is a need to understand the contribution of each factor towards landslide occurrence as well as the inter-relationships amongst the individual factors to determine the spatial probability of landslide occurrences in a particular area.

Landslides are generally localized events as compare to other natural calamities like floods, earthquake, cyclone, tsunami etc. With the population explosion, human beings are forced to occupy those areas of land that are intrinsically fragile and thereby maintaining a delicate balance in nature. Any encroachment in the natural balance of topography will adversely affect and can lead to slope instability resulting in landslides. In the recent years a number of deforestation activities mainly due to overgrazing, forest fire, timber etc. has lead to exposure of soil to vagaries of nature. Deforestation has altered the hydrologic condition of slope/road cutting, which facilitates in rapid runoff and erosion thereby increasing the possibility of landslides.

1.2. Motivation for research

Landslides are one of the common hazards that affect all mountainous areas in some way or the other, by posing threat to settlements, lives, infrastructure and many others. Forecasting the occurrence of landslides is always a critical challenge because of the high uncertainty associated with the event. Hence, it is always difficult to precisely forecast where and when disasters like landslide will occur.

In the region of great Himalayan mountain ranges, one of the main causes of land degradation is landslides and it is recurring phenomenon. Every year in Garhwal Himalaya, due to heavy rainfall and road cuts, landslide gets triggered causing causalities and several dangerous incidences are reported from different parts along the major communication route *(National Highway no 108)* in the state of Uttarakhand, India. This road is the one and only land communication route connecting Gangotri, an important holy place for Hindu religion and other valley of flowers *(Tapovan)* to rest of the nation. Due to slope failures, many traffic disruptions leaving the pilgrims, tourists and local peoples stranded for hours, even days.

If we go to history of Garhwal Himalaya, we can trace a number of major landslide events, which affected lot of people in Uttarakhand state. Few conspicuous memories of major landslides in Garhwal Himalaya includes: On *20th October 1991*, the Uttarkashi earthquake caused numerous landslides, particularly along a 27 km road stretch between Uttarkashi and Bhatwari (Sarkar and Gupta, 2005). One of the worst events happened in *1998;* around 400 people were killed by large landslides near Okhimath and Malpa, in the Alaknanda Catchment (Kuthari, 2007).The Varunavat landslide in the Bhagirathi valley on the upslope of the Uttarkashi town makes the history by damaging a huge loss of both lives and property in the year *2003*. On *July-August 2004,* a heavy downpour in Garhwal Himalaya caused debris slides and debris avalanches where at least 25 people died and 5000 people were stranded for days without food on the Joshimath-Badrinath road.

Considering the disastrous effects of landslides, it is necessary to access the landslides in Himalayan terrain. In order to reduce the damage caused by landslide initiations and reactivations, a landslide susceptibility map is really needed (M. Van Den Eeckhaut et al., 2006). The basic requirement in landslide assessment is the identification of potential landslide areas or zones based on the geological, topographical and geomorphological conditions. This is achieved with the help of landslide susceptibility maps, where the area is divided into homogenous zones with different degrees of susceptibility to the occurrence of landslides.

The main purpose of this work is to establish Landslide Susceptible Zonation, taking into account the terrain conditions through geomorphic, statistical approaches, and slope stability analysis, in an area, which is prone to the occurrence of landslides. It is assumed in this study that the effects of earthquakes and rainfall, which act as triggering factors for landslides, are more or less uniform in the study area due to its limited geographic extent. Hence, the factors will not be considered for the purpose of landslide hazard analysis. Moreover the ongoing tectonic activities in this young fold-thrust belt inferrently shapes the morphometry of the mountains, which results in a complex mass wasting processes, where modelling prediction is a difficult proposition.

Figure 1-3: Active Landslide occurred along National Highway 108 in 2007

1.3. Aim and Objectives of research

The study aims at quantifying landslide susceptibility (spatial landslide probability) using multivariate statistical approach (LRM). Spatial probability will be quantified using multivariate statistical approach like Logistic regression model and slope stability can be assessed by the Slope Stability Probability Classification, developed by Hack in 1996.

1.3.1. The main objective of the research

"To develop a quantified landslide susceptibility map along the major road corridor using a logistic regression model and rock mass classification."

1.3.2. Specific sub-objectives

Based on the main objective, the following specific objectives have been defined:

- To prepare the recent landslide inventory of the study region.
- To generate the database of geofactors to calculate the susceptibility with Logistic Regression Model.
- To evaluate of slope stability of the selected road corridor using Slope Stability Probability Classification (SSPC) system.
- To validate of the result and accuracy assessment of the resultant susceptibility map.

Any landslide susceptibility assessment of an area needs proper understanding of the various factors creating slope instability for the cut slopes all along the road corridor. This is a need of understand and examine the type, characteristics and causes of existing slope failures in the area. It is therefore, relevant to discuss about the landslides and their causes before going on with the methodology for landslide susceptibility assessment.

1.3.3. Research Questions

- What are the different landslide types in the region?
- Is the historical information on landslide sufficient to generate the landslide inventory?
- What are different related geo-factors required to generate the database for model input?
- Is the logistic regression is suitable for the susceptibility assessment in this region?
- What are the major parameters require to access slope stability for SSPC system?
- How the results can be validated?

1.4. Thesis Outline

The structure of the thesis follows the following sequence to achieve the objective of the study.

CHAPTER 1: INTRODUCTION

This chapter gives a general introduction about the background of the research and highlights the current problems in the landslide susceptibility assessment. It also discusses the various objectives as well as the research questions in this chapter.

CHAPTER 2: LITERATURE REVIEW

This chapter engages the previous investigations and research carried out for landslide susceptibility mapping using multivariate statistical approaches and slope stability analysis.

CHAPTER 3: STUDY AREA

This chapter briefs the general idea about the study area, its location, climate, rainfall, major land cover, general geology etc.

CHAPTER 4: CONCEPTUAL FRAMEWORK

The chapter describes the concepts of the models and methodology adopted for carrying out the research work.

CHAPTER 5: DATABASE PREPARATION

The chapter describes all about the data used and the preparation of database for the analysis.

CHAPTER 6: SLOPE STABILITY ANALYSIS

This chapter discusses about the results of the slope stability assessment for the road corridor.

CHAPTER 6: LANDSLIDE SUSCEPTIBILITY ASSESSMENT

The chapter discusses the results of the final susceptibility assessment and validation as well as the accuracy assessment of the result.

CHAPTER 7: CONCLUSIONS AND RECOMMENDATIONS

This chapter summarises the studies and indicates the limitation and suggestions for further research in the area.

2. Literature Review

2.1. Overview of the Research Work

Repetitions of socio-economic losses due to the landslides are great and apparently growing as human development expands into unstable hill slopes are quite noticeable. That is why a number of researchers across the globe are working round the clock to quantify the hazard and risk related to landslides. In recent years, researchers are concentrating more on the quantitative risk analysis by evaluating the spatial and temporal probability of events leading to catastrophic damages. Numerous advances have been made in the field of modelling for landslide initiation, triggering mechanisms, probability for slope instability using high resolution satellite imageries and Geographic Information System (GIS). The ultimate aim of all the research work is to create a landslide susceptible Zonation map with reasonable accuracy.

Landslides constitute a major element in mass wasting phenomena. Analysts always use all types of possible data for creation of historical landslide inventory. They also try to incorporate the aerial photograph interpretation with GIS analysis to acquire the better information. The final landform map is created after detailed analysis of the landslide inventory and a GIS-generated preliminary landuse map. Hazard rating is assigned to each class in the area of interest for further analysis.

2.2. Landslide studies in India

Landslide research works in India received a great attention in the year 1994 through the report presented by the Ministry of Agriculture, Govt. of India, to the world conference on the IDNDR held in Japan (Sekhar, 2006). Rao (1989) stated that five major regions in India which are susceptible to landslide are:

1. Western Himalayas (Jammu & Kashmir, Himachal Pradesh and Uttar Pradesh).
2. Eastern & North Eastern Himalayas (Arunachal Pradesh, Sikkim and West Bengal)
3. Naga - Arakkan Mountain Belt (Nagaland, Manipur, Mizoram, Tripura).
4. Plateau Margins in the Peninsular India and Meghalaya in the NE India.
5. Western Ghats Region in western part of India.

After 1994, though considerable number of researches carried out in Himalayan region, India, most of them focus on landslide hazard zonation, landslide mapping by different remote sensing and GIS techniques. But unfortunately, till now there are only few research articles (Mathew et al., 2007; Saha et al., 2005; Sharma, 1996) are carried out in Indian region by using the multivariate statistical approach for landslide susceptibility assessment.

2.3. Landslide : Types and Causes

Landslide defines a group of processes that causes the downward and outward movement of slope forming materials, including rock, weathered material, soil or a combination of these (USGS, 2004). Landslides are referred to be synonyms with mass movements, slope movements, slope failures etc. A comprehensive rational appreciation of the term was given by Soeters and Van Westen (1996) who called landslides as "the product of local geomorphic, hydrologic and geologic conditions and their modification by geodynamic processes, vegetation, landuse practices and human activities and influenced by the frequency and intensity of precipitation and seismicity".

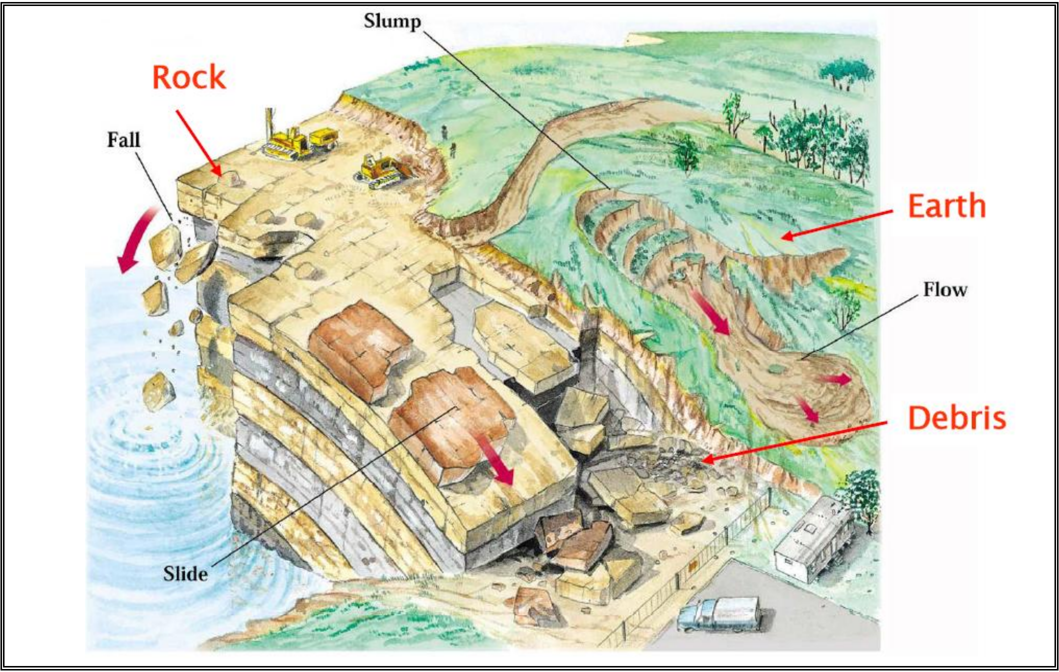

Figure 2-1: Various types of mass movements [Source: (Cruden and Varnes, 1996)]

2.3.1. Types of Landslides

Because of the complexity of landslides, arising from the variation in the nature of the material and processes involved, the classification of landslides should address all these aspects in order to represent it in a meaningful way. A detailed classification system adopted by (USGS, 2004) is given below in table 2-1.

Table 2-1: Abbreviated Version of Varne's Classification of Slope failure movements [Source: (USGS, 2004)**]**

<table>
<tr><th colspan="2" rowspan="3">TYPE OF MOVEMENT</th><th colspan="3">TYPE OF MATERIAL</th></tr>
<tr><th rowspan="2">BED ROCK</th><th colspan="2">ENGINEERING SOILS</th></tr>
<tr><th>Predominantly coarse</th><th>Predominantly fine</th></tr>
<tr><td colspan="2">FALLS</td><td>Rock Fall</td><td>Debris Fall</td><td>Earth Fall</td></tr>
<tr><td colspan="2">TOPPLES</td><td>Rock Topple</td><td>Debris Topple</td><td>Earth Topple</td></tr>
<tr><td rowspan="2">SLIDES</td><td>ROTATIONAL</td><td rowspan="2">Rock Slide</td><td rowspan="2">Debris Slide</td><td rowspan="2">Earth Slide</td></tr>
<tr><td>TRANSLATIONAL</td></tr>
<tr><td colspan="2">LATERAL SPREADS</td><td>Rock Spread</td><td>Debris Spread</td><td>Earth Spread</td></tr>
<tr><td colspan="2">FLOW</td><td>Rock Flow (Deep Creep)</td><td>Debris Flow (Soil Creep)</td><td>Earth Flow</td></tr>
<tr><td colspan="2">complex</td><td colspan="3">Combination of two or more principal types of movement</td></tr>
</table>

2.3.2. Causes of Landslides

Landslides result from conditions that cause an increase of shearing stress acting on the slope or a degree of the cohesion in the slope materials, or both. These conditions include steepening of slope or removal of slope support by river erosion or manmade excavation, addition of weights to the top of the slopes by material deposition, earthquakes and increase in pore-water pressure. Rapid drawdown, subsurface erosion and spontaneous liquefaction may act as conditions responsible in creating slope failures. (Mathew, 2007; Terzaghi, 1950) divided landslide causes into external causes which result in an increase of shearing stress (e.g. Geotechnical changes, unloading the slope toe, loading the slope crest, shocks and vibrations, drawdown, changes in water regime etc.) and internal causes which result in a decrease of the shearing resistance (e.g. progressive failure, weathering, seepage erosion etc.). Earthquakes can also result in the lateral spreading due to liquefaction in gentle slopes. Landslide associated with volcanic activity results in the rapid down slope movement of water and ash that run out to great distances. The classic example of such landslide is huge landslide, which Mt. St. Helens caused in 1980 (USGS, 2004).

Cruden and Varnes (1996), both classified the causal factors of slope failure, including the precondition and triggering ones, into geological, morphological, physical and human causes, as given in table 2-2.

Table 2-2: Causes of Landslides [Source: (Cruden and Varnes, 1996) & (USGS, 2004)**]**

GEOLOGICAL CAUSES	MORPHOLOGICAL CAUSES
i. Weak materials ii. Sensitive materials iii. Sheared materials iv. Jointed or Fissured materials v. Adversely oriented mass discontinuity (Bedding, Schistocity, etc.) vi. Adversely oriented structural discontinuity (Fault, Unconformity, Contact, etc.) vii. Contrast in permeability	i. Tectonic or volcanic uplift ii. Glacial rebound iii. Fluvial erosion of slope toe iv. Wave erosion of slope toe v. Glacial erosion of slope toe vi. Erosion of lateral margins vii. Subterranean erosion viii. Deposition loading slope and or its crest ix. Vegetation loss
PHYSICAL CAUSES	HUMAN CAUSES
i. Intense rainfall ii. Rapid snow melt iii. Prolonged exceptional precipitation iv. Rapid draw down of floods and tides v. Earthquakes vi. Volcanic Eruptions vii. Freeze and Thaw weathering viii. Shrink and swell weathering	i. Excavation of slope and toe ii. Loading of slope or its crest iii. Draw down of reservoirs iv. Deforestation v. Irrigation vi. Mining vii. Artificial Vibration viii. Water leakage from utilities.

Based on the factor of safety of the slope, which compares the shear strength and shear stress existing on the slope material, it is possible to classify the slope into three stages as stable, marginally stable and unstable (Crozier, 1986). It can be represented by the probability distribution curve of the factor of safety [(Popescu, 1996)cited in (Kuthari, 2007)] and the factor of safety also shows a time dependency in creating slope failure, which is shown in figure 2-2.

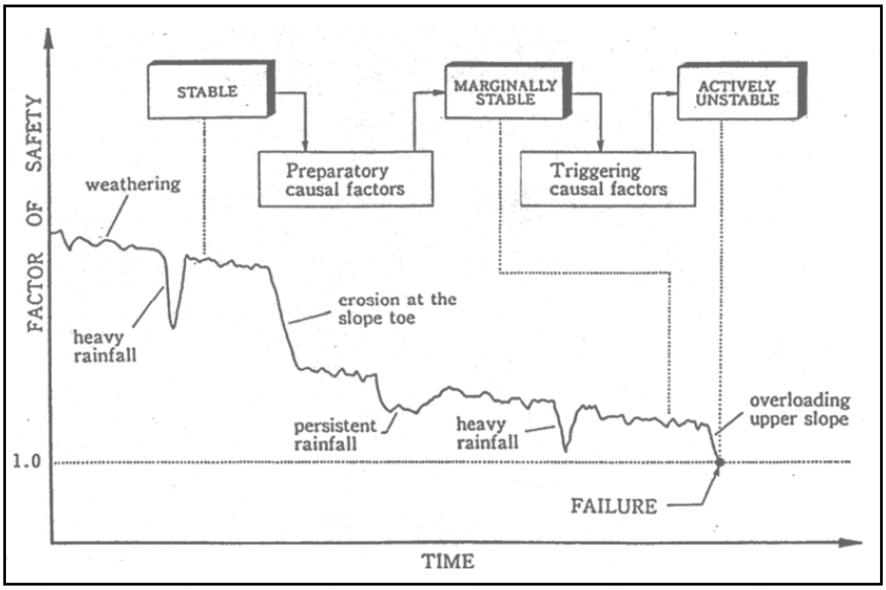

Figure 2-2: Changes in the factor of safety with time [Source: (Popescu, 1996)cited in (Kuthari, 2007)**]**

2.4. Application of Remote Sensing in Landslide related studies

The spatial assessment of landslide hazard requires systematic mapping of the controlling factors as well as the inventory of existing landslides. Remote sensing technology with various spectral, spatial and radiometric resolutions has emerged as one of the most common and widely used tools in accomplishing landslide feature extraction. According to (Metternicht et al., 2005); Remote sensing data is useful in various stages of landslide related studies:

1. Landslide detection.
2. Landslide monitoring.
3. Spatial analysis and hazard prediction.

2.5. Landslide Identification and Mapping

Till late 1990s, the most widely used remote sensing technique for studying the landslides and associated hazard has been stereoscopic-aerial photography. Traditionally several earth scientists assess the characteristics of landslides on the basis of geomorphological investigations carried out through aerial photographs interpretation and field work (Carrara et al., 2003). Inaccessible terrain like high altitude topography, it is always a big challenge to carry out the landslide mapping. But with the launch of IRS Cartosat-I, Stereo pair satellite imagery data of inhospitable terrain are readily available for various studies and investigation. According to (Brardinoni et al., 2003), in rugged forest watershed, canopy cover, it is very difficult to identify the small landslides to a great extent and detecting all landslide features from images.

Accurate mapping of a landslide in terms of magnitude, though it is a challenge is prerequisite to any landslide related research. Some of the common sources of landslide occurrence information are governmental documents, newspapers, archival records, historic travel guide and participatory community reports. However, such records contain some exaggerations but still provide fairly good details of the events occurred. Devoli et al (2006) has used all other sources (e.g. newspaper, old chronicles, and historical monographs at public archives, technical reports and natural disaster database) other than field evidences to prepare national landslide catalogue of Nicaragua analyzing both temporal and spatial distribution, types of landslides, triggering mechanisms, and type of damage of the recorded historical landslides. Such records coupled with detailed field efforts can provide a consistent hazard inventory.

Guzzetti (2005) proposed that the major assumptions for identification and mapping of landslides can be:

1) Landslides leave typical signatures on the terrain surface, i.e. they refer to changes in the form, position or appearance of the topographic surface.

2) The morphological signature left by a landslide can be interpreted to determine the extent of the slope failure and to infer the type of movement (e.g. fall, flows, slides, complex, compound etc.) and the rate of movement.

3) Landslides are controlled by many terrain factors, and are a combined result of the interplay of physical processes and mechanical laws that can be determined empirically, statistically or in deterministic fashion.

4) Landslide occurrence follows the principle of uniformitarianism i.e. the past is the key to present and the past and present is the key to the future.

Another important component of landslide inventory database is mapping the character and surface features of landslide complexes. This is important to classify landslides and monitor their movement. For monitoring the motion of large complex slide, SAR Interferometric analysis was used and it facilitated displacement measurements on space points with greater accuracy (Ferretti, 2000). Recently Barlow et al (2006) proposed to combine high resolution satellite imagery with a Digital Elevation Model (DEM) to replace the aerial photography for automatic detection of landslides from satellite imagery.

2.6. Spatial Landslide Hazard [Susceptibilty] Analysis

The use of landslide susceptibility and hazard maps for landuse planning has increased significantly during the last few decades. The purpose of the susceptibility map is the identification of areas likely to get affected by landslide in near future by various natural and artificial causes. Landslide susceptibility mapping aims to differentiate a land surface into homogeneous areas according to their degree of actual, potential hazard caused by mass-movement with respect to specific locations (Varnes, 1978). Landslide probability quantification involves characterizing the danger in terms of type, size, location and travel distance of landslides, but their reliability depends mostly on the amount and quality of available data, a specific working scale as well as the selection of the appropriate methodology for susceptibility and hazard assessment (Baeza and Corominas, 2001). Van Westen et al (2006) also highlighted that for quantitative output, landslide inventory based probabilistic methods are the most appropriate and in general, the occurrence of landslide events in the past is a good indication of likelihood of the phenomena occurring in the future, under the same geo-environmental settings.

As prevalent in the literature, the commonly adopted approach for susceptibility assessment can be divided into two types, such as: qualitative and quantitative. The qualitative methods are very subjective as well as site specific and up scaling to larger area are often difficult as it needs material data that are difficult to obtain for inaccessible areas. But, on the other side, the quantitative methods provide numerical estimations, in terms of probability of landslide occurrences for each susceptibility class. This approach also uses the relation between the locations of previous landslide events and environmental variables, to predict areas of landslide initiation with similar combinations of factors, using heuristic or statistical methods (Van Westen et al., 2006). Present study is based on the second approach i.e. quantitative approach.

The statistical methods have assumed importance in recent years and preferred over the heuristic methods as they are immune to the variable knowledge base of experts and quantitative in nature. They have become very popular in landslide studies all over world with initiation of Geographic Information Systems (GIS) techniques, which allows integration of data collected from various sources, methods and scales. As a result, various attempts have been made on statistical prediction of landslides using statistical models and remotely sensed data (Carrara et al., 1995; Chung and Fabbri, 1999). The countries where good historical landslides databases are available, some researchers like (Guzzetti, 2000; Guzzetti et al., 2005; Sharma, 1996) have used landslide inventory for probabilistic landslide hazard quantification. Finlay et al (1997) also combined the probabilistic and heuristic method to estimate the annual probability of failure along the cut slopes for Hong Kong area. Guzzetti et al (2005) used discriminant analysis of different thematic variables and Poisson model to evaluate the spatial and temporal probability, at a basin scale. The actual problem with such models is that they require a good multi-temporal landslide inventory on types, sizes and recurrence of slope failures. All these methods carry out the analysis of geo-environmental variables controlling landslide occurrence with respect to previous landslide events, either through a bivariate or a multivariate frequentist statistics. However, these methods give inclusive results with respect to parameter uncertainty. Thus, it is necessary to identify accurately the uncertainty in each parameter estimate that contributes significantly to the model and to investigate the possibility of improving the estimation by means of incorporation of prior information (Mila et al., 2003). Depending upon the type of statistical technique, the meaning of probability changes slightly (Guzzetti, 2005). With the advancement of computing technology, it has become feasible to apply various statistical methods to analyze landslide phenomena and derive at reproducible hazard zonation maps. Currently, most of the statistical analysis is performed with the help of commercial or freeware software packages based on the idea of frequentist statistical framework like maximum likelihood estimates (MLE). MLE based logistic regression, which was first applied in the field of biostatistics now found strong use in landslide studies.

2.7. Statistical Methods

These are the mathematical techniques, where the landslide susceptibility is predicted quantitatively with the help of statistical methods. Statistical methods can be called as data-driven methods. Such methods are mostly applicable at medium scales for limited geographic extent (Suzen, 2002). On the basis of statistical analysis of the factors that have led to landslide studies in past, quantitative predictions are made for areas currently free of landslides (Metternicht et al., 2005). Analysing the relation between the landslides and their causal factors not only provides an insight into the understanding of its operating mechanism, but also forms a basis for predicting future landslides and assessing landslide hazard (Zhou et al., 2002). The following Factors are relevant with respect to such methods (Gorsevski et al., 2000):

a. Usually the strength of the statistical model depends upon the quality of the data used.
b. A data-driven model cannot be extrapolated to another area, unless both have similar geological, topographical and climatic conditions
And c. The climatic conditions may change and hence ‘past is not the key to the future’.

There are two types of statistical techniques used for landslide studies, based on the method of deriving the quantitative contributions of the parameters: Bivariate and Multivariate statistical methods.

2.7.1. Bivariate Statistical Techniques

In bivariate statistical techniques, the contribution of each parameter class is assessed independently and these techniques are bivariate in nature as there are two variables (the parameter class and landslide) considered at a time. It involves the determination of density of landslides in different parameter classes, relative to the landslide density over the entire study area under consideration. Using these density values derived from existing landslide distribution, the landslide hazard is estimated for landslide free areas, by addition of the weights of individual parameter classes. Van Westen (1993) has suggested the following procedure to carry out the bivariate statistical analysis for landslide hazard zonation studies:

- Classification of each parameter map into a number of relevant classes.
- Combination of the parameter classes with the landslide map by overlay analysis.
- Calculation of the weight values to the parameter class based on the cross-tabulated data.
- Assignment of the weight values to the parameter classes and integration of the parameter maps
- Lastly, Classification of the resulting scores into a few hazard classes.

Several methods have been proposed by researchers using bivariate statistical analysis for LHZ mapping. The most widely used methods are Landslide Susceptibility Analysis (Brabb, 1984; Van Westen, 1993), Information Value Method (Saha et al., 2005; Yin and Yan, 1988), Weights Of Evidence model (Lee et al., 2002; Mathew et al., 2007; Neuhäuser and Terhorst, 2007; Wu et al., 2004) and Fuzzy Logic approach (Ercanoglu and Gokceoglu, 2004; Tangestani, 2004). These methods are applied in various research fields also.

2.7.2. Multivariate Statistical Techniques

In multivariate statistical techniques, the combined influence of a set of causal factors responsible for slope failure is determined and the contribution of each of these factors is estimated. There are two main approaches for multivariate statistical analysis for LHZ mapping (Van Westen, 1993):

1. Statistical analysis of point data obtained from checklist of causal factors associated with individual landslide occurrences.
2. Statistical analysis performed on terrain units covering the whole study area.

These methods are rather time- consuming, for both data collection and data processing. The relevant factors are sampled either on a grid basis or in terrain units or geomorphological units. For each sampling units, the presence or absence of landslides is determined. The resultant data is subjected to multivariate statistical procedure. According to Van Westen (1993), this can be executed by following GIS procedure:

- Determination of the list of factors that will be included in the analysis. The alpha-numeric type input maps are converted to numeric types. These maps can be converted into binary pattern (presence or absence values for each land units) maps or presented as a percentage data or the parameter classes can be ranked according to increasing mass movement density. By overlaying the parameter maps with the land-unit map, a large matrix is created.
- Combining the land unit map with the mass movement map to find out the stable and unstable areas.
- The coefficients estimated by the multivariate analysis are used to calculate the landslide susceptibility of the entire study area. The classification results are cross verified for assessing the accuracy of the procedure.
- Division of the landslide susceptibility values into a few hazard classes.

Multiple regression and discriminant analysis require normally distributed input variables (Suzen, 2002). Another multivariate statistical method called Logistic regression (LR) analysis which does not require such normally distributed input variables, has been worked by few researchers in recent past in worldwide (Ayalew and Yamagishi, 2005; Van Den Eeckhaut et al., 2006; Yesilnacar and Topal, 2005).

2.7.2.1. Logistic Regression Analysis

Logistic regression is a mathematical modelling approach, which is used to describe the relationship of several independent variables to a dichotomous dependent variable (Hosmer and Lemeshow, 2000). In this research Logistic regression model is used significantly in whole the area of study for analyze the susceptible values for slope failure. The detailed concept of this model is described in *Conceptual framework chapter (Chapter-4).*

2.8. Why Slope Stability Analysis?

Landslides and slope instabilities are a major hazard for human activities often causing economic losses, property damages and maintenance costs, as well as injuries or fatalities. The primary factors driving this trend includes aging slopes constructed for major transportation systems and the ever increasing need to develop land on steep natural slopes and fills for public and private purposes. Hoek mentioned that, rock falls along the highway and railways in the mountain areas are not same level like the large-scale failures in other areas. So presently, the analysis and solution of landslide problems as well as the prevention of landslide problems require the understanding of geology, geotechnical exploration and practical and engineering solutions with rock slope stability.

An attempt has been made towards rock slope stability analysis using a rock mass classification system regarding their reliability in identifying potentially hazardous rock cut slopes. Rock mass classification systems exclusively use factors relevant to the condition of slope cuttings. Actually, the first attempt for the slope stability assessment of cuttings through rock mass classification system was introduced by Bieniawski (1979). Since then a number of rock mass classification systems have been proposed for slope stability assessment. A detailed list of empirical rock classification methods developed for cut slopes worldwide is presented in Table 2-3.

Table 2-3: Existing rock mass classification system for cut slopes (Pantelidis, 2008)

Name of the System	Abbreviation	Authors	Application	Comments
Rock Tunnelling Quality Index	Q	***Barton***	Tunnels	They are the most commonly used classification systems for tunnels.
Rock Mass Rating	RMR	***Bieniawski***	Tunnels and Cutting	For application in slopes was added in 1979 version of the RMR system.
Mining Rock Mass Rating	MRMR	***Laubscher***	Mines	Based on RMR.
Slope Mass Rating	SMR	***Romana***	Cuttings	Based on RMR (1979). The most used classification system for slopes.
Slope Rock Mass Rating	SRMR	***Robertson***	Cuttings	Based on RMR. The classification is for weak altered rock mass materials from drill-hole cores.
Rock slope Deterioration Assessment	RDA	***Nicholson and Hencher***	Cuttings	For shallow, weathering-related breakdown of excavated rock slopes.
Slope Stability Probability Classification	SSPC	***Hack***	Cuttings	Probabilistic assessment of independently diff. failure mechanics.
Falling Rock Hazard Index	FRHI	***Singh***	Cuttings (Temporary Excavations)	Developed for stable excavations to determine the degree of danger to workers.

In this present research work, Slope Stability Probability Classification (Hack, 1998) is used, which has been developed for the slope stability assessment on cut slopes.

2.8.1. Why Slope Stability Probability Classification (SSPC) System?

Slope Stability Probability classification (SSPC) system was first developed and formulated by Robert Hack in the year 1996. Further, Hack (1998) modified the initial techniques and parameters in the system and gave a better and appropriate indication of maximum influence of each parameter on the final slope stability probability. Because many slope stability systems are based on the system designed for the underground excavation like (Bieniawski, 1989) and (Laubscher, 1990). These have also included those systems for the comparison of other slope systems. The Q-system (Barton, 1976) is also included the same parameters to compare the slope stability analysis with different systems. It is impossible for all systems to indicate the influence per parameter exactly because in some systems, parameters are dependent or parameters are not linear. SSPC has differences in the influencing of parameters from other systems are given below (Hack, 1998):

1. The absence of intact rock strength (except for low intact rock strength in the *Barton's Q-system.*
2. The absence of discontinuity spacing in the *Barton system.*
3. The strong reduction in influence of the water parameter in the *Laubscher system* as compared to the systems of *Bieniawski and Barton.*
4. The absence of a water or water pressure parameter in the *Robertson* modification for the slopes of *Bieniawski system.*
5. The strong influence of susceptibility of weathering in the *Laubscher system*.
6. The strong increase in influence of orientation of discontinuities in relation to the orientation of the walls and roof of underground excavations in the *Laubscher system* compared to the *Bieniawski system.*
7. The systems for surface applications do not include the height of the slope whereas the height of the slope likely has an influence on the slope stability.

According to the above differences in different classification systems, *SSPC* found to be useful for the kind of research in the study area with cutting slopes along a road stretch.

2.9. Why the combination of LRM and SSPC?

As logistic regression model is a multivariate statistical approach, it always requires the combination of both dependent and independent variables. But, the slope stability probability classification is a pure field based approach. To reduce the biasness of the statistical analysis of the dataset, it is always necessary to compare and validate with a field based approach. In recent decades, the SSPC system gives the slope stability probability which is useful for analysis the slope failures. This present research tried to establish the relation between both the systems, which is helps to calculate the accuracy for the landslide susceptibility assessment.

3. Study Area

After carrying out the literature review, the need to select a study area to actually acquiring the genuine problem was felt. Study area was decided after analyzing available data for various slope instability parameters in the landslide prone areas of Uttarakhand. The selection for choosing the area was based on the under mentioned conditions:

1. Availability of historical landslide data.
2. Availability of Geotechnical Survey results.
3. Availability of fine resolution satellite imageries.

3.1. A Brief Description about Area of Research

The area chosen for the study is along road corridor *(National highway No 108)* passing through a highly rugged terrain of upper Bhagirathi river valley in Uttarkashi district of Uttarakhand, suffering from frequent landslides every year. The state of Uttarakhand is divided into two major divisions namely Garhwal division and Kumaon division. Garhwal Himalaya in Uttarakhand state is well known for its fragile landscape and frequent geological hazards, among which landslides are the regular threats over this region.

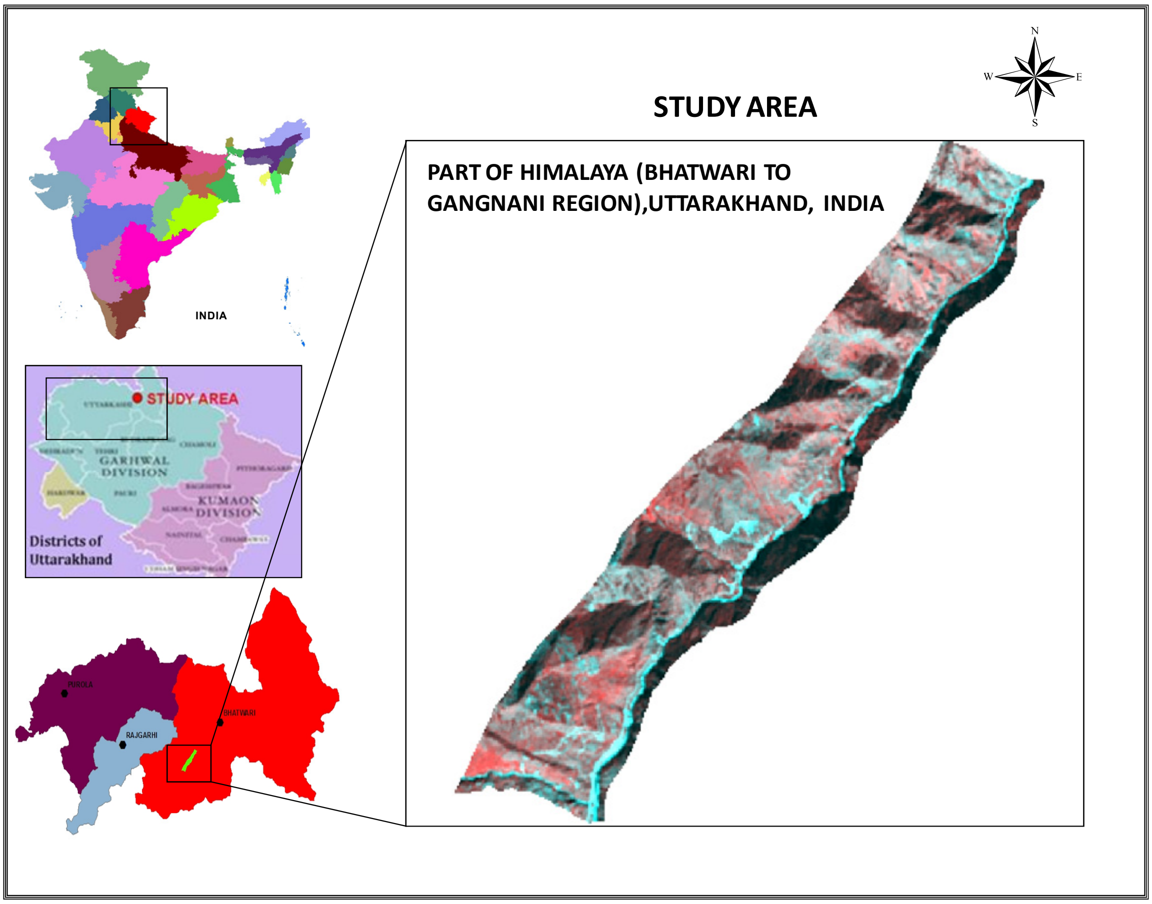

Figure 3-1: Study area location Map

The historic records of landslides along the road in the study is maintained by the BRO *(Border Roads Organization)* itself which taking place. The study area chosen is also ideal for my research as it encompasses the road corridor, which area is around 20 square kilometres, shown above in Figure 3-1.

3.2. Uttarakhand (At a Glance)

Before describing the uniqueness of the study area, which is physiographically part of the Garhwal- Himalaya mountain system, it is germane to briefly explain the geomorphic setting of this major orographic feature of Uttarakhand. It is also relevant to explain in few words, the historical significance of the state as a region of continued human interaction with the environment since time immemorial.

Uttarakhand - the land of gods, the home of Himalayas and truly a paradise on earth, allures everyone from everywhere. The fresh air, the pure water, the chilling snow, the adversing mountains, the scenic beauty, the small villages, the simpler people and a tougher lifestyle is what that distinguishes Uttarakhand from rest of the world. The state Uttarakhand derives its name from Sanskrit for Northern Country or section as it is indeed among the northern most part and formed as 27^{th} state of Republic of India in the year 1999. In January 2007, the name of the state was officially changed from Uttaranchal, its provisional name to Uttarakhand, according to the wishes of a larger section of its people. Uttarakhand shares it border with China (Tibet) in the north part and Nepal in the east. The entire state is hilly terrain incorporating the Tethys, Higher, Lesser and Sub Himalayan part along with the great Indo-Gangetic plain, with covers an area of about 53,500 km^2.

3.3. The Major Communication Route Corridor (NH-108)

In this research, it is proposed to carry out quantitative landslide susceptibility assessment and slope stability assessment of major communication road corridor (Bhatwari-Gangnani Linear Stretch), which is a northern part of the Uttarakhand state, India. The study area is covering approx. 30 km^2 area in 1:10,000 scale between latitudes of 30° 49’ 20” N to 30° 54’ 04” N and longitudes of 78° 35’ 58” E to 78° 40’ 44” E of part of Survey of India Toposheet no 53J/9, along the Bhagirathi river valley in Garhwal Himalaya. The area is transacted by a major National Highway connecting Uttarkashi and Gangotri, in Uttarakhand state, India. A 12 kilometer road stretch between Bhatwari to Gangnani on National highway 108 is finally selected for the research as the landslides affecting or likely to affect the Highway is taken into consideration for the analysis. Slope failures are observed frequently during rainstorm and very often with disastrous condition. Landslides here are the outcome of complex tectonic and neo tectonic settings, unique geomorphic expressions with steep slopes, highly dissected hills, deep carved valleys accompanied by high pace of land degradation in association of climatic and other geo-environmental agents and human activities along the hill slopes. Slope failures are observed frequently during heavy shower and very often with catastrophic consequences.

3.3.1. Geomorphology

The major landforms observed in the study area are structural, glacial, fluvial, and denudational in origin. Inversion of relief in highly metamorphosed rocks of the study area reflects the impact of active weathering process prevailing over the area. The general geomorphic features include the Cuesta and hogbacks type topography, river terraces, highly dissected denudo-structural hill, intermonatane valley, minor and major ridges of quaternary deposits and various geomorphic features like point bar, channel bar, meandering scars are observed along the entire river course.

Figure 3-2: Photograph showing the general geomorphological units of part of the study area

The dip gorges and wide valleys engraved high relief and structural control of the area. The narrow and confined nature of the valley towards the lower portion of the stream indicates the continued nature of these valleys. The middle valley slope generally consists of perglacial and hill slopes scree, landslides and old rock falls.

3.3.2. Drainage

One of the holiest streams in India the "Ganges" also known as Bhagirathi at the upper reaches drains the study area. It originates at Gangotri glacier in Gaumukh in Tethys Himalaya forming a board U-shaped valley near Jhala at its upper course. Afterwards it continues to cut the deep V-shaped gorges while flowing through Greater and Lesser Himalayan course. The river is fed with numerous small first and second order streams from both the sides. Dendritic drainage pattern is predominant over the area and also sub parallel pattern is observed along the hill slopes. The entire road stretch of National Highway 108 is running parallel to the river Bhagirathi.

3.3.3. Climate and Rainfall

The road corridor experiences a subtropical temperature climate throughout the year because of high altitudinal location. The maximum elevation observed in the whole region is about 4500m and minimum elevation is about 1150m with respect to mean sea level. But In this study area, the elevation range in between 1500 meters to 2700 meters has been observed. It receives a heavy rainfall during monsoons. On average there are 100 rainy days in a year and average annual rainfall in the area is around 1200mm. Around 70% of the total rainfall is received during the months of July, August and September in which also maximum landslides occur in the area.

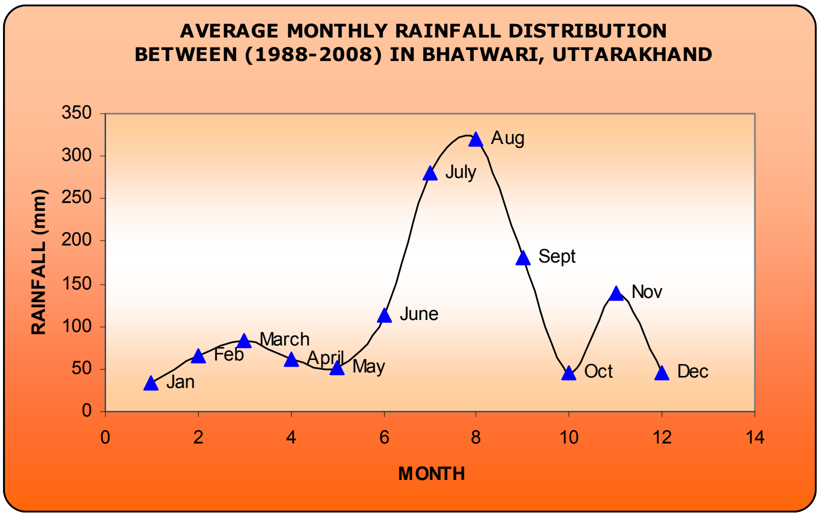

Figure 3-3: Showing the average monthly rainfall of the Bhatwari sector (BRO, 2007)

The rain gauge stations in the study area are Uttarkashi, Tekla, Malla, Maneri, Gyansu, Bhatwari, Jaurab, Bankholi and Gangotri. The maximum average rainfall recorded in the study area was 1750mm per annum and the minimum average rainfall was 1045mm per annum for last two decades (BRO, 2007).

3.3.4. Soil

Wide range of variation in soil type can be observed in the entire road corridor. The total soil cover is existing as a thin layer along the slopes. While the road corridor under geomorphic units like river terraces have thick soil cover where cultivations are practised in abundance. Depending upon these altitudes and geomorphic conditions, the change in soil characteristic is noticeable in the area. Very steep slopes are mostly left without any soil cover.

3.3.5. Natural Vegetation

The high altitudinal zones of the area characterized with beautiful pasture lands which contains grasses with plants, like Piceasp, Pinus, Cesrus, Deodar, Karsu, Quereus semecarpifolia, Rhohododendrron, Camapanualatum, and Betulautilus etc. the moderate to lower altitudinal slopes are generally used in step cultivation for growing potatoes, pulses and green leaves. The natural vegetation predominant over these slopes is Shores robusta, Dalbegia sisoo and Pinus sp.

3.3.6. Anthropogenic Effects

Many times civil engineering construction also leads to the slope failure. In the present study area, it has been observed several places road passes through half tunnels, overhanging slopes portions are left unprotected. These overhanging portions can be observed several places especially between Thrang to Gangnani (around 5 kilo meters road stretch), which also very prone to landslide activities. This road stretch passes through Gneisses and schist, which show the presence of joints in overhanging portions are almost vulnerable and dangerous features. At some places explosives used for blasting as carried out in construction and widening of the road produce vibrations of different frequencies in rocks and thus a temporary change in stress can disturb the equilibrium state of the slope further resulting in slope failure. Hence it should be ensured that large quantities of explosives are not blasted at a time in a particular area.

3.3.7. Geological Setting

The present study area falls in the southern extreme of the world's youngest tectonic mountain chain; The Himalaya. This mountain chain stretches for about 2500 km from Nanga Parbat (Mountain in English) in Jammu & Kashmir to Namcha Barua in Tibet, with a width of about 250 km (Valdiya, 1980).

3.3.7.1. Regional Geology

Geologically, the area of research falls under a part of Garhwal Higher Himalaya. The geological settings of the entire area was studied previously by several eminent researcher like (Chakraborty and Anbalagan, 2008; Valdiya, 1980). The nomenclature for the litho units, as proposed by Valdiya has taken account for the study. River Bhagirathi crosses 3 major lithostatigraphic units in the entire length up to Uttarkashi. In Uttarkashi District, Four major stratigraphic units have been recognized as: The Central Crystalline, Martoli Formation, Dudatoli Group and Garhwal Formations (Agrwal and Kumar, 1973). Each of these units separated by major faults and thrust. The North Almora Thrust and the Main Central Thrust separated the Garhwal group from the Dudatoli Group in the southwest and the Central Crystalline in the northeast respectively.

Table 3-1: Litho-tectonic succession of Study Area [Modified after (Valdiya, 1980)**]**
N.B:- Age of the formation is Precambrian.

Group	*Formation*		*Lithology*
		Upper Crystallines	Phylonite Schist with Garnet-mica Schist.
Almora	*Munsiari –or- Central Crystallines*	*Middle Crystallines*	Mylonitized Porphyroclastic Augen Gneiss, Migmatitic Gneiss, Biotite Gneiss, *Mica Schist and minor Amphibolites.*
		Lower Crystallines	*Porphyroclastic Granite Gneiss, Chlorite Schist, Schistose Quartzite, Biotite Gneiss.*
………………………………………		***Main Central Thrust***	…………………………………………………….

3.3.7.2. Geology along Road Stretch

Actually the area for present study (a road corridor) which starts from Bhatwari up to Gangnani, falls mainly in the Central Crystalline formation or Munsiari formation in Almora Group (Purohit et al., 1990; Valdiya, 1980) of the Higher Himalaya, which is given below. The litho-units are present in close proximity because of the Main Central thrust (M.C.T.), due to which Almora Group of rocks overlies the other Group. In Majority of locations, 3 sets of joints can be seen irrespective of the lithology. A brief overview of the Munsiari Formation or Central crystalline formation is described below.

3.3.7.3. Munsiari Formation

Because of the extensive pressure of metamorphism and gneisses of the Himalaya, this formation is commonly referred as the '*Central Crystallines*' or '*Higher Himalayan Crystallines*' (Chakraborty and Anbalagan, 2008). Lithologically this formation is subdivided into three litho-units. Such as:

Lower Crystallines constitutes low grade metamorphic rock such as Chlorite schist, Schistose quartzite, Biotite gneiss and mylonitic migmatites separated from Garhwal group by the main Central Thrust. The Geological map that is used for the research is given below.

Biotite-Gneiss *Mica-Schist*

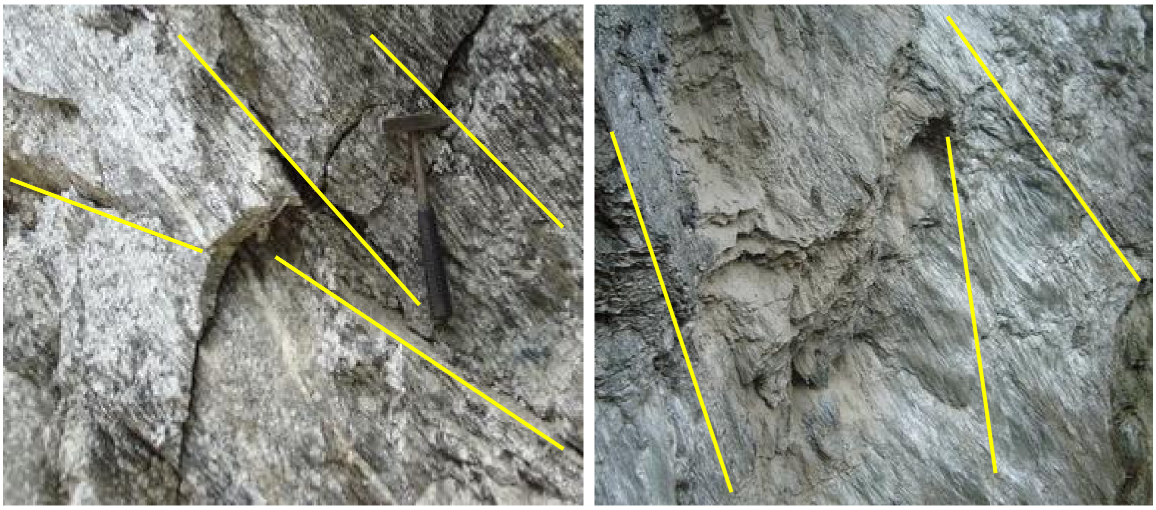

Figure 3-4: Major Rock Types Exposed along the Road Section

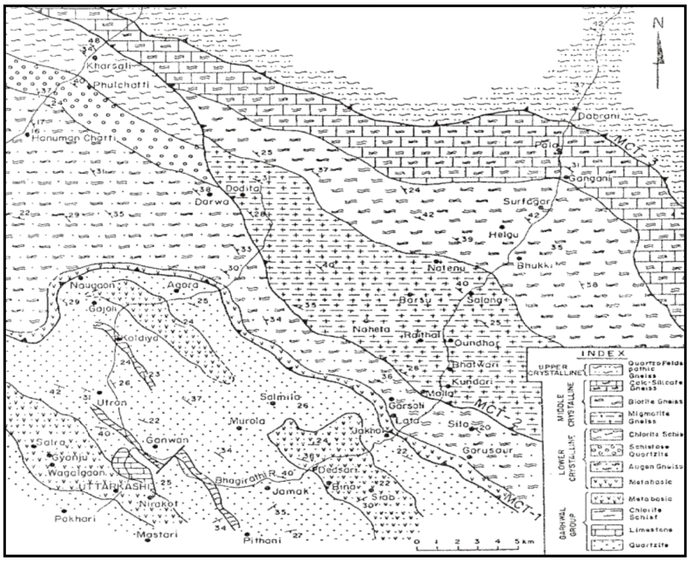

Figure 3-5: Showing the Geology of the Study Area [After (Purohit et al., 1990)**]**

Middle Crystallines is sandwitched between lower and upper crystallines are varying types of migmatites such as gneissic and banded migmatites and Biotite gneisses with Augen gneiss, mica schist and amphibolites etc. Finally northern most *Upper Crystallines* characterized by phylonite schist with medium to high grade of metamorphism as evidence by the presence of kyanite schist, garnetiferous mica schist and Biotite gneiss (Agrwal and Kumar, 1973; Purohit et al., 1990; Valdiya, 1980).

3.3.7.4. Stability Problems along Bhatwari-Gangnani Road Corridor

In road section considered in the study are mainly compares the slopes which are characterized by rocks and the stability evaluation was studied previously by (Chakraborty and Anbalagan, 2008). Where landslides were characterized by transported materials such as debris and rock falls. But the major slope failures in rock mass are governed by geological discontinuities and movement occurs along the surfaces formed by one or several sets of discontinuities.

3.4. Landslides in the Study Area

In this present study the term "landslide" is used to include various types of slope failures on natural and man-modified slopes. The major road corridor (NH 108) is predominantly occupied with various large and small landslides. Most of the landslides in this corridor are generally occurred by anthropogenic activity in nature. Construction and widening of the road along the steep hill slopes are the main cause of the slope instability. The slope failures observed in the Bhagirathi river valley along the road section, involves rock and debris which demonstrated a variety of movements like slide, fall, toe erosion and some where slumps. However, the majority of landslides observed were noted to be rock falls, rock slides and debris slide. While, most of them originate in cut slopes, some of them starts from steep colluvial slopes and all others are originate in weathered bedrock with several joint sets. Some of the landslides represent also complex in nature (i.e. variety of landslides occurred surrounding a particular region).

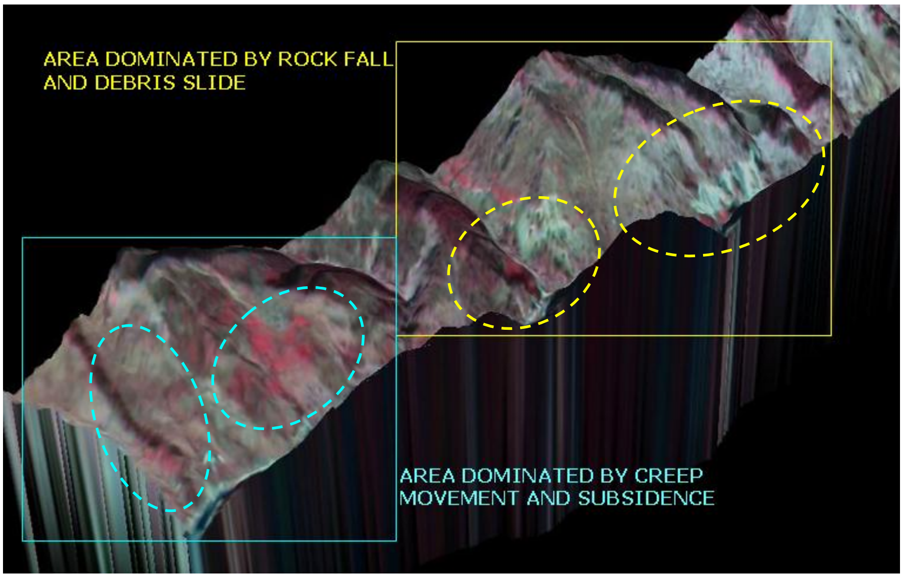

Figure 3-6: Merged Cartosat-I & Liss-IV Image draped over Cartosat DEM

After the detailed survey in field, it has observed that the landslides occurring in the northern part of the study area generally are Rock falls, Rock slides and Debris slides along the steep slopes whereas in the southern part of the study area shows the slow creep process and toe erosion, which leads the land subsidence of the road section. In a road stretch of 12 km length, around 42 landslide events has been recognized during the field survey. The major and prominent landslides which hit the road section have been discussed as follow:

BRO Km Location: 55.0 State: Active
Type: Debris slide along Bhatwari Nalla

Km Location: 55.85 State: Active
Type: Debris slide (Due to toe cutting)

Km Location: 60.0 State: Active
Type: Debris Flow near Thrang

Km Location: 68.15 State: Active
Type: Debris slide (Partially damaged school)

Figure 3-7: Major Landslide Locations in the Study Area

The first landslide event in the study area is observed at Kilo meter 55.0 (Location mark by BRO, India) near upper region of a Nalla (Stream in English) at Bhatwari, which is a fresh debris slide reported on August, 2008 by BRO. Then next major and frequently observed landslide is found at Kilometer 55.85 near Bhatwari Tehsil office. The national highway was totally damaged and subsided to Bhagirathi River due to toe cutting. The same place suffered the subsidence many times from 2006 to till August 2008 and still it is in active state.

Near Pala and Barsu, fresh rock slides are reported by BRO from June to August, 2008. After that, there is a major portion found along the road stretch, a continuous zone of old slide which involves both rock slides and debris slides has been found between Kilometer locations 58.0 to 59.5.

By the field survey, a natural slide located near Thrang Nalla (Km location 60.0) is a natural debris flow still in an active state, which is clearly visible in Satellite Imagery and Google Earth.

Lots of new slope failures have been reported after the Tunnel at Thrang in the last rainy season. Due to absence of any other communication like any other road connection or rail network, this Highway becomes the lifeline for this region to join the holy place to the Capital of the State. That is the reason most of the vehicles for Gangotri Pilgrimage got blocked on the way due to the frequent recurrence of the slides in this road corridor.

Apart from the previous records, a new fresh active debris slide is reported at kilometer 61.5 near Sarchnala on 17th July, 2008. In this location several accidents has reported quite frequently. A major landslide event has been found near the Gangnani School at kilometer location 68.15 by the field survey. An active debris slide is reported by BRO frequently in this location. Lastly but not the least, another important slide has been observed near Gangnani Bridge at Kilometer 68.85, famous as Gangnani slide which occurred along the road section with a crown height around 50-60 meters with volume more than 5000 m^3 during the field survey in year 2008.

3.5. Landslide Inventory

The following sources and methods were used for preparing the landslide inventory database:

- A merged satellite image of Cartosat-1 and LISS IV was used for deriving morphometric signatures of landslides.
- Landslide records of the Border Roads Organization (BRO), India, were used as historical records.
- Visual interpretation of aerial photographs in 1:50,000 scale.
- Extensive field verification using a GPS survey of the landslide locations interpreted from satellite images and listed in the records of BRO.
- Interviewing people residing in the area and visiting professionals working in the area was helped to prepare the landslide inventory.

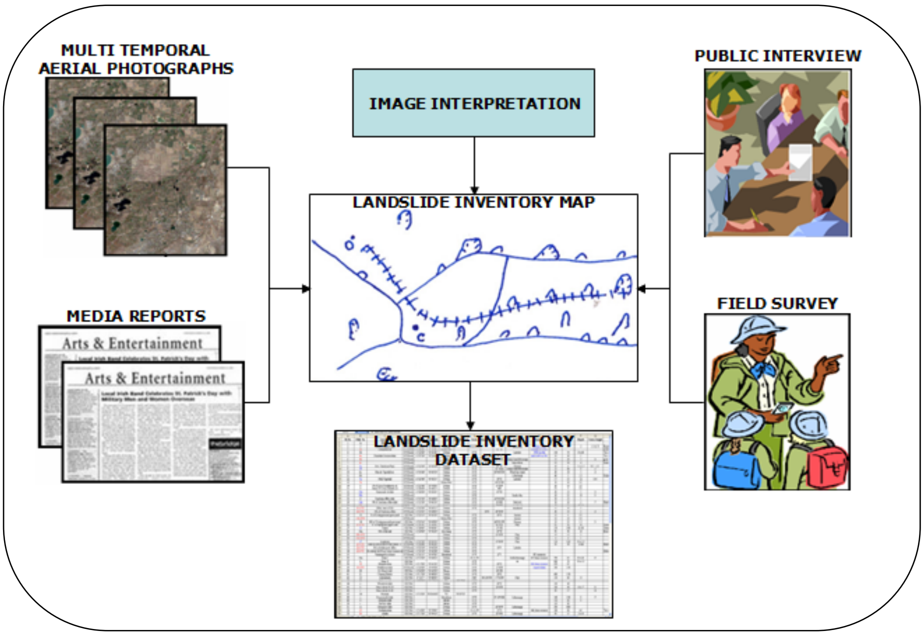

Figure 3-8: The methodological schema for landslide inventory preparation

3.5.1. Landslide Data Collection

The data collection phase involves the preparation of a tabular data format that is needed for the digital landslide inventory generation. As per the requirement of the historic record of landslide events on NH 108, the Border road organization is chosen as the primary organization for collection of the historic records. BRO is the only organization in India, who regularly maintained and updated the records of landslide events in this area. After checking all the records available, finally 26 years of historic records of landslide events have been collected from BRO since 1982 onwards. It was found that all records were association with the kilometer location mark by BRO (Chakraborty, 2008) (provide in Appendix 1B).

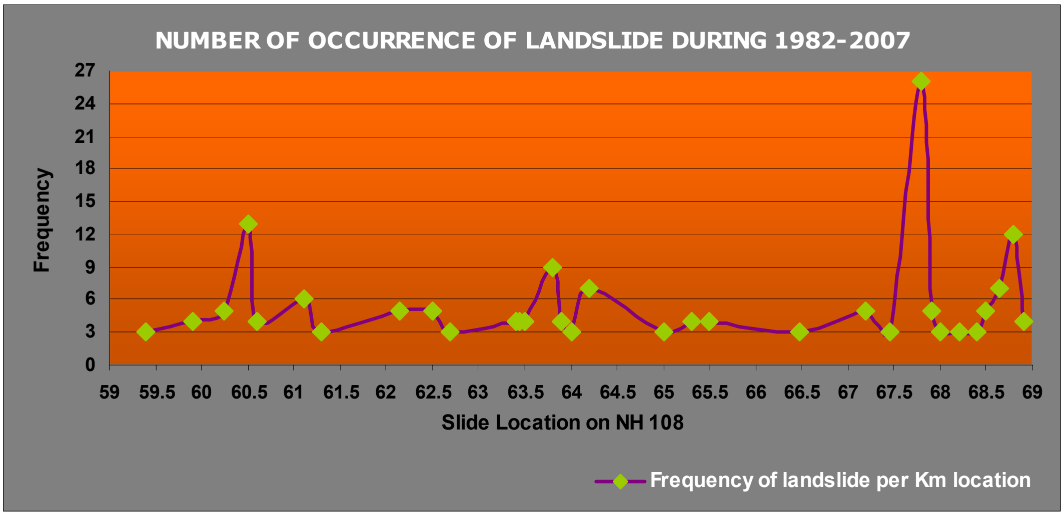

Figure 3-9: Showing the number of failures occurred at each Km location along NH 108

Therefore, it was easy to sort out all the landslide events, which were occurred in the present study area. In present study area, the road stretch extends from 55.5 Km to 69 Km according to BRO location mark. During the field survey and according to BRO, the information about the recent slides occurred per km location from 2007 to 2008 has been collected. The following table shows the frequency of landslide event per km location on NH 108 of recent one year.

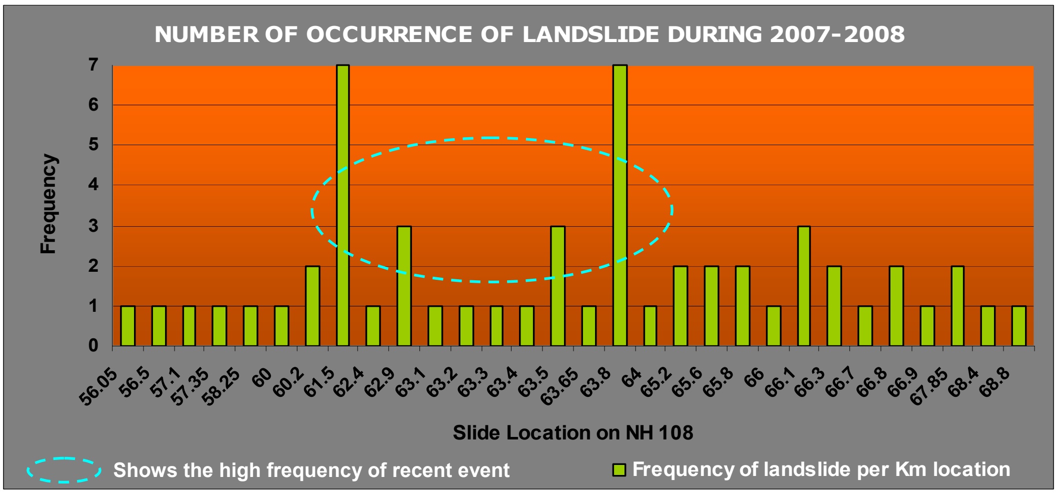

Figure 3-10: Showing the landslide frequency per Km location of recent event along NH 108

3.5.2. Data Preparation

Landslide incidence map was prepared by visual interpretation from merged satellite data such as shape, colour, association etc. The 3m spatial resolution of merged data is very much useful to determine the spectral characteristics of smallest landslide features. The information regarding the old slides from the topographical map is very crucial as some of the old slides are covered by vegetation and it is very difficult to map these on recent satellite data. During the field survey, it was observed that two types of landslide classes prominently visible in the study area. In the study area, the landslides mapped vary from small to large in volume. It is difficult to separate out a single cause for many of the slides as more than one factor seem to cause the slope failures.

(A) Rock Slide near Gangnani bridge **(B) Showing Rock Fall (Shooting Stone Area)**
(C) Slide near the Blasting Zone **(D) Rock Slide due to Road Cutting**

Figure 3-11: Various Landslide Events observed during Field Survey

Based on the activity the landslides are divided into two groups namely active and old slides. For the purpose of applying logistic regression model for susceptibility assessment, all slide events were categorized into one group and the area was classified as slide and no slide (like 1 and 0 respectively). The logistic regression analysis applied in this study is not based on the types of slope failures; rather it considers all landslides together in order to have a good representation of 0 and 1 in the dependent variable on the final result. Sufficient care was taken to avoid the road side failures to exclude from the landslide database. Some field photographs of different landslide events in the study area are shown in figure above. The landslide locations and their extent, finalized after the field work, have been converted to a vector GIS data layer. A total number of 41 landslides have been mapped on the satellite image at 1:10,000 scales of the study area. Each landslides given their corresponding attribute such as location, activity, type of slide, point location, date of activity, volume of the material and area of each polygon etc. (the attribute table is given in Appendix 4). A detailed landslide inventory map with point location mark is shown in the figure below.

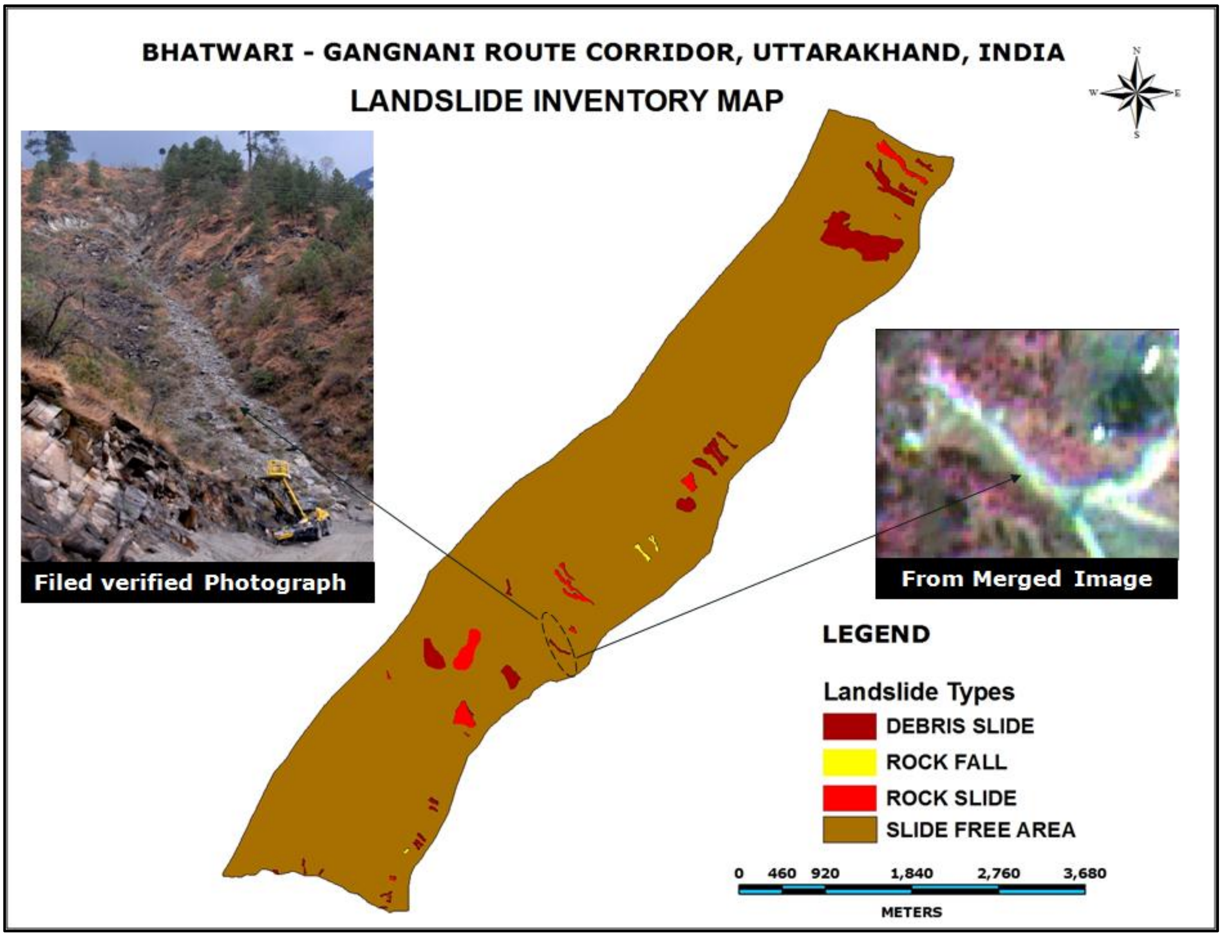

Figure 3-12: Landslide inventory map of the study area

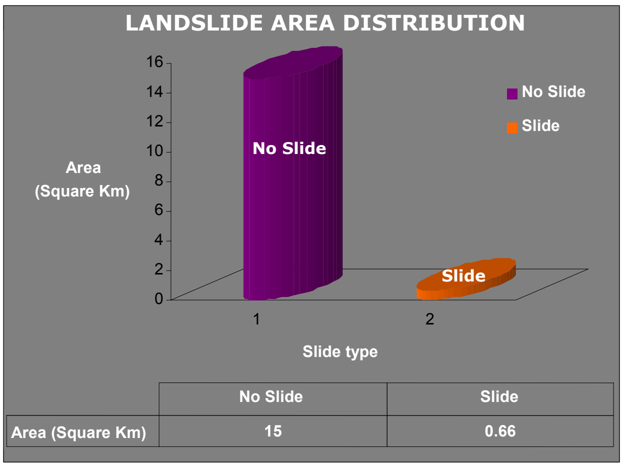

Figure 3-13: Area of landslides in study area

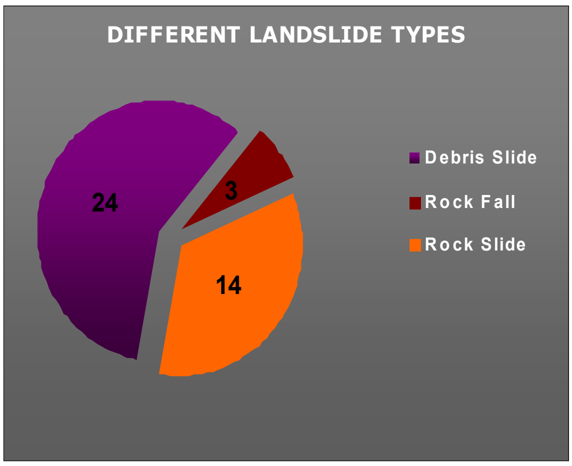

Figure 3-14: Number of slides in different Landslide types

The landslide database has been converted to a raster layer with 20m cell size, in order to use in logistic regression analysis involving pixel based overlay of different input layers. There are 1668 such cells present having landslide with respect to total cells (39119 cells) present in the study area. 4.26 % of the total cells consist with landslide and others are considered as non-landslide cells.

4. Conceptual Framework

4.1. General Overview of the Methodology Adopted

This chapter discusses the methodology adopted for achieving the different objectives of the research. To assess semi quantitative landslide susceptible zones along a major communication route corridor in Bhagirathi valley, India, the following methodology was followed.

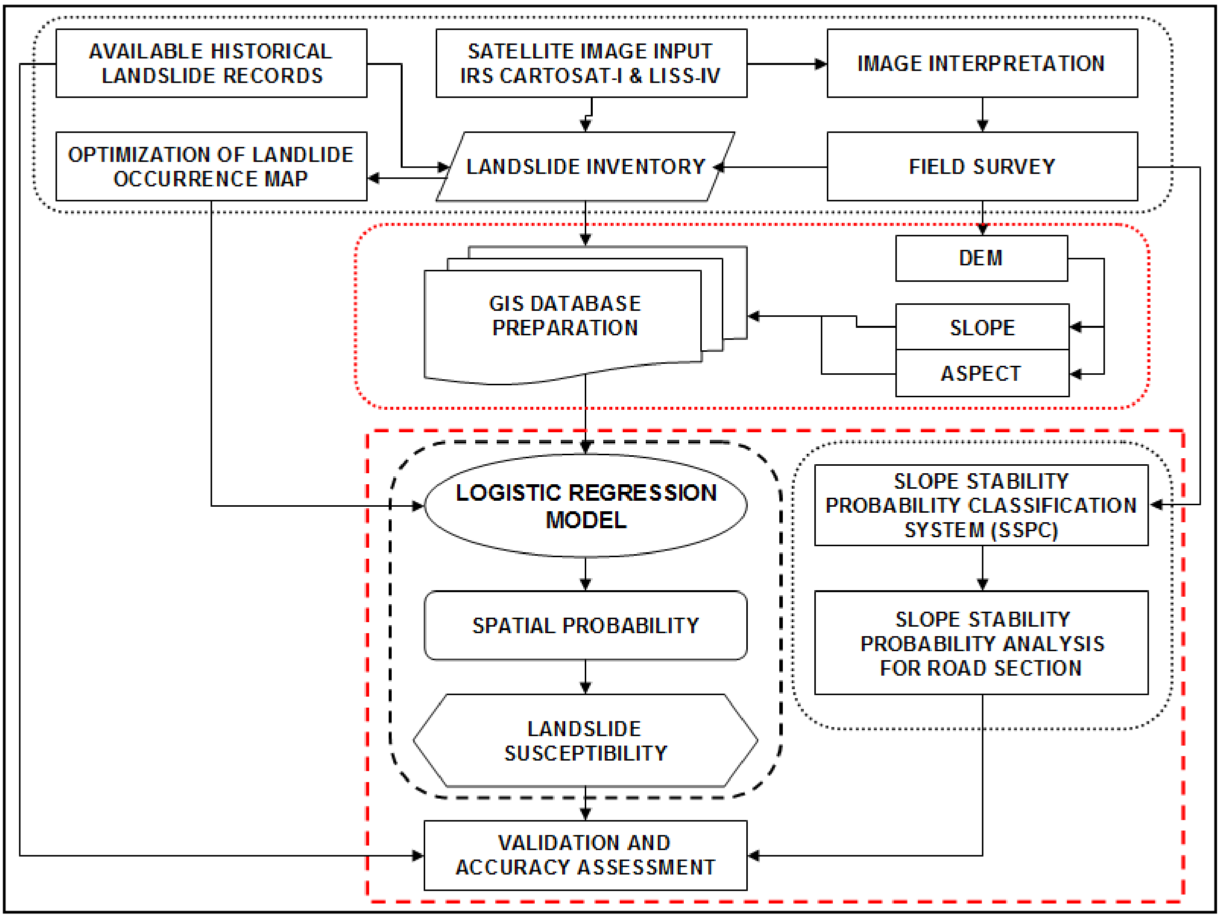

Figure 4-1: Flowchart of the Methodology adopted

The above methodology gives an approach to understand the potential of the earth observation techniques for mapping landslides and assessing the landslide susceptibility using a very well known multivariate statistical model like 'Logistic Regression Model' and a new classification system for slope stability probability assessment like 'SSPC' developed by (Hack, 1998). The methodology is applied in a part of National Highway 108 in Garhwal Himalaya, in Uttarakhand State, India. In the present research, the following approaches have been used to assess the landslide susceptibility.

For a semi quantitative landslide susceptibility assessment, it is essential to prepare a detailed landslide inventory of the study area. An absolute landslide inventory can be prepared by using the historical landslide information and multi-temporal satellite images interpretation with field survey and public interview. For computation of landslide spatial probabilities (susceptibility), it requires generation of high resolution Digital Elevation Model (DEM) which is followed by preparation of derive Morphometric parameters like slope, aspect, relief, etc. It is also necessary to extract the thematic maps using relevant parameters from remotely sensed images using visual and digital interpretation techniques (like landuse/land cover, geological structure, geomorphology, lithology, drainage condition), which is very necessary for this kind of research. Based on these thematic maps, it is proposed to calculate the spatial probability of landslide susceptibility for each class and each pixel, using a well-established multivariate statistical approach from past landslide incidences. In the multivariate statistical approach like Logistic regression, it always gives the relation between dependent and independent variables. At the same time, slope stability probability can be calculated for each slope units in different homogenous conditions for the whole road section in the study area by field survey, because it is necessary to establish the relation between slope stability and Landslide susceptibility for whole region. After establishing the relation, a landslide susceptible zonation map can be prepared. An accuracy assessment is required to analyze the result after preparation of susceptibility map.

4.2. The Model

The models chosen for this present research is statistical and probabilistic based model. They include: Logistic Regression Model (LRM) for landslide susceptibility assessment and Slope Stability Probability Classification (SSPC) system for slope stability assessment. In the following paragraphs, a brief concepts and review of both the model LRM and SSPC is described. Only few important assumptions and mathematical equations, which are relevant to present study, are clarified here.

4.2.1. LRM – Logistic Regression Model

Different multivariate statistical approaches have been used by various researchers all over the world for Landslide hazard zonation mapping, which is mentioned in the literature review chapter. Multiple linear regression, discriminant analysis and general linear regression etc. are the commonly used methods. The nature of the dependent and independent variables play the most important role for selection of the appropriate model.

4.2.1.1. Advantages of Logistic regression Model (LRM)

When the dependent variable is dichotomous in nature,(as in case of landslides), where the presence or absence of landslides in a given unit defines the dichotomous in nature, then discrimant analysis or Logistic regression analysis are very suitable. Actually natural data are usually categorical or continuous in character. That is why Logistic regression is better than discriminant analysis when dealing with such type of dataset. In addition, discriminant analysis requires normally distributed independent variables, which are not always coinciding with in the case of data o natural phenomena like geology, geomorphology and landuse or land cover etc. According to Ohlmacher and Davis (2003), using discriminant analysis, observations are classified into two major groups by their location or area where a landslide has occurred or has not occurred. In addition, each observation consists of a vector of independent variables. When dependent variable is binary in nature and the independent variables are categorical, continuous or a combination of both, Logistic Regression is the suitable multivariate approach (Atkinson and Massari, 1998). Logistic Regression has some similarity with general regression but it is related through an appropriate link function. Just like ordinary regression, LR has straight forward statistical tests, the ability to incorporate non-linear effect and it has a wide variety of diagnostics (Lee, 2005*)*. Since the probability of an event must lie between 0 and 1, it is impractical to model probabilities with the linear regression techniques, because the linear regression model allows the dependent variable to take values greater than 1 or less than 0. LRM is a type of generalised linear model that extends the linear regression model by linking the range of real numbers between 0 and 1 (SPSS, 2007). The advantage of the multiple logistic regression over the linear regression is that with the help of an appropriate link function, the requirement of continuous or numerical nature of the variables has been suppressed (Suzen, 2002). Another advantage is that the predicted value can be thought of as probability as it is constrained to fall between 0 and 1.

4.2.1.2. Concepts of LRM

In this research, the attempt to relate a set of independent variables like the controlling factors of landslides to a dependent variable (Landslide in this case) generates a multivariate problem. In order to analyse such problems, some mathematical model is used, which deals with the approach that can be used to describe the relationship of several independent variables to a dichotomous dependent variable, such as landslide (0 and 1).

LRM is based on the logistic function f (z) which is defined as:

$$f(z)=\frac{1}{1+e^{-z}}$$ ***[1] General logistic function***

Where; z varies from $-\infty$ to $+\infty$.

The logistic regression curve is given in the figure below.

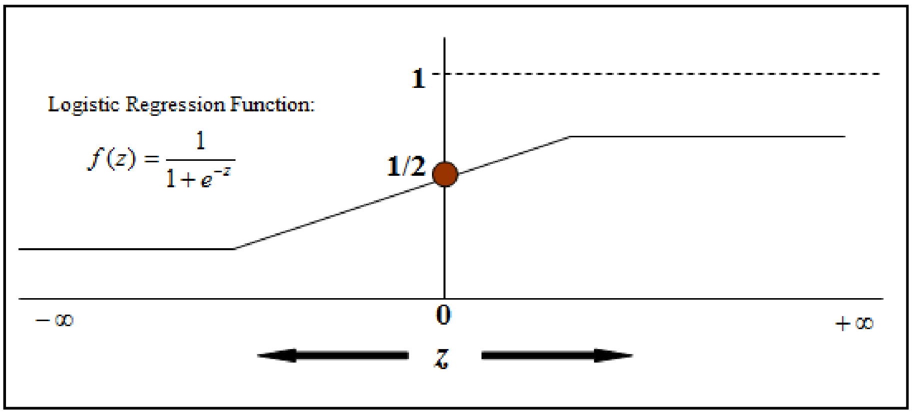

Figure 4-2: Logistic regression function curve [Source: (Kleinbaum, 1994)]

In this above figure, it is clearly shows that if z value varies from $-\infty$ to $+\infty$, and $f(z)$ will change from 0 to 1. This characteristic feature of logistic function makes logistic regression model is accepted world over as it can be used to describe the probability value, which is a number from 0 to 1. Another distinctiveness of the logistic regression function is its shape, which is an elongated S-shaped curve. This can be related to the probability of slope failure. Initially; when z increases from $-\infty$, $f(z)$ gradually increases, but it is close to zero. As z increases further, value of $f(z)$ abruptly rises and finally when $f(z)$ approaches towards $+\infty$, it moves closer to one. This can be thought of analogous to slope failure scenario, where the contributions from some of the contributions from some of the controlling factors which may be overlap or overshoot the threshold value, the probability of the slope failure also abruptly increases (Kleinbaum, 1994).

To obtain the logistic model from the logistic function (from equation 1), z is written as a linear combination or summation of some constant value, which is the intercept of the model and products of independent variables and their respective coefficients.
Such as:

$$z = \beta_0 + \sum_{i=1}^{n} \beta_i X_i$$ ***[2] Linear combination function***

Where; β_0 is the intercept of the model

X_i is the independent variables

β_i is the corresponding coefficients for each independent variables

And i varies from 1 to n for 'n' no. of variables.

Therefore, z is the index that combines the independent variables.
By substituting the equation [2] from equation [1], we can get;

$$f(z) = \frac{1}{1 + e^{-(\beta_0 + \sum_{i=1}^{n} \beta_i X_i)}}$$ ***[3] Logistic Regression Model Function***

Finally, the Logistic model for the slope failure can be represented as:

$$\text{P(S= 1} \left| X_1, X_2, \ldots\ldots\ldots\ldots\ldots\ldots X_n \right.) = \frac{1}{1 + e^{-(\beta_0 + \sum_{i=1}^{n} \beta_i X_i)}}$$

[4] Function of fitting the LRM to the Dataset

Where; P(S= 1 $\left| X_1, X_2, \ldots\ldots\ldots\ldots\ldots\ldots X_n \right.$) is the probability of a land unit or a cell undergoing slope failure, given the presence of independent variables X_1 to X_n.

The parameters β_0 and β_i are unknown and have to be estimated based on the data of the independent variables and the landslide condition of the pixels, using maximum likelihood method. Another way of expressing the logistic regression model by using the logit form as such:

$$Logit(p_x) = \log(odds) = \log\left(\frac{p_x}{1 - p_x}\right) = \beta_0 + \sum_{i=1}^{n} \beta_i X_i$$ ***[5] LR Function in Logit form***

In LRM, the dependent variable is a Logit, which is natural logarithm of odds.
The expression $\left(\frac{p_x}{1 - p_x}\right)$ refers to the odds of the slope failure for a cell with certain x_i.

Probability, Odds and logit are different ways of expressing the same thing. Logit of the logistic model gives an expression for the logarithm of odds of the slope failure for specific set of x_i.

In LRM, the parameters β_i are the similar to the regression coefficients in an ordinary multiple regression model. However, the interpretations of the values were more important while executing the logistic regression (Hosmer and Lemeshow, 2000). Here the values are used to quantify the landslide probability with contributions from various predictors or geofactors. The LRM tries to estimate β_0 and β_i by the "best fitting" the observations on independent variables xi s for the sample locations for which the status of dependent variable is known as present or absent. Using these estimates, the probability of slope failures for remaining cells are calculated, for the observed values x_i s for all the cells. Although logistic regression finds a best fitting equation just as linear regression does, but the principles on which it works is different in nature. Instead of using least-squared deviations criteria for the best fit, it uses a iterative maximum likelihood method, which maximizes the probability of getting the observed results given the fitted regression coefficients used in the multiple LRM is different from those used in linear model. Actually, the distribution of a dichotomous dependent variable is binomial and it is assumed that the mean of this distribution is related to the independent variables through a logistic distribution function. If the likelihood is maximum, then its logarithm is also maximum and this value when multiplied by -2 is called the negative log likelihood. Using the LRM, the accuracy of the prediction may be well enough. In this present research, SPSS (Version 15) is used for the logistic regression analysis of the sampled dataset for whole the study area quite effectively.

4.2.2. SSPC (Slope Stability Probability Classification) System

In this present research, SSPC has been carried out for assessment the slope stability along the road corridor and it worked very nicely. Actually, SSPC was first developed by Hack in 1996 but later Hack modified the system according to the results of the older one on 1998. This is a new approach towards the rock mass classification. Because it calculates directly the probability of slope stability with use of various rock mass parameters. A brief description about the concepts and the parameters used in this classification system is given below.

Hack (1998) gave the concept of this newly developed classification system as follows:

1. Introducing the principle of *three step classification system* to describe the 'exposure', 'reference' and 'slope' rock mass.
2. The assessment of the slope stability by determining the probability of occurrence of different failure mechanisms instead of single point rating value.
3. Correct (without any ambiguity) and simple procedures for the data collections in the field.

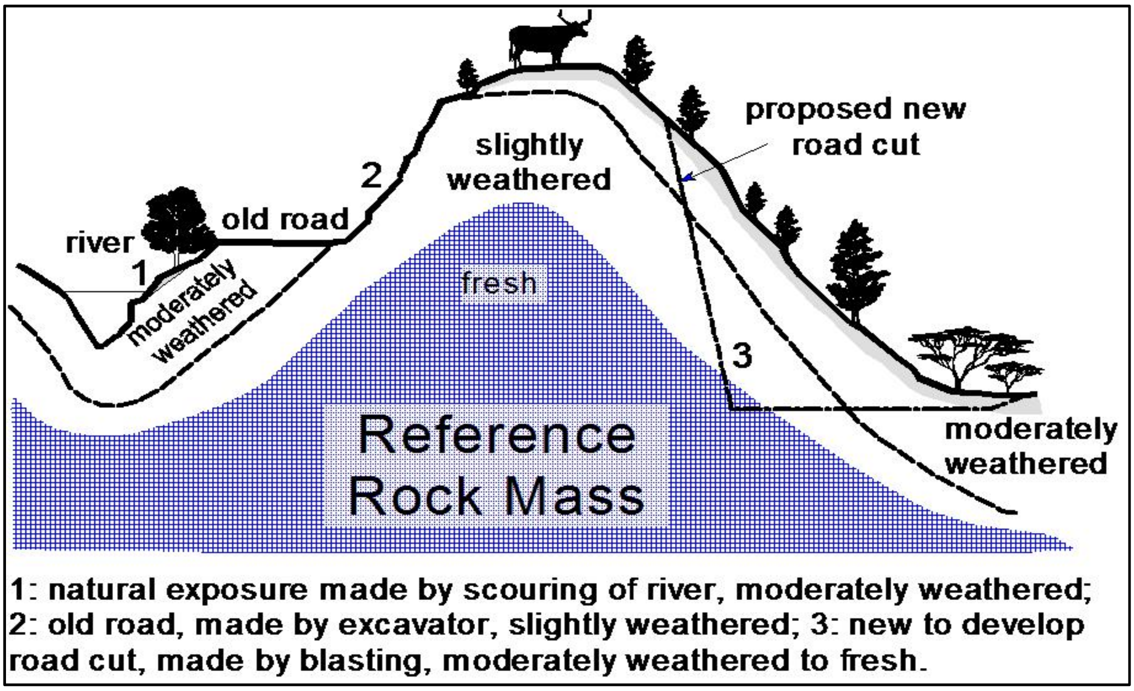

Figure 4-3: Sketch of exposures in rock masses with various degrees of weathering and different types of excavation and showing the concepts of the Reference Rock Mass [Source: (Hack, 1998)**]**

According to Hack (1998): SSPC system works with three major rock masses which is totally different from other rock mass classification system, which is shown in figure 4-3.

1. The rock mass in the exposure: - Which is known as *Exposure Rock Mass (ERM).*
2. The rock mass is an imaginary, unweathered and undisturbed condition prior to excavation: - which is known as *Reference Rock Mass (RRM).*
3. Lastly; The rock mass in which the existing or new slope is to be situated: - which is known as *Slope Rock Mass (SRM).*

These above three steps are used in SSPC for calculating the probability for slope stability. But actual stability assessment is made for the *slope rock mass (SRM).* Because, in that condition actual blasting or manmade excavation is influencing the stability of slopes. This is derived from *reference rock mass* by adjustment of the parameters of the *reference rock mass* with the slope specific parameters. The *existing rock mass* and *slope rock mass* are both same in nature if the existing slope is examined and assuming there is no future weathering in that slope condition. A proposed methodology has been taken to carry out the slope stability assessment, which is given below:

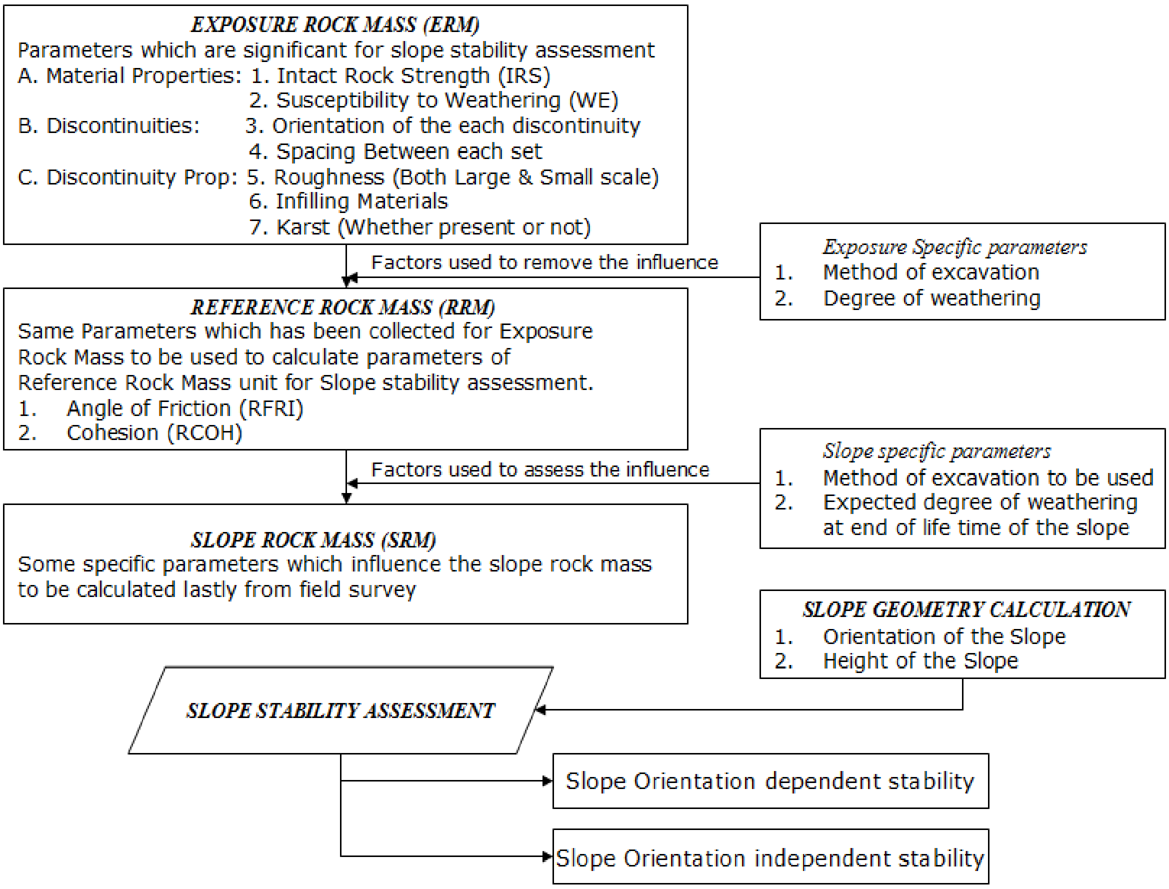

Figure 4-4: Flowchart shows the three step concepts, which works in the SSPC system [Source: Modified Flow Diagram of (Hack, 1998)]

According to the present study, the three step concepts of SSPC system has been worked nicely for calculating the slope stability assessment in the study region. In SSPC system, it always requires to determine all properties of Exposure rock mass parameters, which can be calculated in the field survey.

4.2.2.1. Exposure Rock Mass

1. Intact Rock Strength (IRS): This is the most essential parameter of the exposure rock mass for estimate the slope stability. The intact rock strength can be estimated in the field by standard geological hammer (weight about 1 kg actual). This calculation is totally based on the British Standard (BS5930, 1981).

2. Weathering: The degree of rock mass weathering is like whether the rock mass is fresh or weathered. So in SSPC, weathering condition can be estimated practically in the field and also following the British Standard. It can be translated to a numerical value like unweathered or fresh means value should be 1.00 or weathered then it is divided into different classes.

3. Discontinuity: [Types, Orientation & Spacing]

To access the discontinuity, it is prior to locate visually the sets and types discontinuity (e.g. Bedding, Joints etc.). After checking the types of discontinuity, the characteristics of discontinuity orientation and the spacing in between each set of joints also be calculated. In this study, the SSPC calculation form is used for whole calculation of slope stability assessment. All present discontinuity sets should be calculated thoroughly because determining the sliding and toppling failure probability can be estimated using these parameters.

4. Discontinuity Property: Discontinuity persistence along strike and dip should be calculated for each discontinuity sets but it is not used in SSPC system for calculating final probability. Another very important discontinuity property like roughness can be visually estimated that again divided into two scales, like small scale and large scale. Lastly, infill material is also required to be calculated for each discontinuity unit in terms of the values and presence of Karst formation is quite necessary to access for each discontinuity sets. Only two classes in this parameter like Karst present (0.92) or no Karst (1.00).

5. Susceptibility to Weathering (WE): In SSPC, Susceptibility to weathering is also required for the exposure characterisation. Like if there is no susceptibility to weathering in surrounding exposures which is existed time before, this is used as specific parameters for influencing the exposure rock mass in SSPC system.

Finally, in the field survey, the existing slope condition should be calculated visually which is not required for a new slope stability assessment. However, it can be used as better reference for establishing the reliability of the outcome result of the SSPC. In this criterion, we have to mention whether there is large or small or no problem exists.

4.2.2.2. Reference Rock Mass

In reference rock mass, the parameters for each conditions of discontinuity set (RTC) can be measured in the exposure (TC) corrected with influencing factor like degree of weathering in the exposure (WE). Another major parameter of reference rock mass like reference rock mass cohesion (RCOH) and reference rock mass friction (RFRI) can be calculated using a linear combination of reference intact rock strength (RIRS), reference discontinuity spacing (RSPA) and a parameter describing the weighted condition of the discontinuity (RCD). All the reference rock mass parameters can be calculated from IRS, SPA and CD (which has already been collected from the field) but some correction factors like degree of weathering and method of excavation can be used for better result. All the calculations are described in the form which has used for data collection and data process for assessment of slope stability.

4.2.2.3. Slope Stability

Assessing all results of reference rock mass, finally slope stability can be calculated for a proposed slope in the slope rock mass by using both the results of exposure rock mass and reference rock mass with slope geometry data. In the slope geometry, it has to calculate the slope orientation with slope dip and height of slope. For this case, a new method of excavation for new slope (SME) and degree of weathering of rock mass at the location of slope (SWE) can be noted according to the British Standard.

After incorporating all parameter values, SSPC has calculated two different stability according to orientation like 'slope orientation independent stability' and 'slope orientation dependent stability'.

For both the cases, SSPC uses some basic requirement like material property and discontinuity property (discontinuity spacing and conditions). So for assessment of the slope independent stability, it has to calculate the slope intact rock strength (SIRS), slope spacing condition (SSPA) and slope condition of discontinuity (SCD), which is conceptually a strong approach towards the stability classification. It also carried out the calculation for the slope rock mass friction (SFRI) and slope rock mass cohesion (SCOH), which is prior requirement for slope stability assessment.

If the slope rock mass friction (SFRI) is smaller than the dip of the slope, then the maximum possible height (H_{max}) can be calculated. After this, the ratio of (slope rock mass friction and slope dip) and (maximum height (H_{max}) and natural height of the slope (H_{slope})) also be determined. By plotting the curve between the ratios, we can access the slope stability in independent orientation. Like if 75% probability comes for a slope exposure that means with reality there is no major problems within the particular slope unit and it may be considered as stable. [The total calculation is shown in chapter-6].

For calculating the slope orientation dependent stability, it is quite necessary to determine the apparent discontinuity dip (AP), which can be estimated for each discontinuity set using slope dip amount with slope orientation and the slope condition of discontinuity (STC). Depending upon the orientation of the discontinuity with relation between orientation of slope and the value of slope condition of discontinuity, the probability of the slope can be determined. According to this discontinuity condition, we can calculate the sliding or toppling probability for each discontinuity set, which gives us a new idea about the quantitative assessment of the slope stability probability. For the whole assessment and fieldwork, SSPC form is used which is formulated by Hack in 1998 and are attached as Appendix 4.

5. Database Preparation

As mentioned earlier, various factors responsible for slope failure should be taken into consideration while modelling for landslide susceptibility. The reliability of resultant map will depend on accuracy of maps generated for various inputs that have been considered for modelling. So database preparation is the preliminary and essential step in the susceptibility assessment procedure. Preparation of the various parameters like landuse or land cover, geomorphology, geological structures, drainage and road network etc. by field based mapping is always be costly and time consuming. By use of Remote sensing data, we can optimize both the time and cost factors.

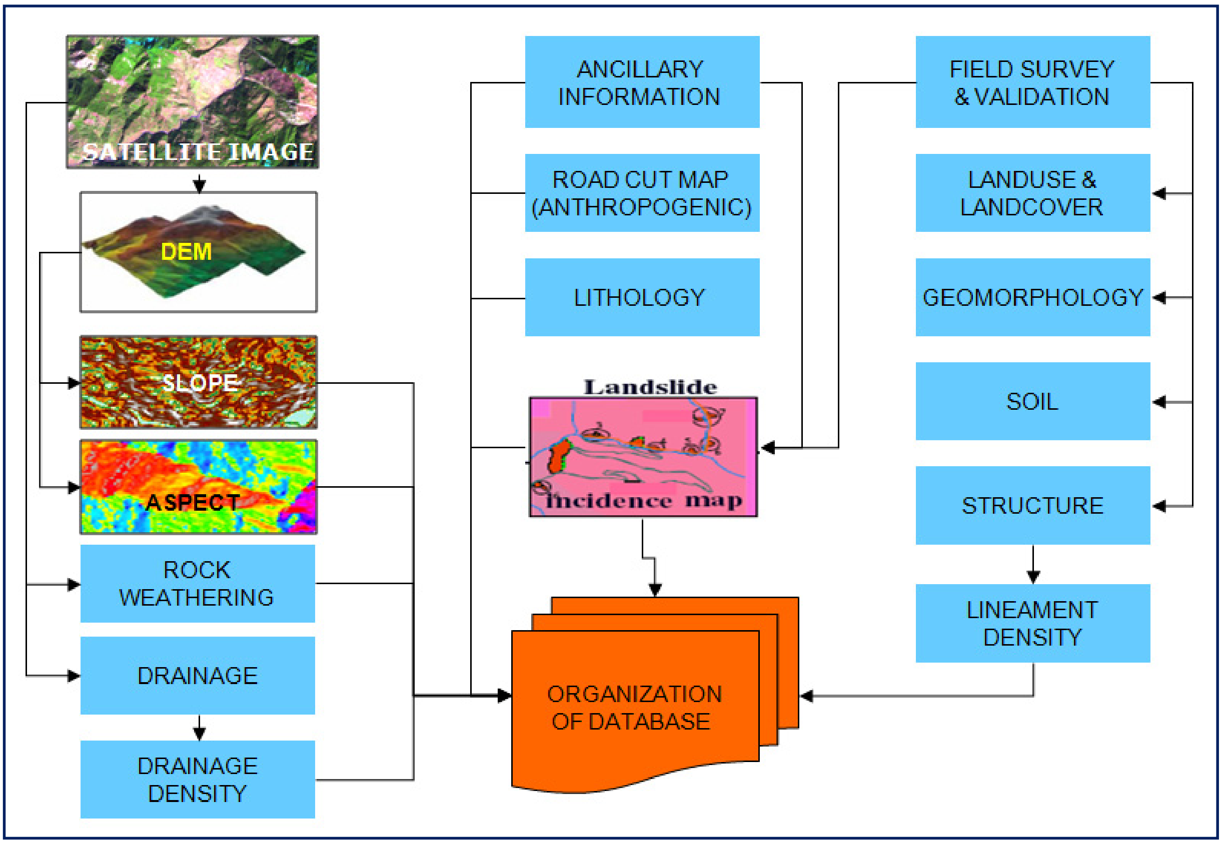

Figure 5-1: Methodology adopted for organization of database

Most importantly, Remote sensing data is an excellent source for preparing the landslide inventory. In the present study, all the required input data layers have been prepared with the help of remote sensing data together with field survey. Since remote sensing data has been used mostly in this present work, a brief description about the important data used is described below.

5.1. Data Used

For the preparation of landslide susceptibility map, remote sensing data and ancillary dataset are collected from various sources. A brief description of the dataset and respective sources are given below in the table.

Table 5-1: Data type and sources

Serial No	**Data**	**Type**	***Source***
1	IRS P5 CARTOSAT-1 PAN (Stereo)	2.5m spatial resolution with Single band	*IIRS (NRSC)*
2	IRS P6 RESOURCESAT-1 LISS IV (MSS)	5.8m Spatial resolution with three Spectral Bands	*IIRS (NRSC)*
3	Google Image	1m Spatial resolution (Approx)	*ITC, The Netherlands*
4	Topographic map No.53J/9 (Restricted)	Contour type Scale 1:50,000	*Survey of India*
5	Historical landslide records	Tabulated format (Excel sheet)	*Border Road Organization (BRO)*
6	Lithology map (Modified)	Vector layer	*IIRS (NRSC)*
7	Soil type and Soil thickness Map	Vector layer	*IIRS (NRSC)*

In order to achieve the objectives of the present study, two different satellite images have been used. High resolution satellite image of IRS Cartosat-1 was used for DEM generation and landslide identification. Google image was also used for identification of landslide bodies. Medium resolution satellite images of IRS LISS IV were taken for mapping the landuse and land cover and geomorphological features. Ground control points (GCPs) were used for image registration purpose. All the images were used for preparing various input parameters for the model. Some detail specification of both the Indian satellite images are given below:

Cartosat-1 & LISS IV

The system of IRS P5 consists of two panchromatic solid state cameras Fore and Aft, which mounted at +26 degrees and -5 degrees with respect to nadir to generate stereoscopic view of the area along the track. It is very much useful for terrain modelling and mapping purpose. The both Fore and Aft bands having same wavelength (0.50 µm to 0.85 µm) with swath width (30km and 27km respectively) and revisit time around 5 days.

The IRS P6 has three sensors onboard. LISS IV is one of them, with three spectral bands, two in the VISIBLE range and one in the NIR range. It gives a nadir resolution of 5.8m with swath width 23.5km and revisit time around 24 days. This sensor has the additional feature of off-nadir viewing capability.

PRODUCT DETAILS (Source: NRSC, ISRO)

Cartosat-1		LISS IV	
Satellite ID	: P5	Satellite ID	: P6
Sensor	: PAF	Sensor	: L-4
Path-Row	: 0529-256	Path-Row	: 202-041
Date, Time	: 08APR07 05:26:23	Date, Time	: 27-MAR-07 05:37:42
Orbit Number	: 10418	Orbit Number	: 17861
Number Of Bands	: 1	Number Of Bands	: 3
Bands Present in Product	: P	Bands Present in Product	: 2 3 4
Scan Lines	: 12000	Scan Lines	: 5010
Pixels	: 12000	Pixels	: 4200
Bytes Per Pixel	: 2	Bytes Per Pixel	: 1
Image Record Length (Bytes)	: 24000	Image Record Length (Bytes)	: 4232

5.2. Hardware & Software

1. ERDAS 9.1 with LPS, ARC GIS 9.1, ARC VIEW 3.2a and ENVI 4.3 are used for image processing and GIS analysis.
2. LPS with terrain editor used for DTM generation.
3. SURFER (Surface Mapping System) version 7 is also used for DTM processing.
4. SPSS-15 used for Statistical analysis of Logistic regression analysis.
5. Endnote 11 and Microsoft Office 2003 were used for thesis writing and presentation.

5.3. Data Pre-processing

Before using the acquired raw satellite data, it is very much necessary to correct the distortions from the images in order to enable correct measurement of the area, precise localization and multi-source data integration (Zhang and Zhang, 2007). The geometric errors can be removed by using the standard correction factors and with the help of precise ground control points (GCPs) during the rectification of the raw dataset. Total 25 well-distributed stable points on both images were selected as ground control points (GCP) for the geometric rectification of Cartosat -1 image in UTM projection with WGS 84 North spheroid and zone 44. The RMSE (Root Mean Square Error) was 0.792 pixel observed after the geometric correction. Image to image rectification technique was applied because it minimizes the residual rectification error (Dai and Khorram, 1998). LISS IV image was rectified by image to image registration with Rectified Cartosat-1 image. After rectification of both the images, Image fusion technique was applied for merging the LISS IV with Cartosat-1. After checking several techniques available for resolution fusion, Brovery transform was found suitable for this condition. Contrast enhancement using linear stretching in histogram has been applied to enhance the image in its high information areas. The standard FCC has been used for visual interpretation to prepare various data layers for model inputs.

5.4. DEM Extraction from Cartosat-1

The digital elevation model was generated by Cartosat-1 stereo pair (Fore and Aft) images. The ground control points (GCP) were collected using Differential GPS (DGPS) survey to refine the orbital parameters. The detail methodology was adopted as follows:

- Identification of ground control points with the help of Cartosat-1 image and Google image (Pre-field Work).
- Collection of GCPs by DGPS survey (in the field).
- Post-processing of DGPS data using Leika's Ski-Pro Software.
- Matching the Collected GCPs in both images by Leika's Photogrammetry Suite (LPS).
- Finally, extraction of DEM and accuracy assessment.

5.4.1. GCP collection and Post Processing of Data

For this study, the fore and aft scenes were studied carefully in the pre field stage for collection of distinct ground control points like sharp bends, road crossing, bridge, house corner, etc. A total number of twenty-four sharp points were marked as GCP in the 7 days field survey. By the help of DGPS, the X, Y, Z coordinates were collected from the field survey. But after the post processing, the DGPS points with help of Ski-Pro, only eighteen points were found correct. From them, ten points were considered as full control points and eight points as vertical control points or check points.

The reference coordinate system was assigned in UTM projection with spheroid and datum as WGS 84. A block file was created in LPS and both fore and aft scenes were added in the frame. The coefficients were directly taken from the .rpc text files provided with Cartosat-1 data. Internal orientation was done to define the pixel coordinate positions of the calibrated points with each image of the block. External orientation was done to define the position and orientation of the perspective centre (Kuthari, 2007). After this, aerial triangulation process was used for processing the data for DEM extraction. Three or four points like Bridge corners were taken as full checkpoints in this process. After all automatic tie points were also generated for uniform distribution of points and the orbital parameters of both fore and aft scenes were refined using ground control points (Shown in figure below).

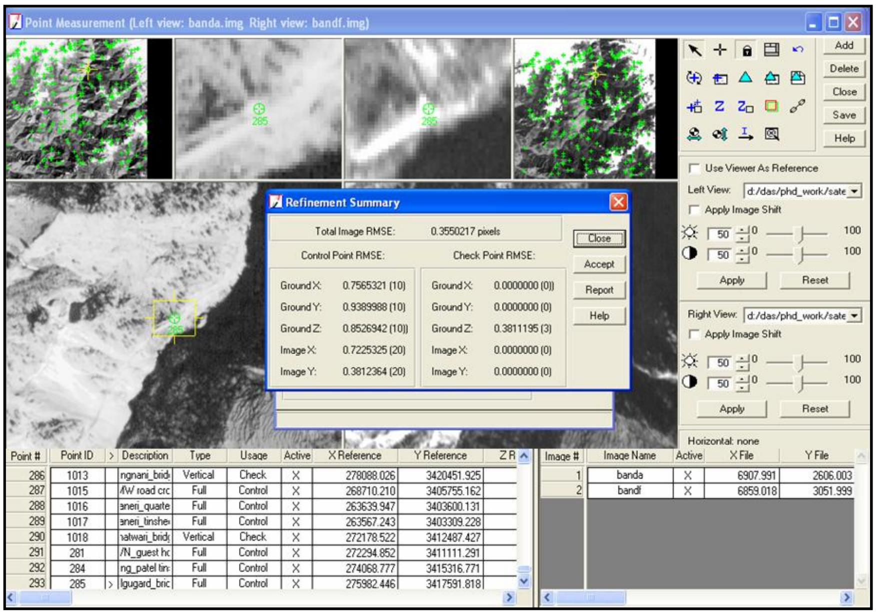

Figure 5-2: Refinement of the GCPs in both images

5.4.2. DEM Generation

The block adjustment technique was applied for aerial triangulation to establish the geometrical relationship between the two scenes, model and the ground. This technique was preferred over normal triangulation routines because with this the errors associated with matching of the GCPs are well distributed and minimized considerably (LPSmanual, 2003). A total RMSE (Root mean square error) of 0.355 pixels was achieved after the above method, which shows the best triangulation result (Shown in the above figure). After all the triangulation processes, digitally matched image pairs were subsequently used in Ortho BASE Pro, to automatically extract the three dimensional terrain models. The raster DEM was then extracted with all information about the extraction report, the accuracy and quality report of the output DEM, which is shown in figure below.

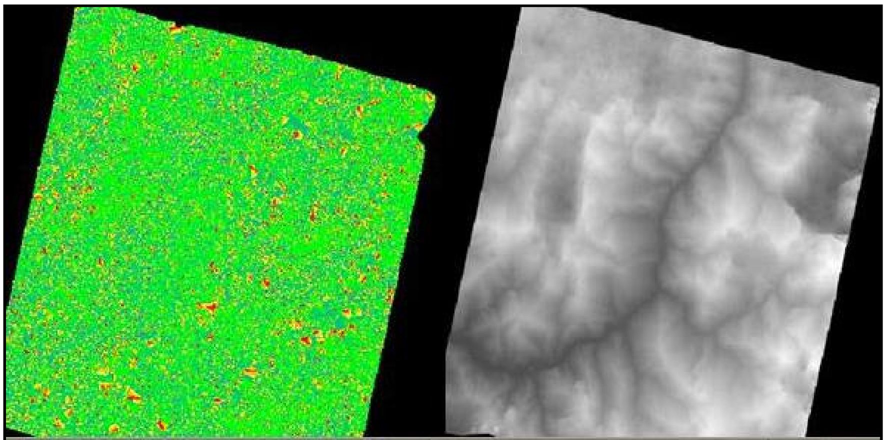

Row	Class Names	Color
1	Excellent	
2	Good	
3	Fair	
4	Isolated	
5	Suspicious	
6	Measured	

Figure 5-3: Point status output image (Quality) after DEM generation

After accuracy assessment of the resultant DEM, three-dimensional interpretations are required. The area of interest is also overlaid on the derived DEM, which is shown in figure below.

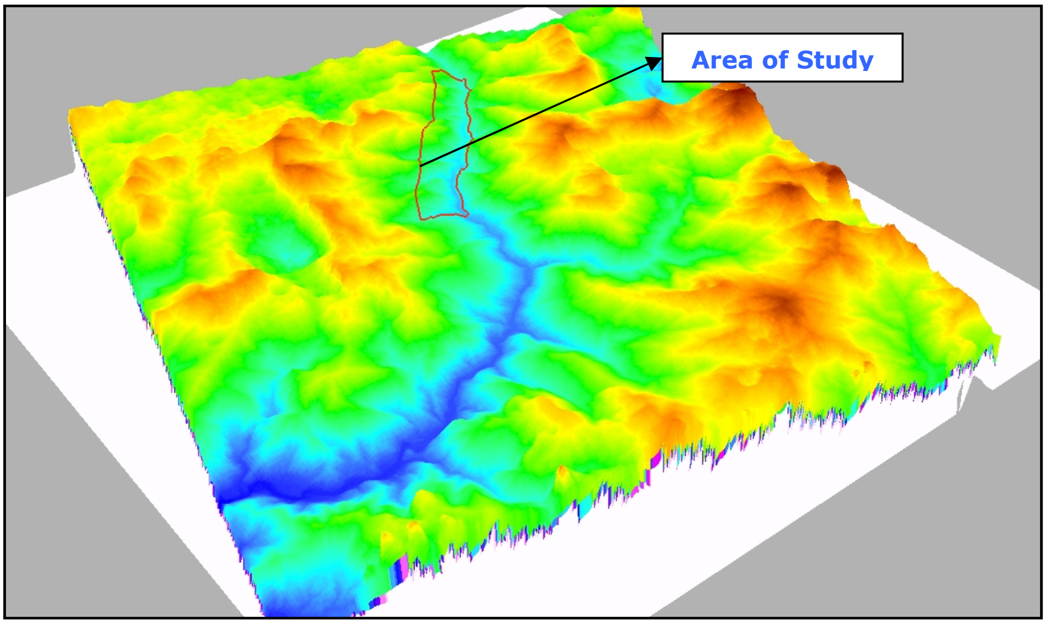

Figure 5-4: Area of study draped on the Resultant DEM derived from Cartosat-1

5.5. Model Parameterization

Being a maximum likelihood model, Multiple Logistic Regression is governed by including more explanatory variables. The main concept behind that the more variables are included, the more complete of the model will be, provided that they play a major role in determining the response variables. However, selecting those explanatory variables with significant contribution is always a challenge (Ayalew and Yamagishi, 2005). Slope and vegetation cover play a vital role in controlling landslides, besides other geo-environmental factors. In tectonically active regions, geological structures and lithology also plays a major role. In the present study, eight landslide influencing geo-environmental factors has been considered. These factors are like geological structure (lineament density), lithology, DEM derivatives (slope and aspect), geomorphology, landuse land cover, drainage density, soil depth, weathering and anthropogenic (road cut) etc. Each factor was divided into possible number of classes that are likely to affect landslide occurrence. Another important aspect for generation of landslide susceptibility map is scale of input data. It is the potential and specific requirement for data input for the analysis. Scale is very important for the consideration of aerial extent of final output, the level of information collected. Analyzing three different scales, a large scale (1:10,000) has been selected finally. The brief description of all factor maps prepared with this scale is given below. Detailed description of landslide density in each class of different factor maps is given in the Appendix 5.

5.5.1. Base Map

First, a base map was prepared from the topographical map (Source: Survey of India) and IRS Satellite (Cartosat-1 & LISS IV) merged data. The location map includes important towns and village locations from topographical map. The point locations are also taken from the topographical map and field observation. The Road corridor is approximately a 12 km stretch from Bhatwari town to Gangnani.

5.5.2. Lithology Map

The lithology map was prepared by comparing with all existing information from NRSC and satellite image interpretation of study area and field verification. In addition, existing geological maps for part of the study area (Prepared by Purohit and Valdiya) were referred to have the broad idea about the geology of the region. The main lithological units were correlated with known stratigraphic succession of the region for universal understanding. The prepared lithology map and percentage of each class is given below.

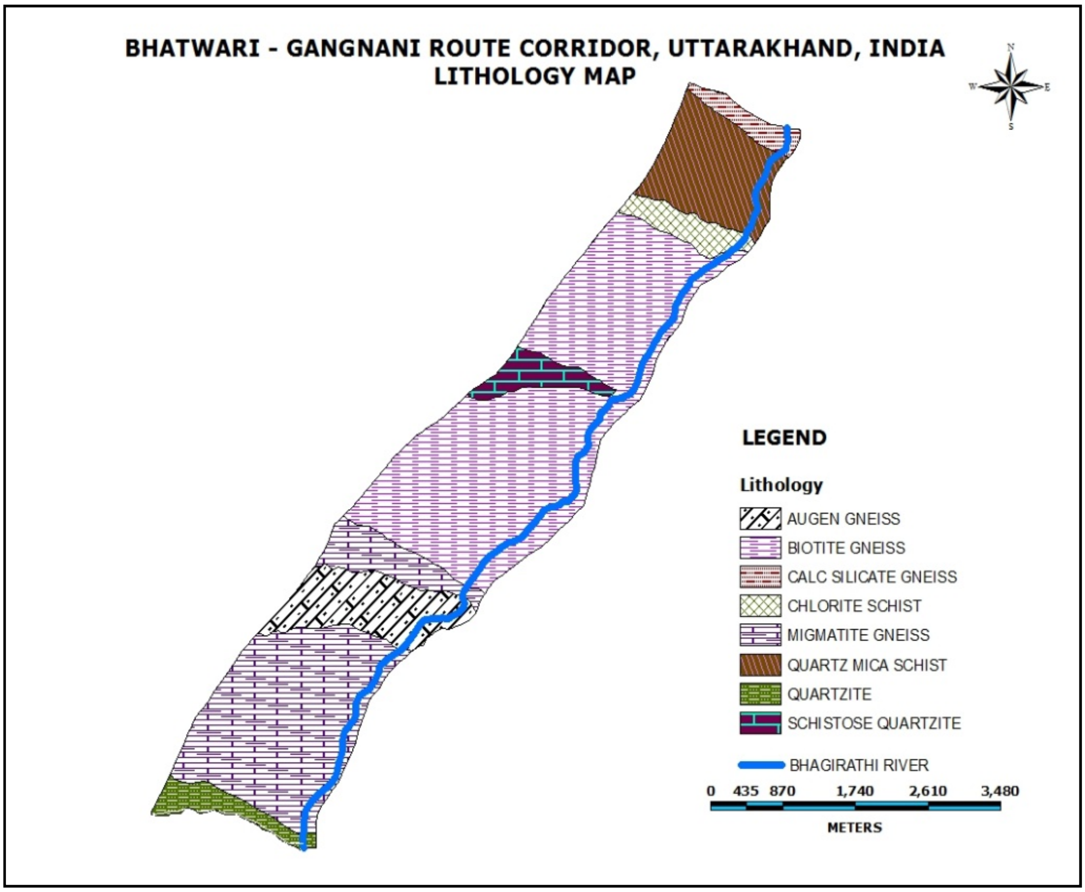

Figure 5-5: Lithology Map of the study area

Different rock types (lithology) behave differently with respect to the occurrence of landslide, because of their variable mineral composition that determines their strength. The stronger rocks give more resistance, hence are less prone to landslide occurrence and vice versa. The rock types found in the study region in the area are quartzite, quartz mica schist, biotite gneiss, calc-silicate gneiss, augen gneiss and migmatites gneiss (Purohit et al., 1990; Valdiya, 1980). The major portion of the area consists of variety of gneisses type (75% of whole area).

5.5.3. DEM derivatives

Topographic parameters such as slope gradient and slope aspect play a crucial role in steep mountainous terrain for influencing mass movement process (Guzzetti et al., 2005). Thus, in present study, both slope and aspect map was derived from IRS Cartosat DEM.

5.5.3.1. Slope Map

Slope is also another important criterion for assessing the slope stability for the road corridor. Slope instability would normally be expected to increase with increase in steepness and slope length. As a result, there is an increase in velocity and volume of surface runoff. The detailed description of slope stability assessment is given in the chapter 6. For the present study, slope (0-76 degree found for whole area) was divided into six classes with 10 degree interval as per slope classification (Kanungo et al., 2006). 25 to 60 degree slope was found in major portion of the region. The classified slope is given below.

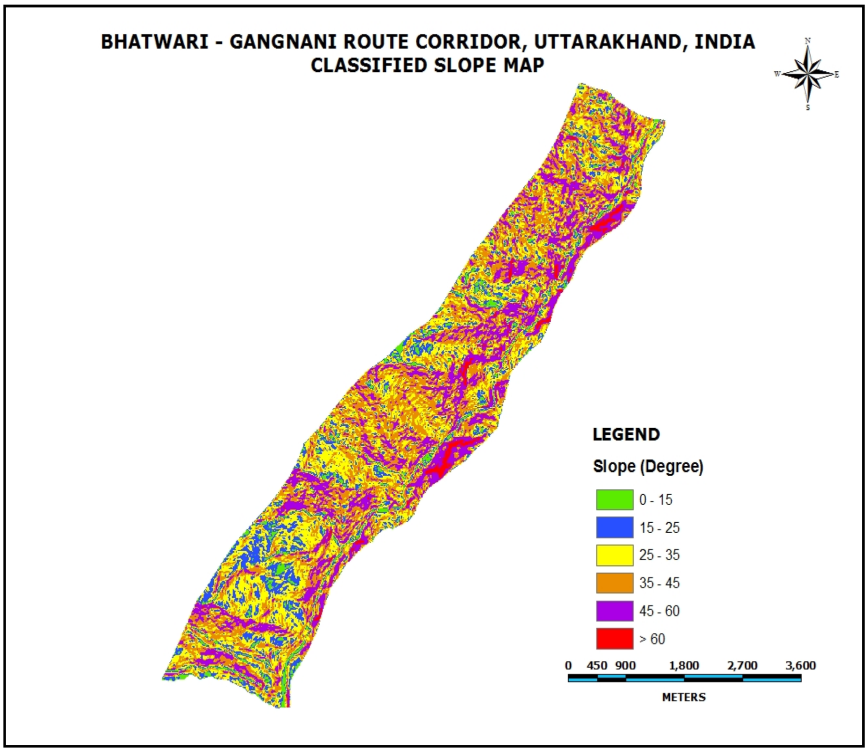

Figure 5-6: Classified slope map of the study area

5.5.3.2. Aspect Map

Aspect also plays a significant role in slope stability assessment in the Himalayan terrain, where most of the south-facing slopes are poorly vegetated, resulting in rapid mass wasting on moderate to steep slopes. In this study, aspect was divided into eight classes. Such as N, NE, E, SE, S, SW and NW (Kanungo et al., 2006). The classified aspect map is given below.

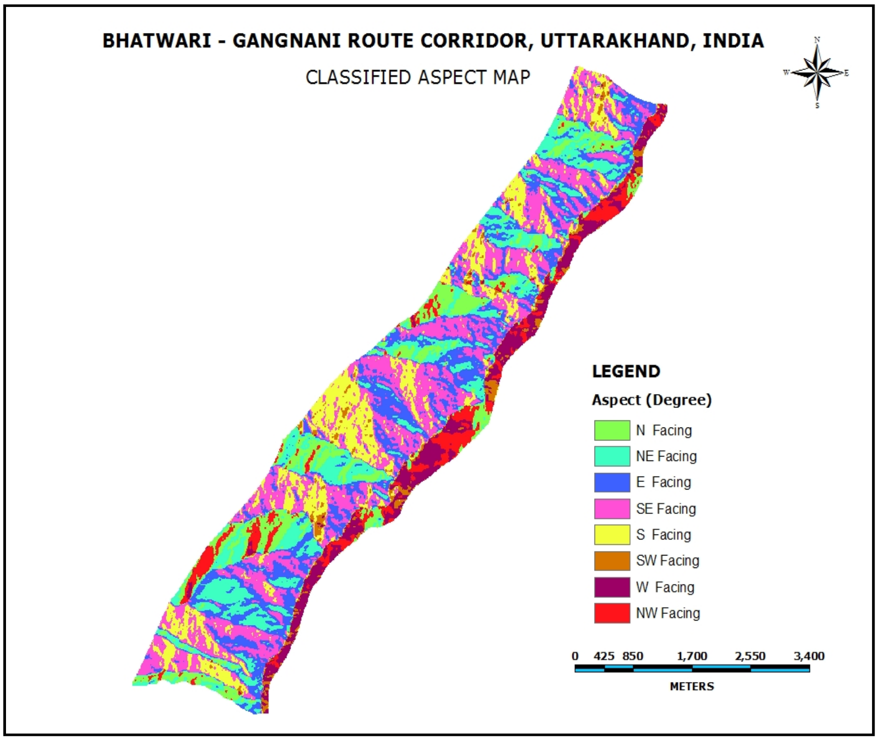

Figure 5-7: Classified aspect map of the study area

5.5.4. Geological Structure / Lineament & Lineament Density Map

Lineaments, including linear geological structures, contribute significantly to mass movement processes in hilly terrain. For the purpose of a landslide susceptibility analyses, the density of lineaments are necessary to prepare because they are likely to be affected by the mass movement process around the lineaments (Purohit et al., 1990). It varies depending upon the nature of terrain, nature of study and overall pattern of landslide distribution in particular area. For the present study, lineaments were extracted from the satellite image interpretation and edge enhancement and filtering techniques as well as field verification.

Lineament density map was prepared by generating a grid map of 500m * 500m and superimposing the lineament over the grid map. The density was calculated by the total length of lineament per grid and the value was converted into a point. According to their values, again it was classified into different classes. The lineament map and the classified lineament map are shown below.

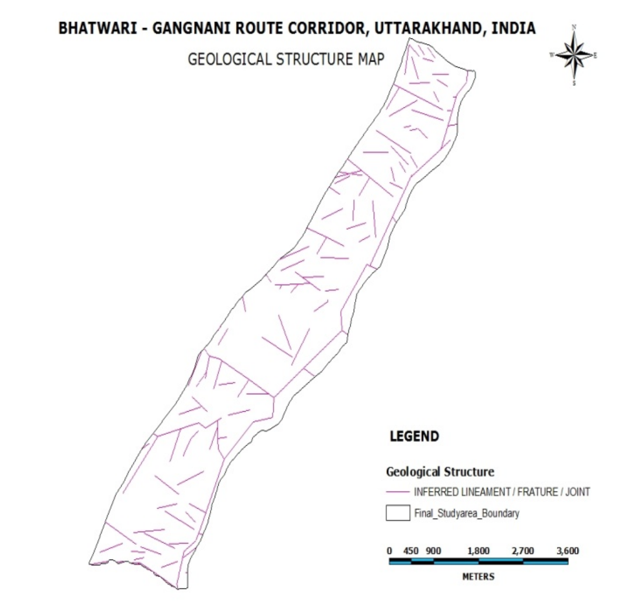

Figure 5-8: Structure map

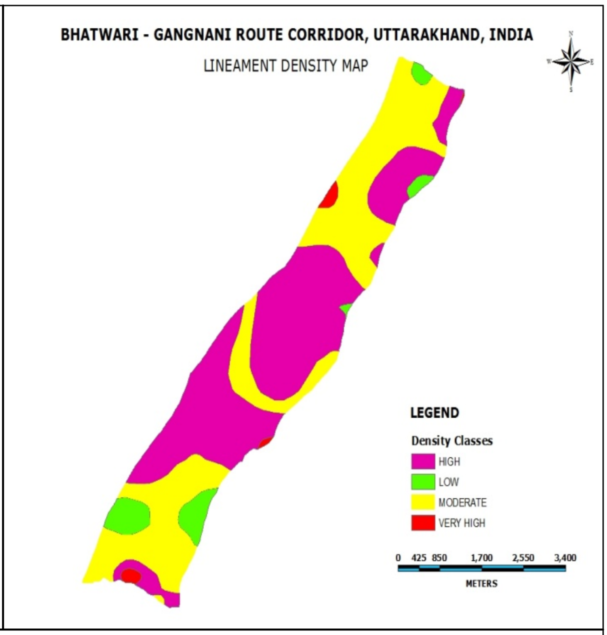

Figure 5-9: Lineament density map

5.5.5. Geomorphology Map

The geomorphological map was prepared by interpreting the earth observation satellite data and comparing with the existing map (NRSC, India). Also integration of geological and topographical maps as well as field observation has been carried out for preparing the map. General geomorphic features in the area include cliffs, rock slopes, major and minor ridges and quaternary deposits along the river valleys. The effect of the high relief and structural control is well reflected by deep gorges and narrow valleys carved by numerous channels.

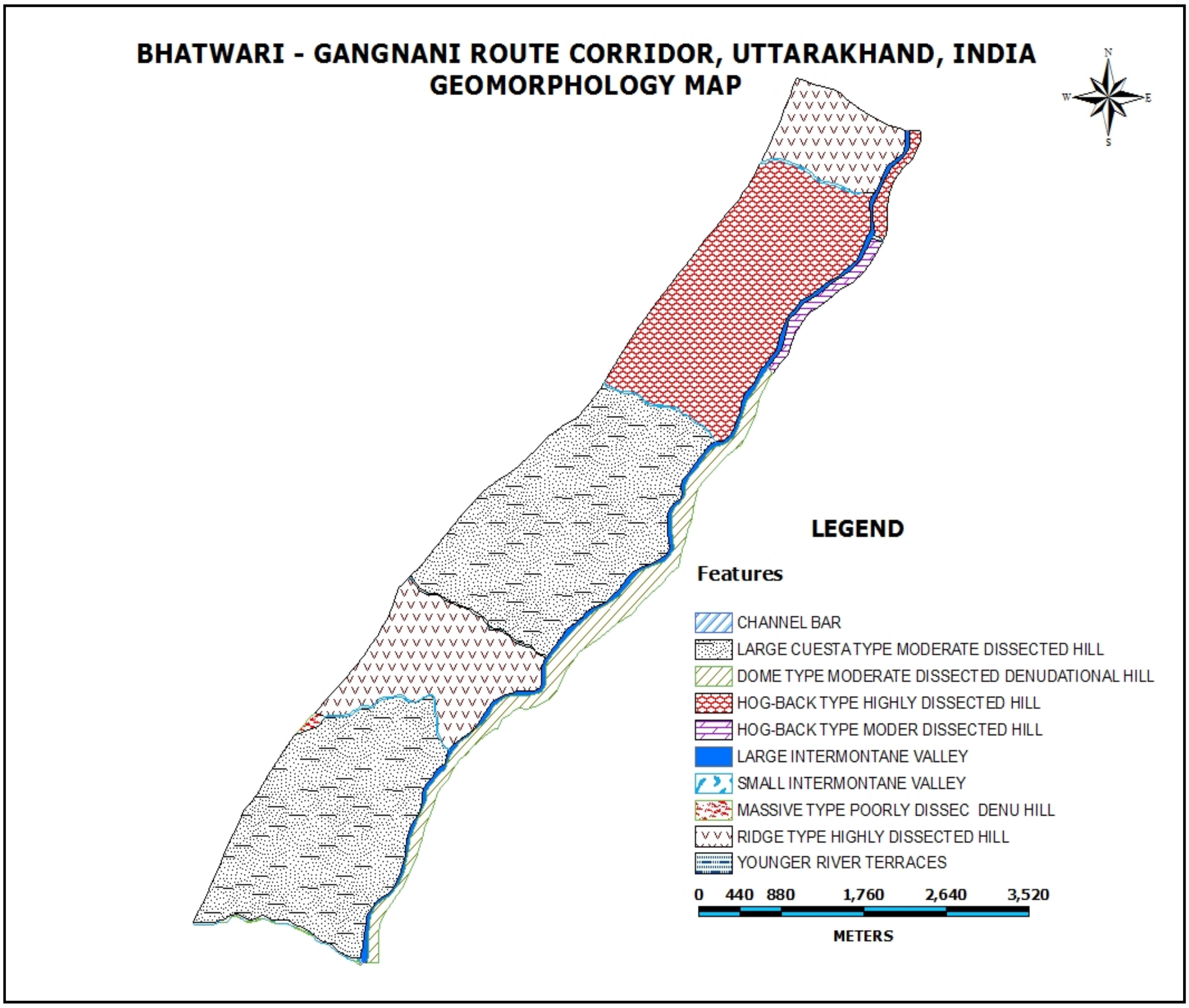

Figure 5-10: Geomorphological map of the study area

` The narrow and confined nature of these valleys towards the downstream in a cross section indicates the continued vertical uplift of the area. Major geomorphic units categorized in the area dome type moderately dissected denudational hills (DTMDDH), massive type poorly dissected denudational hills (MTPDDH), ridge type highly dissected structural hills (RTHDSH), Cuesta type moderately dissected structural hills (CTMDSH), hogback type highly dissected structural hills (HTHDSH), narrow and wide intermonatane valleys. The geomorphological map is shown above.

5.5.6. Landuse / Land cover Map

Land cover plays an important role in Landsliding in hilly terrain. Their relationship can be complex, depending on the nature and type of land cover. Therefore, ground investigation of land cover can be a solution other than the digital classification. Thus, land cover classes were mapped from the satellite images on 1:10,000 scale using visual interpretation method and other auxiliary information, such as pre-existing maps aided by ground checks. Ten dominant land cover classes have been classified in this present study region. The classes are like dense forest, open forest, degraded forest, scrubland, barren land, built-up land, agricultural land, river channel, sand area. The prepared landuse or land cover map is shown below.

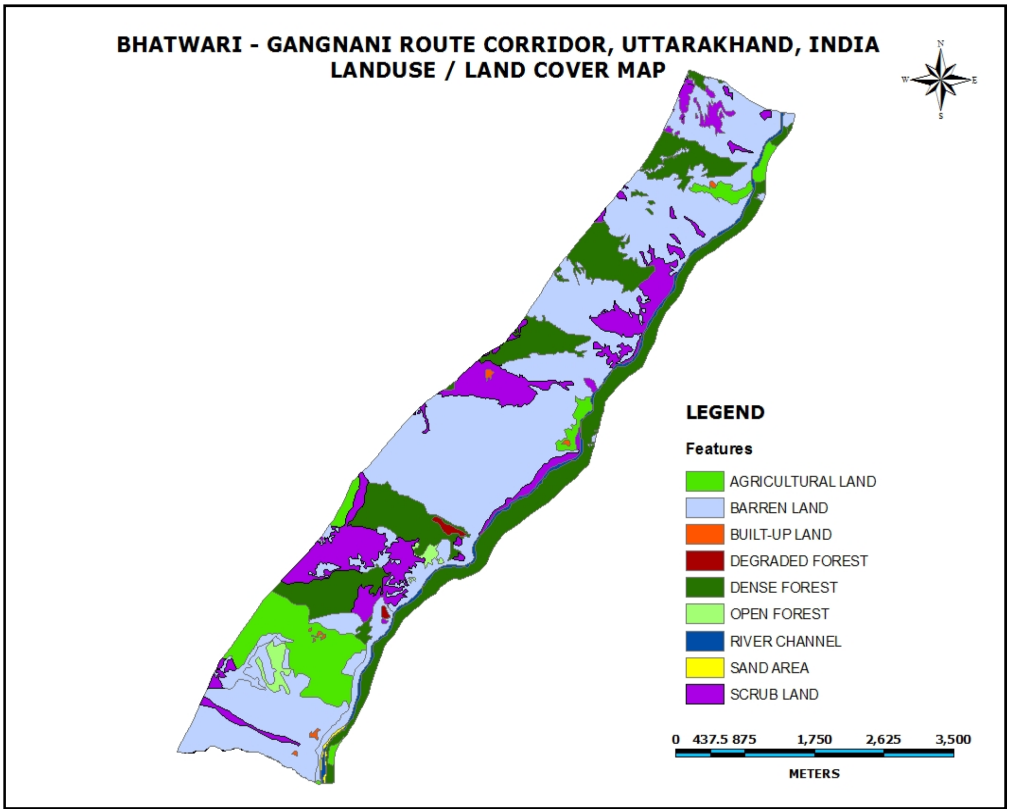

Figure 5-11: Landuse / Land cover map of the study area

5.5.7. Drainage Map and Drainage Density map

The drainage map was prepared by interpreting the satellite images with ancillary information. The main drainage pattern of the area is having dendritic pattern. Up to fifth order drainage has been found in the study area. With this information, a drainage density map was prepared using the density calculation formula (Total length of drainage network per a grid about 500*500 m^2). After calculating the density values, again it was classified into different classes. The final drainage density map is shown below.

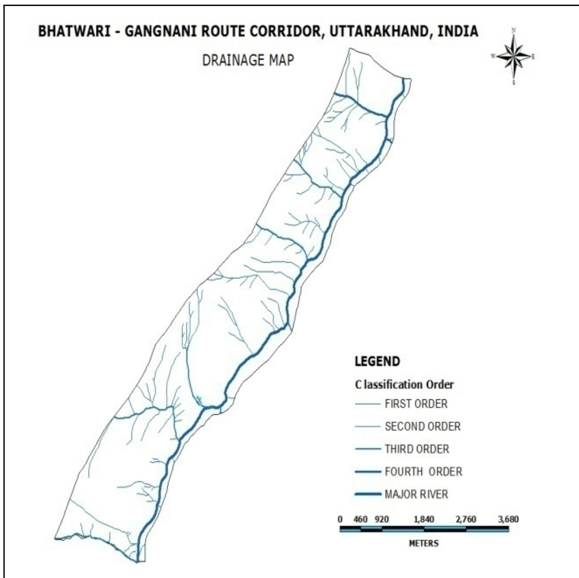

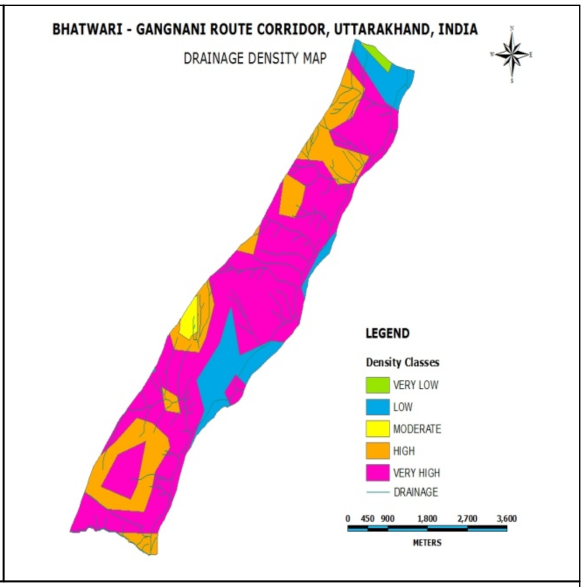

Figure 5-12: Drainage network map

Figure 5-13: Drainage density map

5.5.8. Soil Depth Map

Soil depth plays important role for sliding particularly slumping or circular failures. But in the present study, many landslides were found in areas having shallow and deep soil depth.

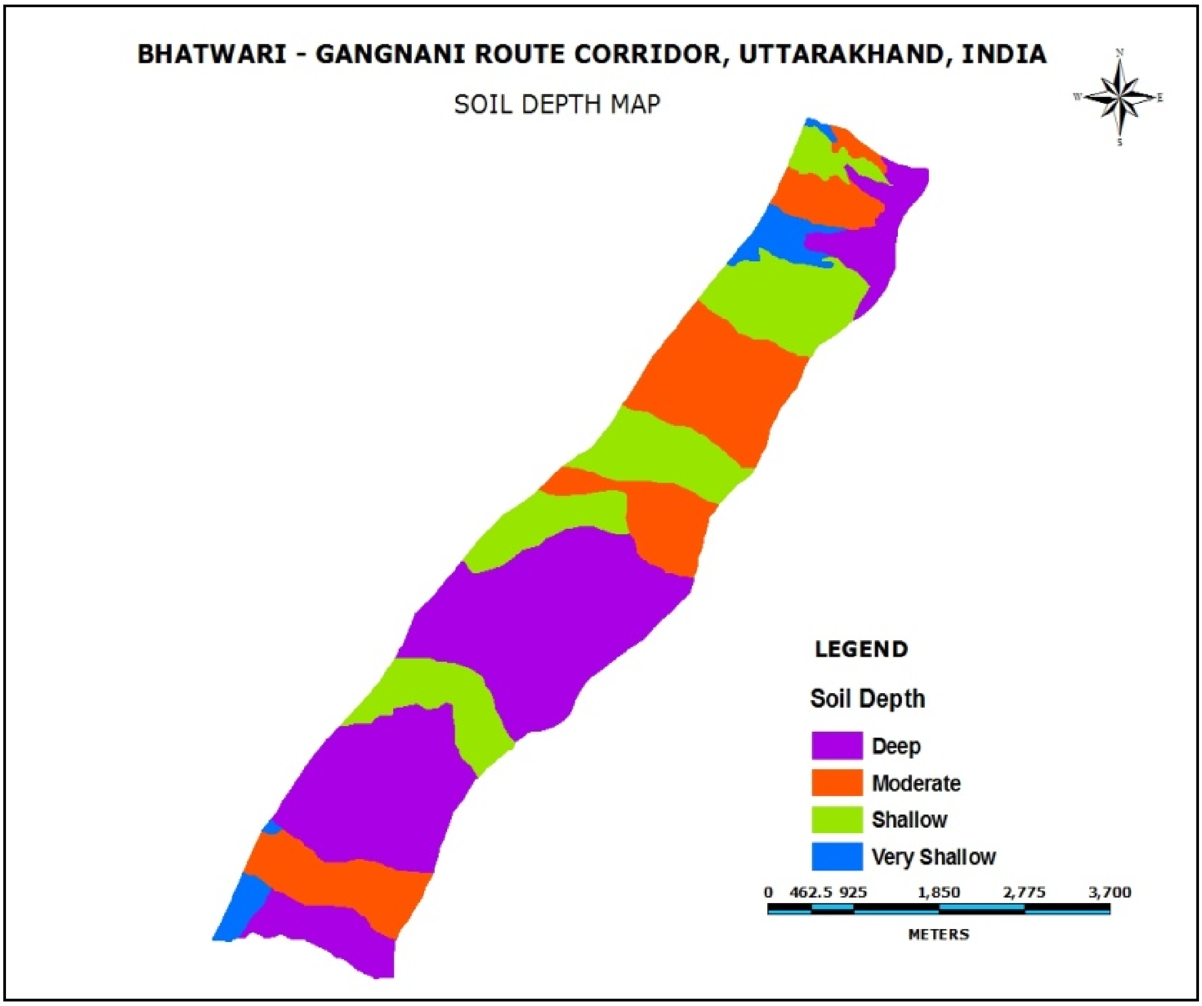

Figure 5-14: Soil depth map of the study area

Four soil depth categories like deep, moderate, shallow and very shallow were derived in the study area in consultation with the broad soil map in 1:250,000 scale available from the leading Indian mapping agency, the **National Bureau of Soil Survey and Landuse Planning**. The map information was also included with additional analysis of high resolution satellite images, and field mapping. This was the only possible and authentic source of information for soil map in this region.

5.5.9. Weathering Map

The weathering map was prepared by referring to the field observation and pre existing map (prepared by NRSC) as well as geology and geomorphological map. For example, rock types like schist and gneiss are expected to more weather than quartzite. By this process, a weathering map was prepared and it was also classified into different classes. The final weathering map is given below.

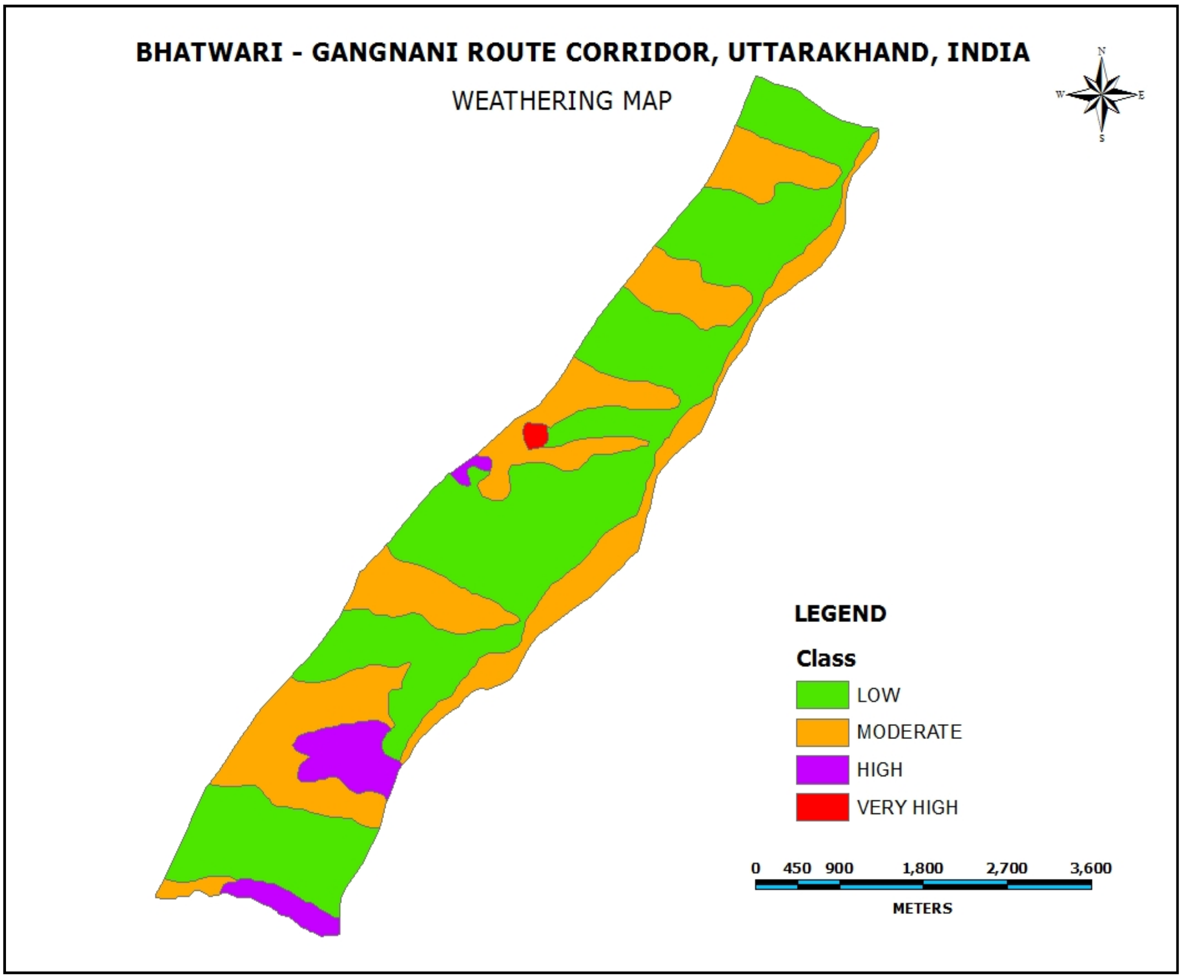

Figure 5-15: Weathering map of the study area

5.5.10.Proximity to Road

Road construction in hilly areas severely alters the slope stability making them prone to slope instability and landslide. The best way to include the effect of a road section in a slope stability study is to make a buffer around them (Ayalew and Yamagishi, 2005). All slope cuttings or road cuttings due to road construction were mapped using satellite data and field investigation. Thus two types of map were prepared like Road buffer map and road / slope cutting map (Anthropogenic map), which is shown below.

5.5.10.1. Road Buffer Map

A road buffer of 50 meters was made around the centre of road that may likely influence the slope failures. This was guided by the fact that slope alteration due to road construction does not go beyond 50 meters on both side of the road. The road buffer map is shown below

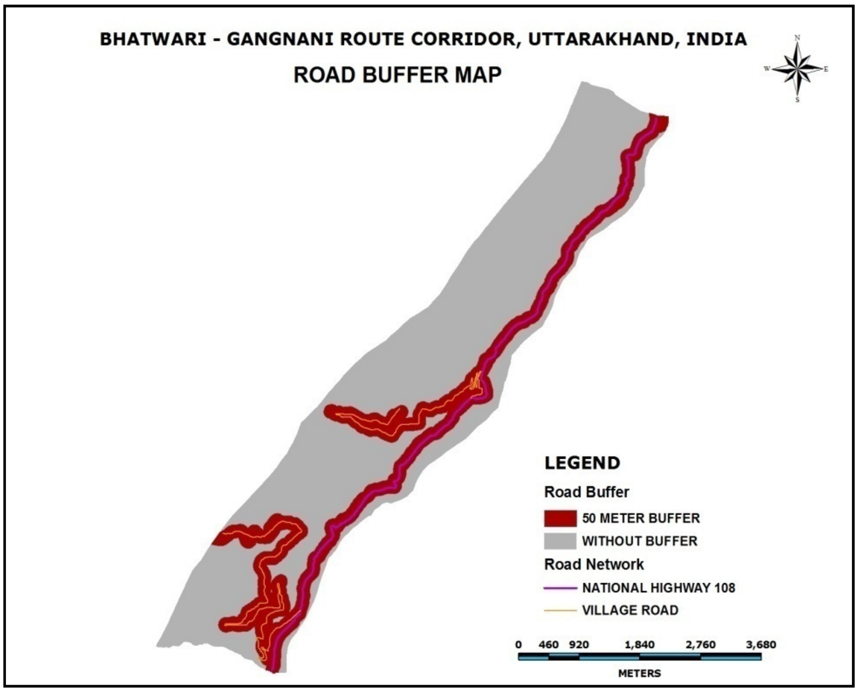

Figure 5-16: Road buffer map

5.5.10.2. Anthropogenic Map (Road/Slope cut map)

This is an important map considering the fact that road construction, mining in hilly areas severely alter the slope stability making them vulnerable to slope instability and Landsliding. Sometimes stable slope causes instability due to weight factors. Therefore, all vulnerable slope cuttings either due to road construction or blasting are mapped as much as possible using EO satellite data and field investigation. The road information from the base map, landslide map, and slope map was crosschecked for finalizing this map. The anthropogenic map is shown below.

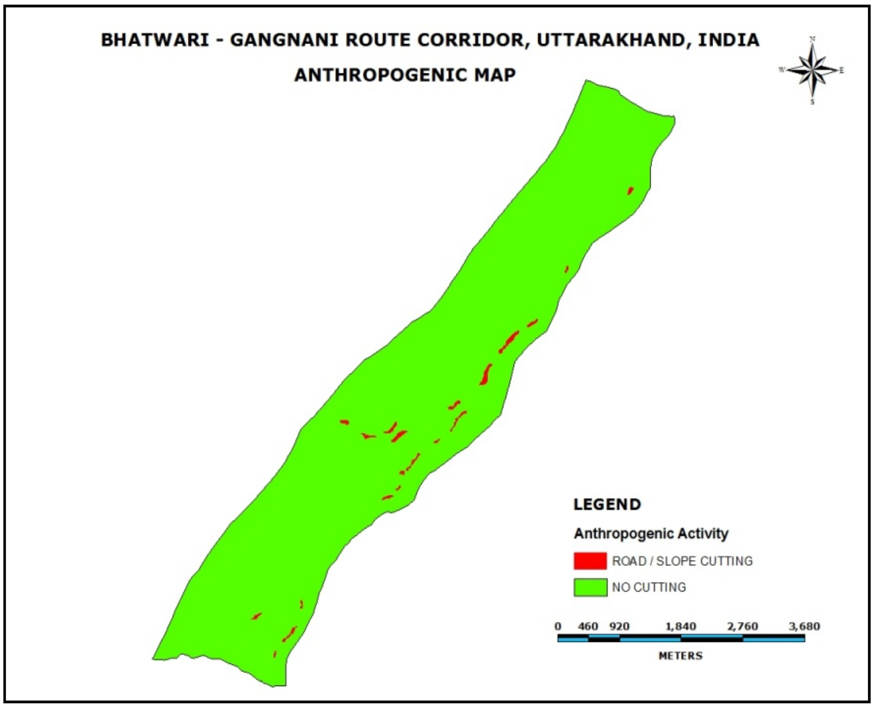

Figure 5-17: Anthropogenic map of the study area

6. Slope Stability Analysis

As described in the chapter on methodology, two types of analysis were carried out: slope stability assessment using SSPC system and landslide susceptibility assessment using logistic regression approach. This chapter describes the results of the Slope Stability Probability Classification (SSPC) system for calculation of slope stability for road sections with side slopes in hard rock.

SSPC system is a field-based approach, which calculates the slope stability probability by two different approaches. The first one is '*Orientation Dependent Stability'* related to the orientation of the discontinuities and the slope unit and the second one is '*Orientation independent Stability'* related to the strength of the rock mass in which the slope occurs, which is independent to the orientation of both the discontinuities and the slope unit (Hack, 1998). As a field based approach, this method is very much useful for validating the output susceptibility map.

6.1. Parameterisation for SSPC System

In this present study, SSPC fitted well to calculate the slope stability probability of each homogenous rock mass along the road corridor. Preparing homogenous section from a satellite image is particularly impossible. Therefore, the homogenous sections or rock masses were observed from the field itself. For calculating the slope stability for whole 12 km road stretch, around 32 homogenous sections were marked for observation. The location map depicting all the data collection points to establish the SSPC system is shown below.

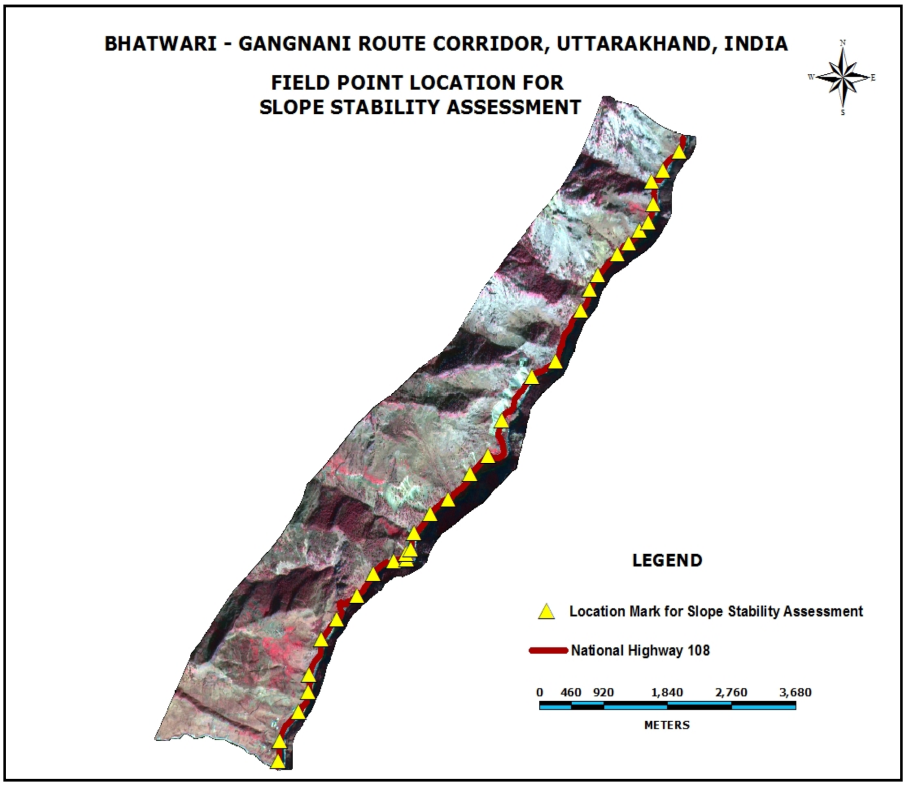

Figure 6-1: Shows the field location for slope stability assessment

As mentioned in chapter 4, before calculating the slope stability assessment, it is essential to calculate the rock mass parameters. The rock mass properties like intact rock strength, discontinuity spacing and condition, are determined in the field itself. SSPC system considers three rock masses which were described above in chapter 4. Therefore, the rock mass strength and degree of weathering condition was calculated from the field. The orientation of discontinuities in combination with the shear strength along all the discontinuities determines the possibility of movement along the discontinuities. It has a major influence on the mechanical behaviour of rock mass. First it requires checking the possible discontinuities present in each rock mass and according to each rock mass, the orientation of discontinuity like dip direction and dip amount should be calculated. For 32 locations, the orientation of each discontinuity sets were calculated in the field. One of the filed data collection result sheet is given below.

Table 6-1: Showing the rock mass parameters collected from field

SSPC ROCK MASS CLASSIFICATION					
LOCATION: BHATWARI BRIDGE (57.1) EXPOSURE-1 DATE: 27/09/2008 TIME: 10:20 hrs					
Exposure specific parameters and properties:					
Method of Excavation:	no damage			factor:	1.00
Degree of weathering:	slightly			factor:	0.95
Intact rock strength:					100 M Pa
DISCONTINUITIES ORIENTATION, SPACING AND CONDITION					
Type	**Ba1**	**J2**	**J3**	**J4**	**J5**
Dip direction	65	212	30	132	125
Dip	35	65	67	75	26
Spacing (m)	0.500	0.250	1.000	0.500	0.500
Persistence // dip	>5	>5	>5	1	0.5
Persistence // strike	>3	>25	>25	0.5	0.4
Rl	0.80	0.75	0.80	0.80	0.95
Rs	0.65	0.75	0.80	0.75	0.80
Im	1.00	0.55	0.55	0.85	0.55
Ka	1.00	1.00	1.00	1.00	1.00

The above sheet shows, the collection of data for each discontinuity sets present in the rock mass. Based on the block size and block formation by visual assessment, the spacing and persistence of discontinuities were calculated. Shear strength of each discontinuity is determined with visual and roughness established by touch. The shear strength in terms of roughness in large scale *(Rl)* can be determined by visually and the small scale roughness *(Rs)* factors are a combination of visible roughness of an area of about 20x20 cm^2 and tactile (roughness established by touch). The small-scale roughness like stepped, undulating, planar can be calculated with reference to the given form. The tactile roughness was calculated by touch like rough, smooth and polished. . The reference form is given below.

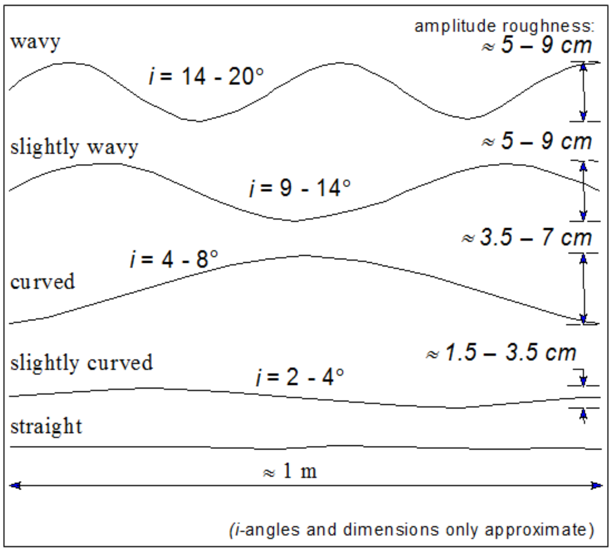

Figure 6-2: Large scale Roughness Profile [Source: (Hack, 1998)]

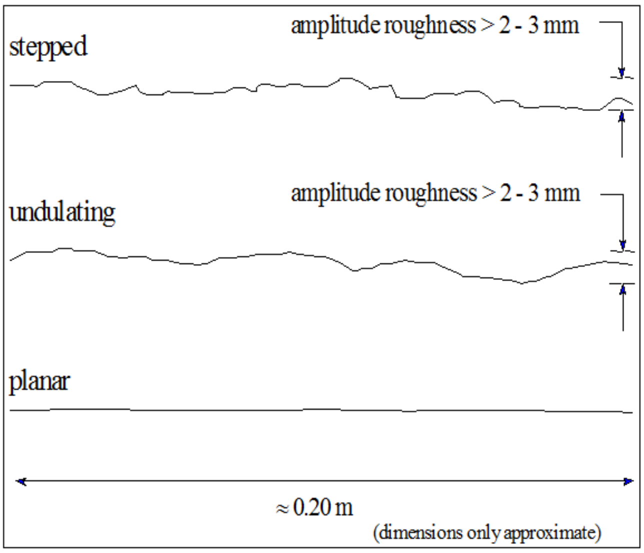

Figure 6-3: Small scale roughness profile

The infill material *(Im)* in discontinuities and the presence of Karst *(Ka)* along discontinuities are characterized, which has shown in the above calculation sheet. All the values given for these four factors can be simply multiplied to calculate the condition factor for a discontinuity *(TC)* (Hack, 1998):

$$TC = Rl * Rs * Im * Ka \qquad [1]$$

After calculating all factors, we can calculate the spacing parameter (SPA) based on the discontinuity sets with smallest spacing. The following formula shows the SPA calculation.

For three discontinuity sets:

$$SPA = factor_{maximum} * factor_{intermediate} * factor_{minimum} \qquad [2]$$

Table 6-2: Shows spacing parameter (SPA) calculation

		spacing (m)	factor
Spacing factor:	J2	0.250	0.67
	Ba1	0.500	0.70
	J4	0.500	0.67
SPA = Factor1 * Factor2 * factor3			0.314

Likewise, for two discontinuity sets:

$$SPA = factor_{maximum} * factor_{minimum}$$

Then the condition of discontinuities in a rock mass (CD) was calculated by the formula based on the mean of conditions of three discontinuity sets weighted against the spacing of the sets. The given formula is used for the calculation.

$$CD = \frac{\frac{TC_1}{DS_1} + \frac{TC_2}{DS_2} + \frac{TC_3}{DS_3}}{\frac{1}{DS_1} + \frac{1}{DS_2} + \frac{1}{DS_3}} \qquad [3]$$

Where; $TC_{1, 2, 3}$ are the condition and $DS_{1, 2, 3}$ are the spacing of the discontinuity sets 1, 2, 3.

Table 6-3: Calculation of condition of discontinuities in a rock mass

Condition of discontinuities:					
	Ba1	**J2**	**J3**	**J4**	**J5**
TC = Rl*Rs*In*Ka=	0.52	**0.31**	**0.35**	0.51	**0.42**
Used in calculation:	no	yes	yes	no	yes
CD (overall condition of discontinuities):				**0.35**	

Rock mass friction and cohesion

The rock mass friction angle and cohesion can be calculated by the optimizing the Mohr-Coulomb failure criterion with the intact rock strength *(IRS)*, spacing parameter *(SPA)* and condition of discontinuities *(CD)* using the given formula (Hack, 1998).

$$\varphi_{Mass} = IRS * 0.2417 + SPA * 52.12 + CD * 5.779$$
$$Coh_{Mass} = IRS * 94.27 + SPA * 28629 + CD * 3593 \qquad \textbf{[4]}$$

If *intact rock strength* > 132 MPa, Then *IRS*=132MPa

Where, φ_{Mass} = *angle of internal friction of the rock mass (in degrees)*

Coh_{Mass} = *rock mass cohesion (in Pa)*

From above equation, it was observed that above a value of about 132 MPa, the stability of slopes did not further increase with increasing intact rock strength. A higher value of the intact rock strength maximum may be necessary for significantly higher slopes with higher stresses. For both the spacing parameter (SPA) and discontinuity condition (CD), the combination of the discontinuity sets that result in the minimum rock mass friction value was always taken.

Maximum Slope Height Determination

In SSPC system, it was mentioned that the stability of a slope is independent of the height of the slope if the slope has the dip angle less than the friction angle. If the dip angle is higher than the friction angle, then the maximum slope height was determined by the cohesion of the rock mass. Hack has also stated that for a rock mass unit weight of $25kN/M^3$;

If $dip_{slope} \leq \varphi_{Mass}$; then Maximum slope height ($H_{\max}$) is infinite.

Otherwise, $$H_{\max} = 1.6 * 10^{-4} * coh_{Mass} * \frac{\sin(dip_{slope}) * \cos(\varphi_{Mass})}{1 - \cos(dip_{slope} - \varphi_{Mass})} \qquad \textbf{[5]}$$

Table 6-4: Showing the rock mass friction, cohesion and maximum possible height observed for the slope exposure in the field

Rock mass friction:	φ_{Mass} =	43 degrees
Rock mass cohesion:	Coh_{Mass} =	19668 Pa
Maximum possible height:	$H_{\max}$ =	7.2 m

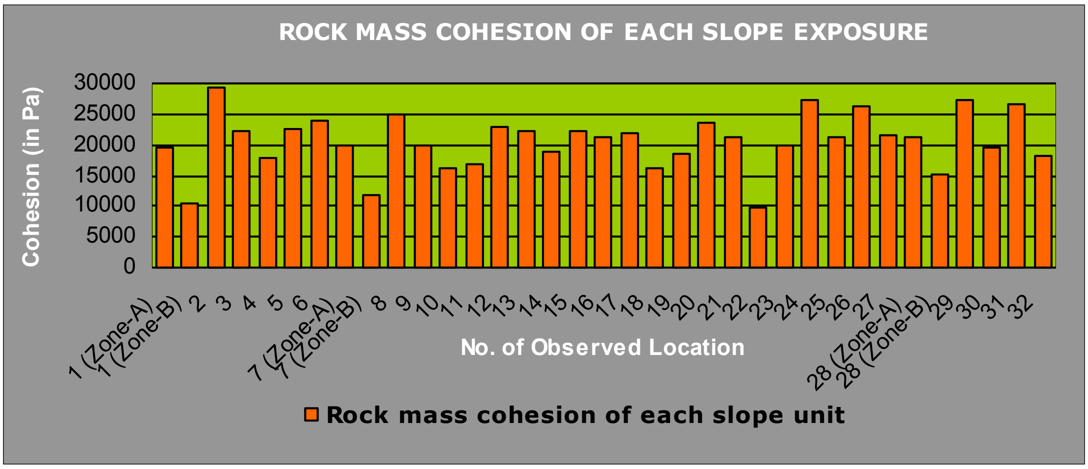

Figure 6-4: Shows the rock mass cohesion observed for each slope exposure

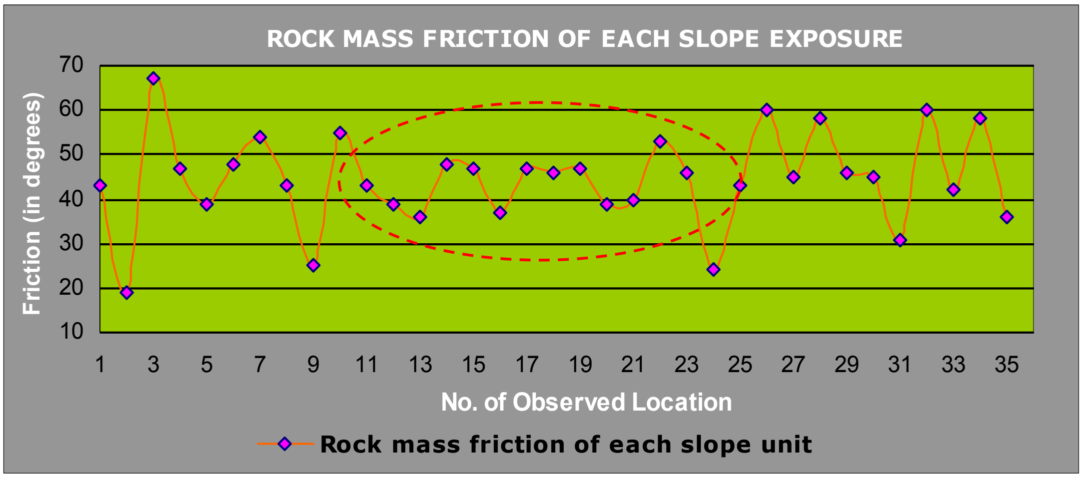

Figure 6-5: Angle of friction of rock mass observed for each slope exposure

From the field survey, 32 number of slope exposures were observed according to the homogenous conditions. The above table shows that the cohesion of rock mass is uniform in nature and varies between 10000 to 20000Pa. The angle of friction varies from 18-70 degree for whole slope exposures but it was observed that 35 to 50 degrees have more frequency. According to these rock mass cohesion and friction angle, the slope stability can be assessed easily, which has been described below.

6.2. Slope Stability Analysis

As mentioned above, the slope stability is determined by two different processes according to their relation to the orientation. Such as:

1. Orientation independent stability
2. Orientation dependent stability

6.2.1. Orientation Independent Stability

The orientation independent stability is related to the strength of the rock mass in which the slope occurs, which is always independent to the orientation of both the discontinuities and slope. Therefore, for these observed slopes, a mathematical model was used to predict the orientation independent stability. Most of the slope failures were approximately linear, although these are not following one and the same existing discontinuity plane. It was observed that a small fracture in the intact rock may results in linear failure planes developing partly through intact rock and partly through the existing discontinuity plane. This effect can be prominently observed in rock masses when the block size is smaller. Therefore, intact rock strength, block size and the shear strength along the discontinuities have an influence on the development of failure planes, which is not related to the single discontinuity plane.

Actually, in SSPC system, both the slope stability can be calculated in terms of probability in percentage, which is shown in figure below. For the calculation of orientation independent slope stability, it is very necessary to observe the rock mass friction, slope dip, height of the slope and maximum slope height, which were already calculated above.

Table 6-5: Calculation for assessment of the orientation independent slope stability probability

SLOPE STABILITY PROBABILITY Orientation Independent Stability		
Excavation method: existing slope - no damage	factor:	1.00
Expected weathering for new slope at end of engineering lifetime: existing slope: slightly	factor:	0.95
Existing slope:		
Dip direction:		105 deg
Dip:		**82 deg**
Height:		**20 m**
Visual assessed stability	**Large problems, major slide just left of exposure**	
Slope Intact rock strength	IRS =	100 MPa
Slope spacing	SPA =	0.314
Slope condition of discontinuities	CD =	0.347
Rock mass friction	FRI =	**43 deg**
Rock mass cohesion	COH =	19668 Pa
Maximum possible height	**H_{max} =**	**7.2 m**
RATIO FOR GRAPH USE	**φ_{Mass} /slope dip=**	**0.473**
	Hmax/Hslope=	**0.358**
Orientation independent stability (%)		**<5**

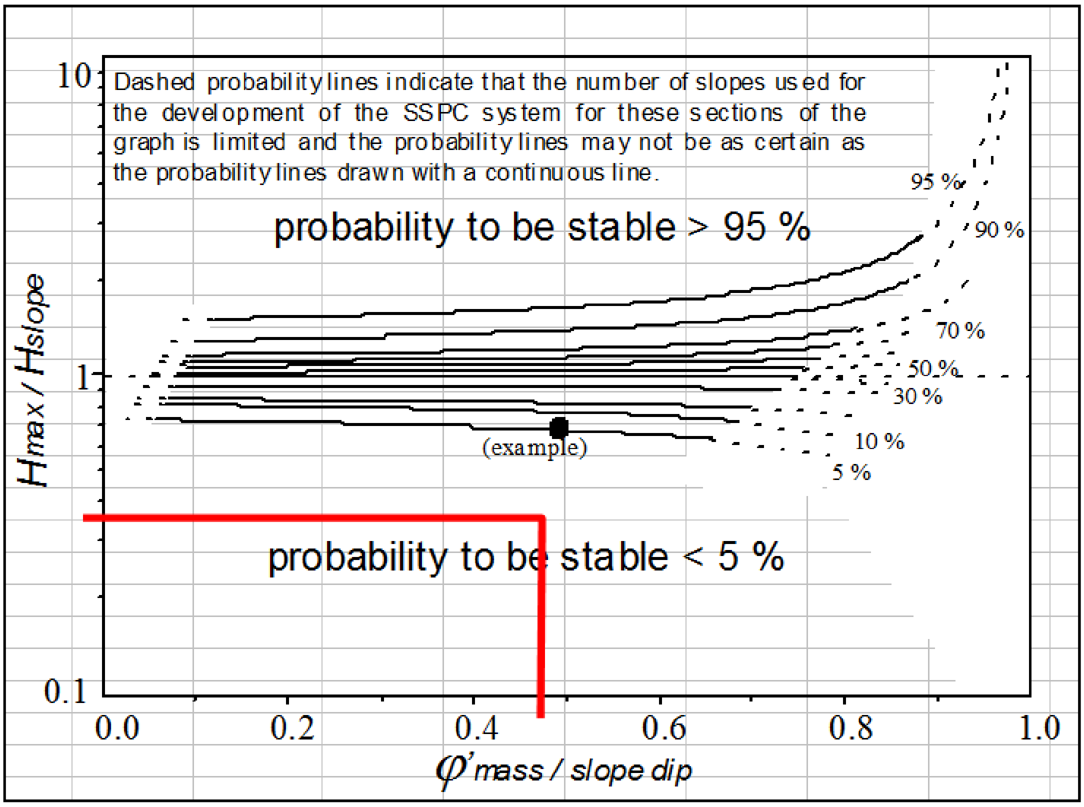

Figure 6-6: Graph shows the probability of independent slope stability

According to above graph of SSPC system, the axes are horizontally normalized on the ratios of rock mass friction (φ_{mass}) to the slope dip (dip_{slope}) and vertically on the maximum possible slope height (H_{max}) as a ratio of the true or actual slope height (H_{slope}). From the above graph, the ratio graph shows the stability of slope is less than 5% means it is highly unstable, which was also checked by visually in the field survey. It was assumed that φ_{mass} and Coh_{mass} are dependent on the rock mass parameters measured in the field like intact rock strength *(IRS)*, spacing of discontinuities *(SPA)* and conditions of discontinuities *(CD)*. By this process, the orientation independent slope stability was calculated for all observed 32 slope exposures from the field survey. All the independent slope stabilities are given in a tabulated format further.

6.2.2. Orientation Dependent Stability

Failures in the rock slope always depend on the orientation of the slope and the discontinuities in the rock mass. Therefore, it is necessary to know which discontinuity set plays an important role for the slope failure. Two criteria were developed in SSPC system to predict the orientation dependent stability of a slope. Such as:

1. Sliding criterion and 2. Toppling criterion

6.2.2.1. Sliding Criterion

A relationship was found in between the condition value of discontinuity *(TC)* and the apparent angle of the dip of the discontinuity plane in the direction of the slope dip *(AP)*. The condition value of discontinuity (TC) was already calculated in equation (1). And the apparent dip of the discontinuity plane can be calculated with the following formula.

$$AP = \arctan(\cos\delta * \tan dip_{discontinuity}) \qquad \textbf{[6]}$$

Where; $\delta = dipdirection_{slope} - dipdirection_{discontinuity}$

If $AP > 0^\circ$ then AP = apparent discontinuity dip in the direction of the slope dip.

And If $AP < 0^\circ$ then AP = apparent discontinuity dip in the direction opposite the slope dip.

The sliding criterion is therefore considered as the boundary of sliding in slopes. Therefore, the sliding occurs in the slope if the condition of discontinuity satisfies the following condition (Hack, 1998).

$$TC < 0.0113 * AP \qquad \textbf{[7]}$$

The calculation sheet of the sliding criterion after the field survey is given below.

Table 6-6: Calculation for assessment of the slope stability probability for sliding criterion

SLOPE STABILITY PROBABILITY Orientation Dependent Stability (*Sliding Criterion*)					
	Ba1	J2	**J3**	**J4**	**J5**
Dip direction	65	212	30	132	125
Dip	35	65	67	75	26
AP	**28**	-32	**31**	**73**	**25**
TC	**0.52**	0.31	**0.35**	**0.51**	**0.42**
Probability stable for sliding (%)	**>95**	100	**75**	**<5**	**>95**

From the above calculation sheet, it shows that the stability probability for sliding is <5%. It means that the stability is much less for sliding along the joint number J4 with dip 75° and orientation N132°. The sliding criterion was confirmed visually in the field survey.

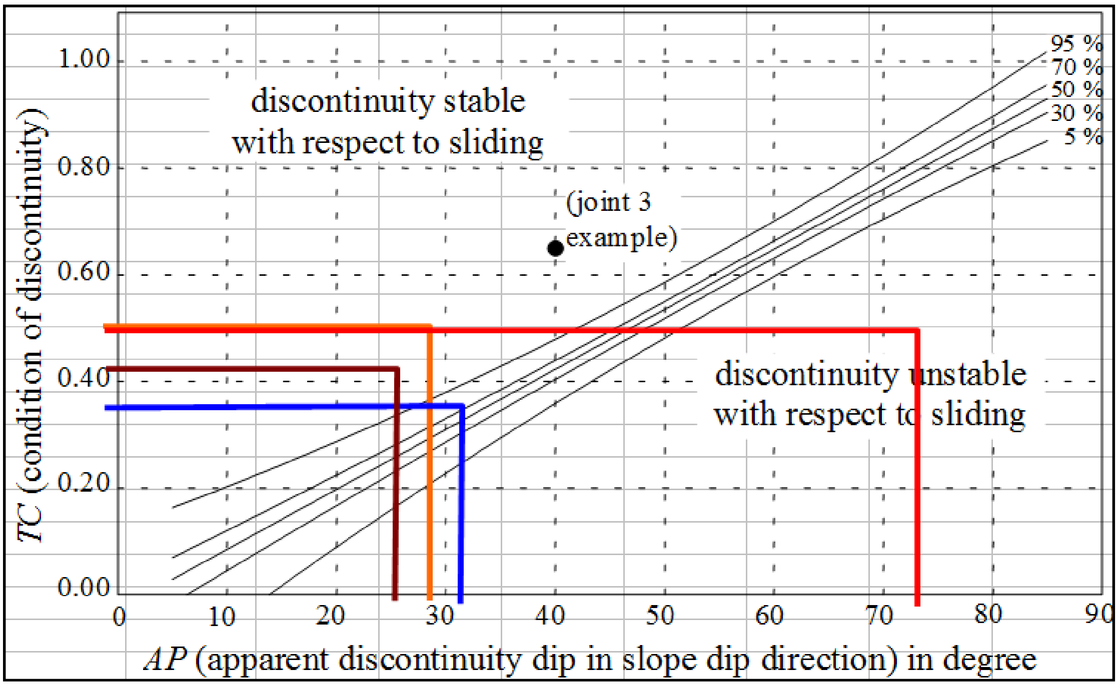

Figure 6-7: Graph shows the stability probability for each discontinuity with respect to sliding

At the end, it was observed that if apparent dip of the discontinuity is less than zero, then sliding criterion may not be possible to occur in that discontinuity set.

6.2.2.2. Toppling Criterion

Corresponding to the sliding criterion, toppling criterion can be estimated with considering the interlayer slip in between the discontinuities. The mathematical formula derived by [(Goodman, 1989) cited in (Hack, 1998)]. According to the mathematical condition, the toppling criterion in SSPC is derived as follows.

$$TC < 0.0087 * (-90^{\circ} - AP + dip_{discontinuity}) \qquad \textbf{\textit{[8]}}$$

According to the above equation, the toppling criterion was developed for each discontinuity sets. The following table and graph shows the toppling criterion which was observed from the calculation.

Table 6-7: Calculation for assessment of the slope stability probability for toppling criterion

SLOPE STABILITY PROBABILITY					
	Ba1	**J2**	J3	J4	J5
Dip direction	65	212	30	132	125
Dip	35	65	67	75	26
AP	28	-32	31	73	25
TC	0.52	**0.31**	0.35	0.51	0.42
Toppling condition (-90-AP+Slope dip)	-36	**24**	-39	-81	-33
Probability stable for toppling (%)	100	**85**	100	100	100

From the above table, it was observed that when the toppling condition (-90-AP+slopedip) is less than zero, the stability of discontinuity with respect to toppling is 100 %. It means there is no problem of toppling in this area.

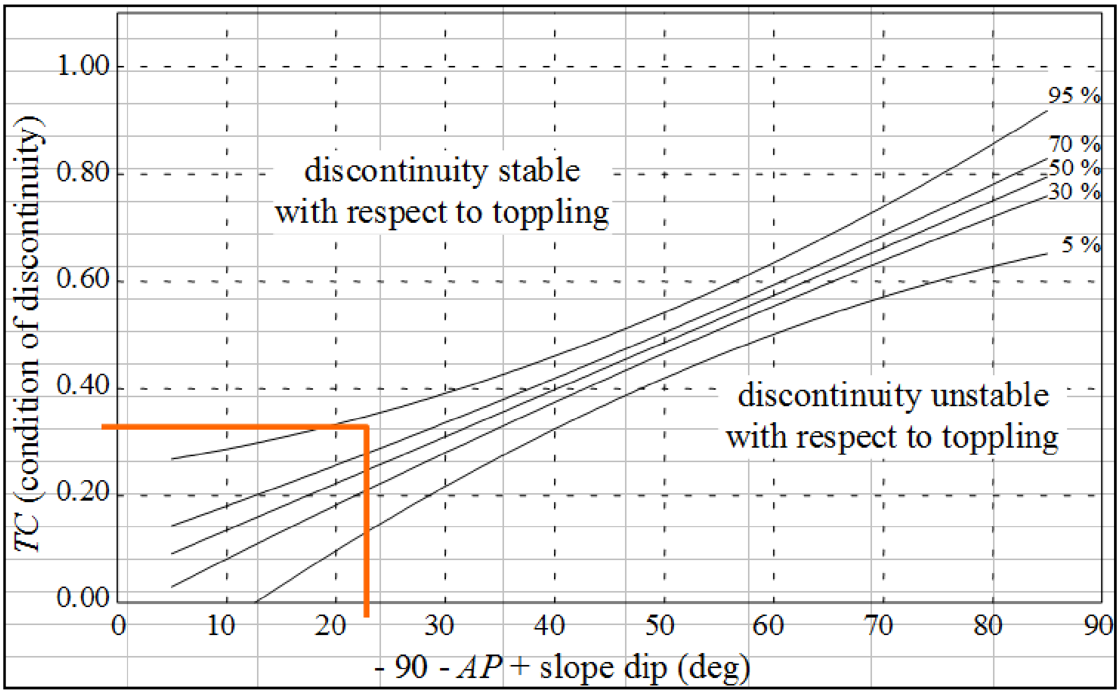

Figure 6-8: Graph shows the stability probability for the discontinuity with respect to toppling

An additional condition is also assumed that, the discontinuity plane should not be near vertical as a vertical plane cannot be a sling plane or it cannot influencing the toppling mechanism. It was checked that: for sliding, the apparent dip of discontinuity (AP) must be less than 85 degree and for toppling, AP must be greater than (-85) degree.

6.3. Slope Stability Map

For this present research, it was observed very critically that orientation independent stability is very useful approach for assessment of the stability of each rock mass exposure. It calculates the probability of stability with respect to independent orientation of slope. Moreover, it was validated directly from the field survey. In slope orientation dependent stability, it is necessary to observe each discontinuity sets, the dependency of each discontinuity with the slope rock mass. Also, measurement errors may be observed like overestimation of slope height, slope orientation etc. Finally, the result was compared with the field observation. The prediction of the SSPC system fits very accurately with the natural condition. Thus, a final slope stability map was prepared with the outcome probability values of orientation independent stability. The probability of stability for each rock mass exposure is given below. The probability observed from SSPC system varies from 0 to 100 %. So it was necessary to convert the probability in range from 0 to 1. For example, the above result shows <5% probability to be stable for this particular rock mass exposure. That means this rock mass exposure is highly unstable and may be prone to failure in near future. Therefore, the probability is high in this condition and converted to numerical value of 0.9.

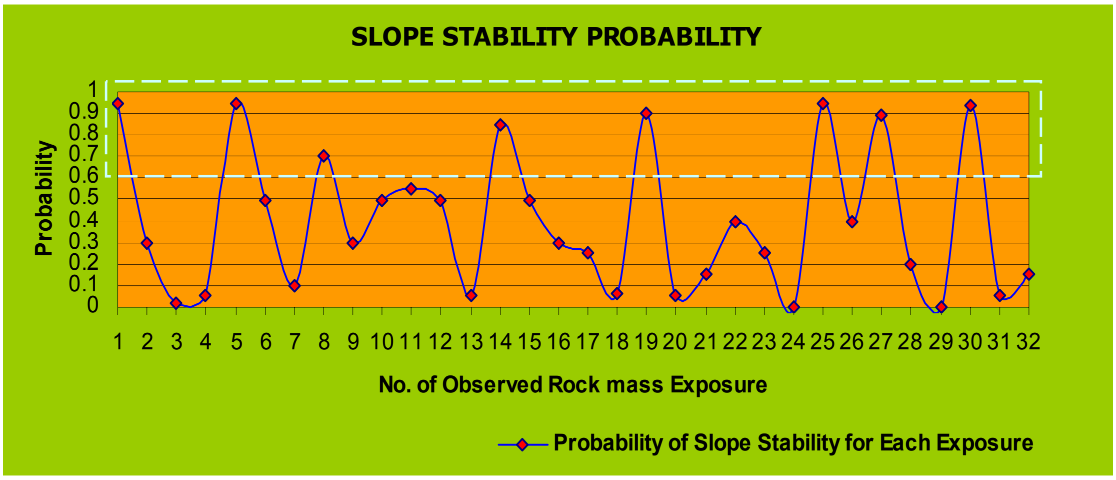

Figure 6-9: Graph shows the output probability of slope stability using SSPC system

From the above graph, it was observed that from 32 locations, in 8 locations rock mass exposures have been found above the probability of 0.6. But, the SSPC system gives the slope stability in percentage. According to the stability percentage, a slope stability map was prepared with different slope stability classes. The low slope stability percentage shows that the slope exposure is unstable in nature and high slope stability means that exposure having no problem for slope failure. The slope stability map is given below.

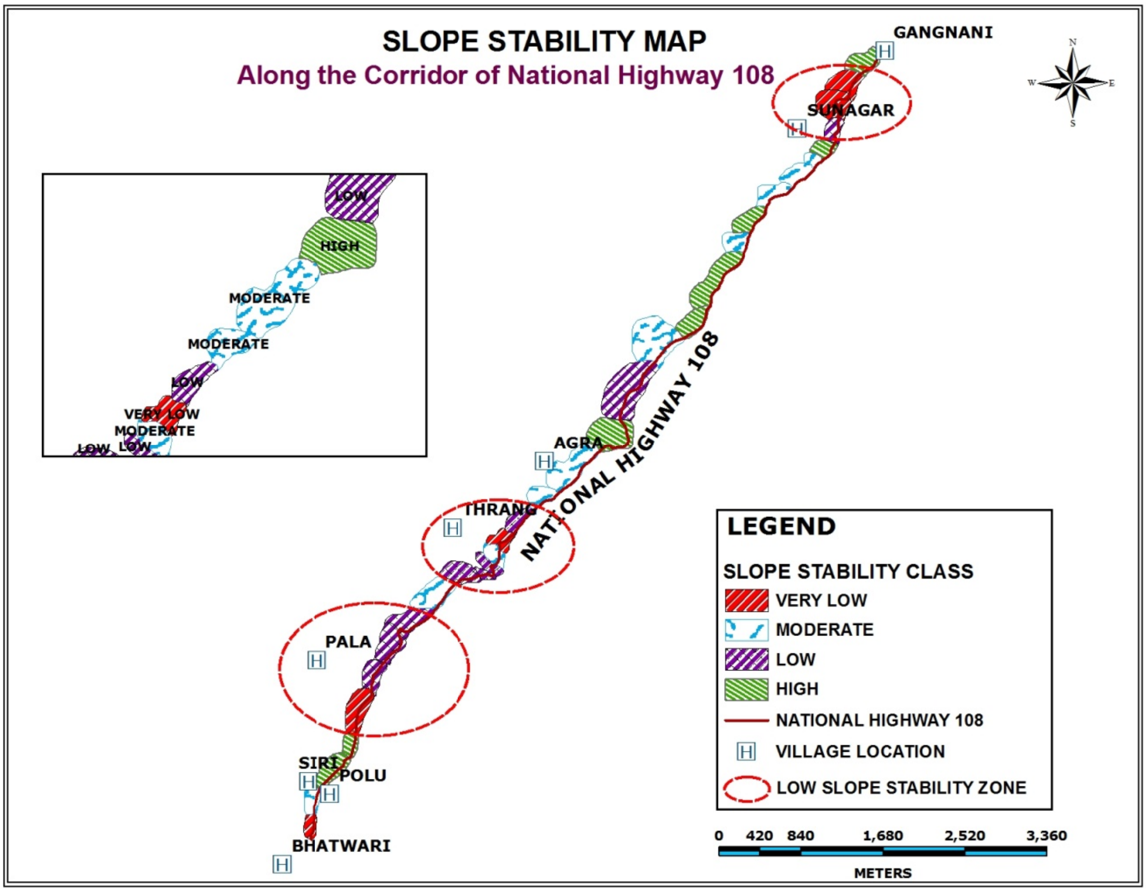

Figure 6-10: Slope Stability Map along the corridor of National Highway 108

The above figure shows the slope stability map obtained by SSPC system with four different classes. The classes are based on the stability percentage observed which varies from 0 – 100%.The classes range from very low to high probability. The class distribution is given in figure below.

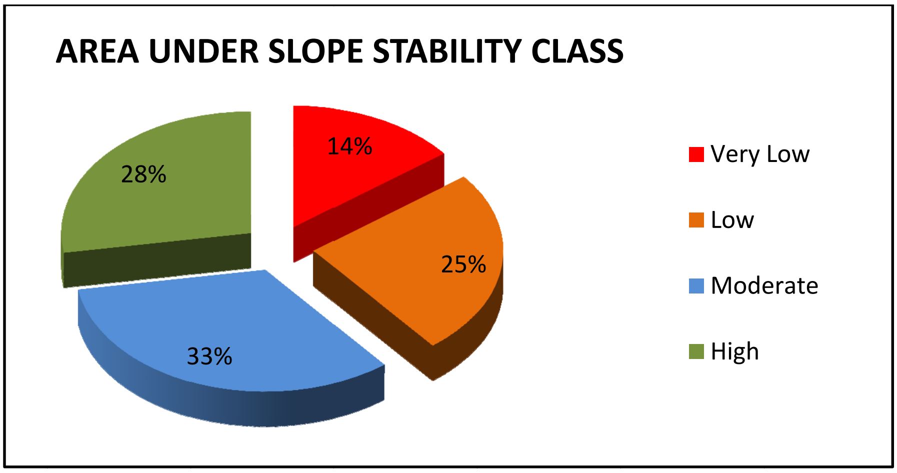

Figure 6-11: Shows the area under slope stability class

The above figure shows around 40% of the area of exposure along the road corridor under the low slope stability class and 60% shows high slope stability. This result was also validated by assessing the slope condition in the field. As SSPC system is a field based approach, the observed slope stability map can be used further for the validation of the susceptibility map generated using logistic regression.

7. Landslide Susceptibility Analysis

The spatial probability of landslide occurrence, known as susceptibility, is the probability that any given region will be affected by landslides with influences of a set of environmental variables [(Brabb, 1984) cited in (Guzzetti et al., 2005)]. It also defined as in the following equation:

If L: a given region, which will be affected by landslides
Then Susceptibility 'S' becomes:
$S = P$ [L is true, given (morphology, lithology, structure, landuse, geomorphology, etc.)] ***[1]***

As explained before in chapter-2, susceptibility can be estimated using a variety of statistical techniques. Depending on the type of statistical technique, the meaning of the probability changes slightly (Guzzetti et al., 2005). But for this present research, Logistic regression approach was implemented for estimating the spatial probability of study region.

7.1. Logistic Regression Model for Susceptibility Analysis

Logistic regression is capable of handling a combination of continuous and categorical variables. In case of categorical variables, there is no meaningful numerical value attached to each class. Therefore, it is necessary to create dummy binary variables for each class of categorical variables and to represent the presence or absence of that variable class by 1 and 0 respectively (Ayalew and Yamagishi, 2005; Ohlmacher and Davis, 2003). If the number of parameters is small, then this approach is good. If there are many parameters, then it would produce a long regression equation and may even create numerical problems. It may also work against the basic assumption like the absence of strong correlations among independent variables, which is known as multicollinearity (Ayalew and Yamagishi, 2005).

It is also an important issue that how many samples should appropriately be taken for the logistic regression analysis. After the literature review, it was found that there is difference of opinion regarding this matter. Some researchers have used the data from all over the study area which shows the unequal proportions of landslide and non-landslide pixels (Ohlmacher and Davis, 2003). In this method, a large volume of data is included. Some authors also used an unequal proportion of 1 (landslide present) and 0 (landslide absent) to prepare the database for logistic regression analysis (Atkinson and Massari, 1998). Yesilnacar and Topal (2005) used the total number of landslide pixels and randomly selected cells from the landslide free areas. He has divided the dataset into six different training datasets to determine which dataset will work well in the logistic regression model according their accuracy percentage. Also researchers like Dai and Lee (2002) and Suzen (2002) have also used the equal number of landslide and non landslide pixels.

7.2. Estimation of Logistic Regression Coefficients

In order to estimate the logistic regression coefficients, the basic requirement is an input database consisting values of the independent variables and the status of the dependent variable (landslide present or absent) for the corresponding units of each cell. As in the present study, the number of landslide pixel is comparatively low (4.26%), all landslide pixels have been taken into account to increase the accuracy. In addition, equal number of non-landslide pixels was randomly chosen from the landslide free area to decrease the effect of unequal proportion of both landslide and non-landslide pixels. It is also important to know which parameter is more influencing towards landslide. For this purpose, landslide density corresponding to each parameter helps to solve these problems. But before this, it is necessary to get knowledge about both the independent and dependent variables.

7.2.1. Independent Variables

For the analysis purpose, eleven independent variables or parameters have been prepared in ARCINFO GRID format with 20m cell size, which is already described in chapter- 5. According to their cell size, the area was calculated for each class of each independent parameter. As it was explained before, in logistic regression analysis, numerical value should be attached to each class of all independent variables for further analysis. All prepared class codes for each parameter class has been given in annexure.

7.2.2. Dependent Variables

The dependent variable in this analysis is landslide occurrence map. For the purpose of analysis, the landslide map was rasterized and converted into ARCINFO GRID format with 20m cell size. After rasterizing, it has been found that total 1668 number of landslide cells present in the study area. The density of landslide with corresponding to each class has been calculated by the density calculation formula. The following graph shows the landslide density with respect to slope class.

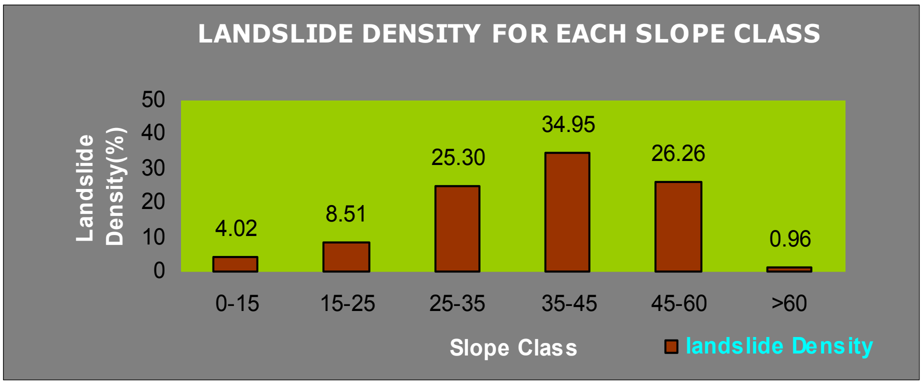

Figure 7-1: Landslide densities computed for the parameter slope

In the above graph, landslide densities have been computed for six categories of slope angles. It shows that, the density of landslide is high (around 35%) in 35-45 degree slopes and 25% for both 25-35 and 45-60 classes. From the above graph, it was clearly shown that slope angle from 15 degree to 60 degree plays an important role for slope failure. This process can calculate the landslide density for all 11 independent variables (Graphs shown in annexure).

7.3. Sampling Procedure

Sample data is always necessarily required to fit the logistic regression model. Sampling the data for each layer will affect both the nature of the regression relation and the accuracy of the resulting estimates (Atkinson and Massari, 1998). Before sampling, it is necessary to create a database for the whole study area. The database can be prepared by the surfacing techniques available in ERDAS 9.1. By the surfacing, all the cells can be arranged in actual sequence with respect to their class code. After analysing the whole database, it was found total 1668 cells having presence of landslides in the study area. Therefore, according to requirement, a random selection has been done from the area excluding the landslide locations, to select equal number of cells (1668) which do not have the presence of landslides and has been kept as raster data layer. A table has been created containing a column with landslide status (means 1668 with presence of landslide and 1668 with absence of landslide).

But for the Logistic regression analysis, the input table needs to be filled with the values of independent variables for the 3336 cells for landslide and non landslide samples. The randomly selected sample map has been cross tabulated with each of the independent variable maps. This produces the output data layers, which contain corresponding data values only at the spatial locations of the random landslide locations and null values at all other locations. From each output map (which is an overlay of the randomly selected landslide sample map and the independent variable map), it is possible to extract the corresponding variables at the locations of the random landslide samples. These values have been filled in the input table for the independent variables at the corresponding landslide sample locations. The same procedure has been adopted for the random samples of non-landslide locations have also been extracted and the input table for logistic regression model has been updated with these values. Thus the final input table for logistic regression contains 12 columns. The first column contains the status of landslide as 1 or 0 and the remaining 11 columns contain the values of independent variables at the corresponding sample location. The input table has been prepared in EXCEL format or ASCII format. The format of this table with few entries is given in Annexure. Like this same process, three training datasets was prepared for the logistic regression model.

7.4. Statistical Results and Discussion

The spatial relationship between landside and landslide influencing parameters was evaluated using the logistic regression method. The statistical analysis has been carried put using the statistical analysis software namely SPSS. Three different test datasets were chosen and the logistic regression model was run with each dataset. The overall statistics of three sample datasets was found to be quite similar indicating the quality of the dataset.

Table 7-1: Summary of the training dataset

Training set no.	_2ln Log likelihood	Cox and Snell pseudo R^2	Nagelkerke Pseudo R^2	Chi-square	Overall accuracy %
1	2532.888	0.556	0.341	986.868	82.9
2	2478.871	0.543	0.323	929.171	86.3
3	2308.304	0.527	0.300	849.701	88.7

In the above table, it was observed that the overall accuracy of the sampling dataset number 3 is 88.7%. It was the highest among all of the others and it is quite acceptable (Yesilnacar and Topal, 2005). The observed accuracy of the third training dataset is given below (After output of SPSS).

Table 7-2: Classification table of training dataset for Logistic regression base model

Observed	Predicted		
	1	0	Percent Correct
1 (Landslide)	1495	173	89.6%
0 (Non-landslide)	204	1464	87.8%
Overall Percentage	50.9%	49.1%	88.7%

According to the summary and accuracy of the three training dataset, it was finally observed that the third sample dataset is quite useful for the logistic regression model. After finalizing the dataset, multiple relations between the factors and landslide distribution were tested with multiple regression analysis using SPSS software. The output result is shown below:

Table 7-3: Summary statistics of the logistic regression model

Statistics	Value
Total number of pixels	39,119
-2ln L (L=likelihood)	2308.304
-2ln L_0	948.712
Model chi-square	849.701
Pseudo R^2	0.527

The above table summarizes the overall model statistics of the regression conducted in this study using SPSS. A key for usual analysis of the test is generally the model chi-square value which provides the usual significance test for Logistic regression (Ayalew and Yamagishi, 2005). Here, in this study, model chi-square is quite high to conclude that the independent factors have a great influence on the occurrence of landslides. Actually, the chi-square statistic is a difference between -2ln L (L=likelihood) for best fitting model and -2ln L_0 for the null hypothesis in which all the coefficients are set to be zero. High value for model chi-square indicates that the occurrence of landslides is quite less likely the influencing parameters without landslides than the full regression model (where all parameters are included). The pseudo R^2 value always gives an indication of how model fits the data. According to Ayalew and Yamagishi (2005), pseudo R^2 equal to 1 means perfect fit, whereas 0 shows no relation with the data. But, when pseudo R^2 is greater than 0.2, this is an evidence of relatively goodness of fit [(Clark and Hosking, 1986) cited in (Akgun and Bulut, 2007)]. In the present study, pseudo R^2 was observed as 0.518, which indicates a reasonable fit to the data. The model also gave the regression coefficients for all class of each independent parameter, which was used for generating the landslide probability map. The regression coefficients are given below.

Table 7-4: The regression coefficients obtained for eleven independent parameters

Parameter Estimates

Landslide	B	S.E.	Wald	Sig.
Intercept	1.823	1.149	2.518	.113
[Slope=1]	-.107	.463	.053	.017
[Slope=2]	.083	.438	.035	.051
[Slope=3]	.172	.425	.163	.036
[Slope=4]	.261	.423	.380	.038
[Slope=5]	.403	.425	.899	.043
[Slope=6]	0	.	.	.
[Aspect=1]	1.150	.288	15.882	.000
[Aspect=2]	1.382	.249	30.709	.000
[Aspect=3]	1.160	.245	22.404	.000
[Aspect=4]	.880	.249	12.500	.000
[Aspect=5]	1.277	.268	22.730	.000
[Aspect=6]	-.157	.372	.177	.674
[Aspect=7]	.240	.288	.693	.405
[Aspect=8]	0	.	.	.
[Lithology=1]	.093	.253	.136	.712
[Lithology=2]	-2.012	.373	29.164	.000
[Lithology=3]	-2.639	.427	38.242	.000
[Lithology=6]	1.712	.224	58.386	.000
[Lithology=8]	0	.	.	.
[Geomorphology=3]	-.908	.676	1.802	.080
[Geomorphology=4]	1.264	.665	3.614	.037
[Geomorphology=5]	-1.180	.657	3.221	.073
[Geomorphology=6]	-11.809	142.560	.007	.934
[Geomorphology=8]	-10.209	76.453	.018	.894
[Geomorphology=9]	-.553	.739	.560	.454
[Geomorphology=10]	0	.	.	.
[LuLc=1]	-3.283	.834	15.481	.000
[LuLc=2]	-.835	.608	1.889	.169
[LuLc=3]	.388	1.240	.098	.755
[LuLc=4]	-15.739	.000	.	.
[LuLc=5]	12.019	135.961	.008	.930
[LuLc=6]	-2.973	.629	22.325	.000
[LuLc=7]	-.068	.617	.012	.912
[LuLc=8]	-2.740	.638	18.475	.000
[LuLc=9]	0(b)	.	.	.
[DrainageDensity=1]	.213	.368	.336	.042
[DrainageDensity=2]	-.572	.425	1.812	.178
[DrainageDensity=4]	-.148	.343	.186	.666
[DrainageDensity=5]	0	.	.	.
[LineamentDensity=1]	.073	.637	.013	.039
[LineamentDensity=2]	-.463	.323	2.056	.022
[LineamentDensity=3]	.394	.305	1.678	.195
[LineamentDensity=4]	0	.	.	.

[Soil=1]	1.328	.231	32.998	.000
[Soil=2]	-.142	.119	1.437	.231
[Soil=3]	-.395	.133	8.899	.003
[Soil=4]	0	.	.	.
[Weathering=1]	.236	.361	.426	.014
[Weathering=2]	-.107	.360	.088	.766
[Weathering=3]	0	.	.	.
[Anthropogenic=1]	.953	.222	18.374	.000
[Anthropogenic=0]	0	.	.	.
[Road Buffer=1]	.206	.112	3.377	.046
[Road Buffer=0]	0	.	.	.

B: Coefficients for each class S.E.: Standard Error of estimate values
Wald: Wald chi-square value Sig.: Significance of the value

The multiple logistic regression process started with all 56 predictor variable classes of total 11 independent variables, which has shown in the above table. From the base sample dataset, the variables have been added successive steps such as they have significant changes with 200 times iteration process. But, the regression process selects 25 predictor variable classes, with the addition of the remaining predictor variable classes to the model not bringing any significance changes. Hence, the ignored predictor variable classes are insignificant in causing the occurrence of the dependent variables. Thus, the final model was retained with only 25 predictor variable classes, which has shown in orange colour in the above table. The all classes and their respective codes of predictor variables are given in annexure. Finally the coefficients (B) have been calculated for all retained categories with respect to the dependent variable. The statistical test for providing this has used Wald chi-square value, which can be calculated as $[(B/SE)^2]$ and 95% confidence interval has been used for this statistical analysis. So the variables with estimated coefficients having significance (Sig.) value less than 0.05 are found to be significantly accepted as influential predictor variables (Van Den Eeckhaut et al., 2006).

Here, different classes have different coefficient values according to their influence towards the landslide occurrence. It was observed from the above parameter estimate table; all independent variables have some influencing character according to their significance (Sig.). Some positive and negative coefficient values have been observed for some predictor variable class. Positive means those classes positively responsible for the landslide occurrence and negative coefficient means negatively influence towards the landslide. Therefore, according to the coefficient values of different independent variables like slope (from 25 to 60 degree) and aspect (N to SE facing) shows the positive influence towards landslide. But in lithology class (Mostly quartz-mica schist and calc-silicate gneiss shows the negative influence and Biotite gneiss shows the positive influence). Ridge and hogback types dissected hill shows the negative coefficient while Cuesta type dissected hill shows the positive influence. After all, in landuse or land cover class, river channel, scrubland and dense forest shows the influencing character. In other side, drainage density and lineament density shows the natural condition like high densities of both parameter shows the positive influence. It was also observed, shallow soil depth, high weathering zone, anthropogenic activity section and road buffer show the positive coefficients while deep soil depth shows the negative influence towards the landslide occurrence. By the process, all the coefficients were analyzed and can be used for calculating the probability for each cells of the total map.

7.5. Calculation of Predicted probability

The logistic regression analysis has provided estimates of the intercept of the model and the coefficients of the independent variables. Using all these coefficients and intercept values, the predicted probability can be calculated for the training sample dataset and the whole cells in the study area. It is the proper way to first calculate the probability for the sample data and then calculate the probability for whole area for accuracy and validation purpose. Therefore, the probability can be achieved with the help of given logistic regression equation

$$P(S=1 \mid X_1, X_2, \ldots\ldots\ldots\ldots\ldots\ldots X_n) = \frac{1}{1+e^{-(\beta_0+\sum_{i=1}^{n}\beta_i X_i)}}$$

For each cell, the values of the independent variables have been multiplied with their corresponding estimated coefficient (B) values. Any independent variable class is not retained with any coefficients or any negligible values, and then they should kept as zero for the analysis. For each cell, the products of the independent variable values and their coefficients have been summed up with the intercept of the model to estimate the probability of slope failure for each cell. The result is a raster layer with the cell values representing the estimated probability of slope failure. Probability should be within 0 to 1. At first, probability has been calculated for the training dataset, which is given below.

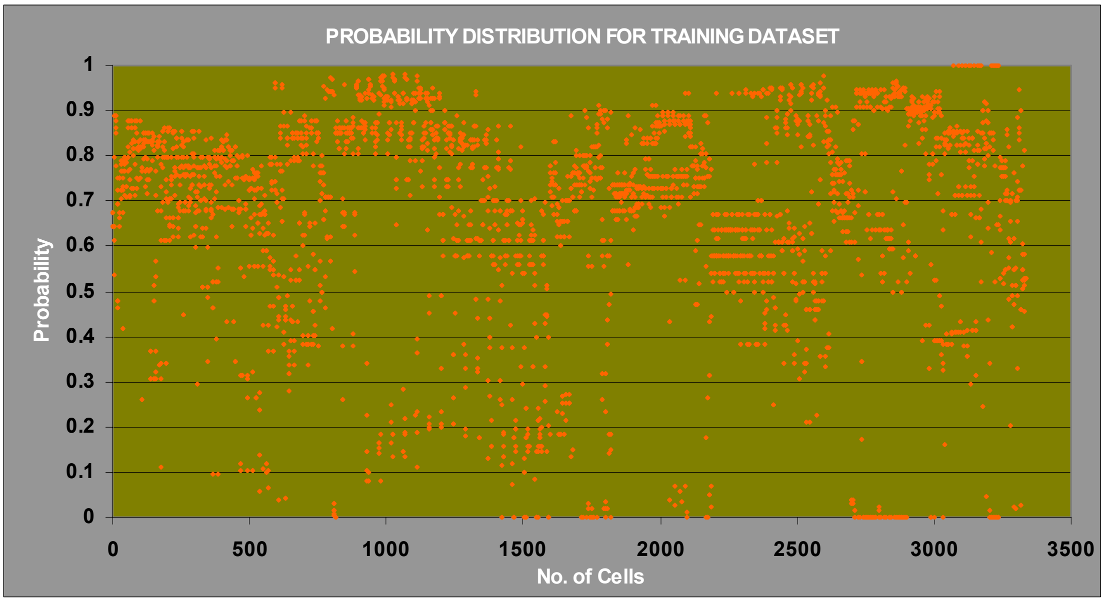

Figure 7-2: Scatter plot of the probability distribution for training dataset

The above scatter plot graph shows, most of the cells of the training dataset having greater than 0.5 probabilities. Because, it is showing for 3346 cells only which has equal number of 1 and 0 (Slide and non-slide cells respectively). However, the numbers, which are closer to 1, indicate the better likelihood whereas the numbers close to 0 show poor likelihood according to the probability. Thus, these sample data is again used for calculating the probability of the whole study area cells. The probabilities for whole cells are shown below.

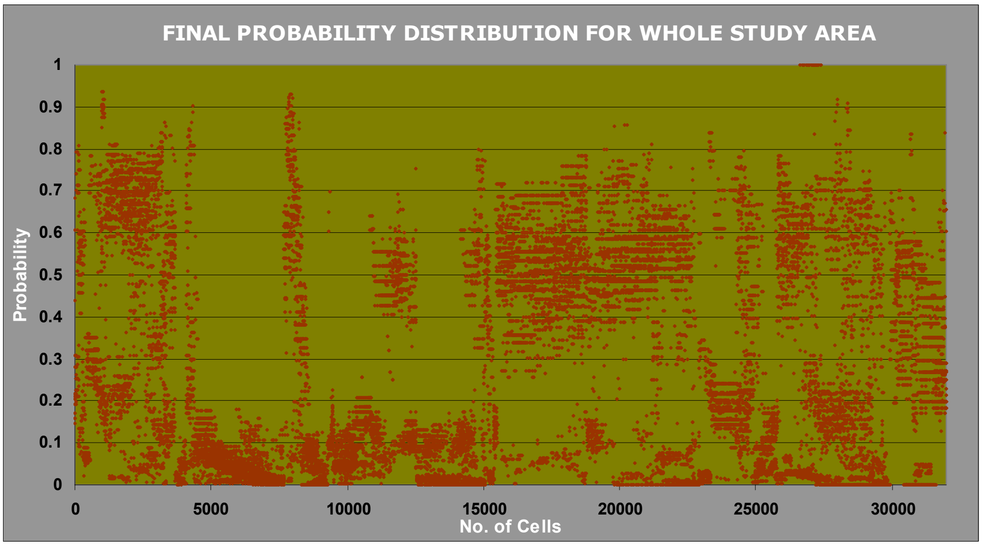

Figure 7-3: Scatter plot of the probability distribution for the whole study area

The above graph shows the well-distributed probability for whole study area cells. After applying the training dataset for whole the study area, it was observed that the probability for whole region varies from 0 to 1, which shows the reliability of the result.

7.6. Landslide Probability and Susceptibility Map

Based on the statistics and the output probability after the logistic regression model, a landslide probability map can be prepared. The final resultant probability map is shown in figure below.

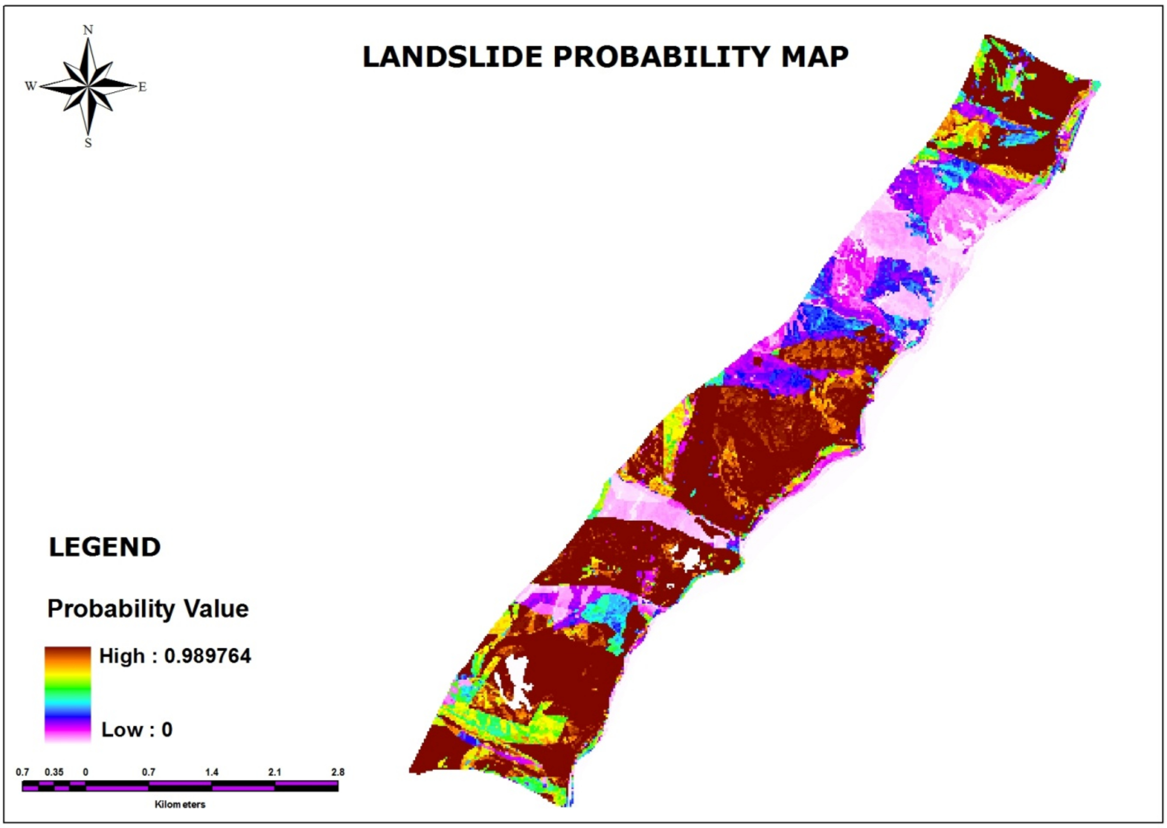

Figure 7-4: The Probability map obtained by the logistic regression model

After obtaining the probability map, it is necessary to divide this map into different susceptibility classes. Generally, the most common method for this purpose depend on the optimum band width classification of the histograms of various parameters (Akgun and Bulut, 2007). Actually in worldwide, various literatures shows that there are many methods available to realise this necessity (Ayalew and Yamagishi, 2005; Lee, 2005; Ohlmacher and Davis, 2003). Ayalew and Yamagishi (2005) have used four classification systems that use quantiles, natural breaks, equal intervals and standard deviations and tried to find out the best suit method for the information. Finally, they found that quantile based classification system has a disadvantage in that it places widely different values in the same class. Natural breaks are better when there is big fluctuation in the data values, which is not the case present probability map. Equal intervals were also determined as not helpful because they emphasize one class relative to others. Final method is standard deviation, which has some merit like it uses the mean to generate the class breaks. According to the histogram of the probability dataset, it was found that standard deviation method is only suitable method for the present study to classify the probability values. The histogram of the total cell distributions is shown in graph below.

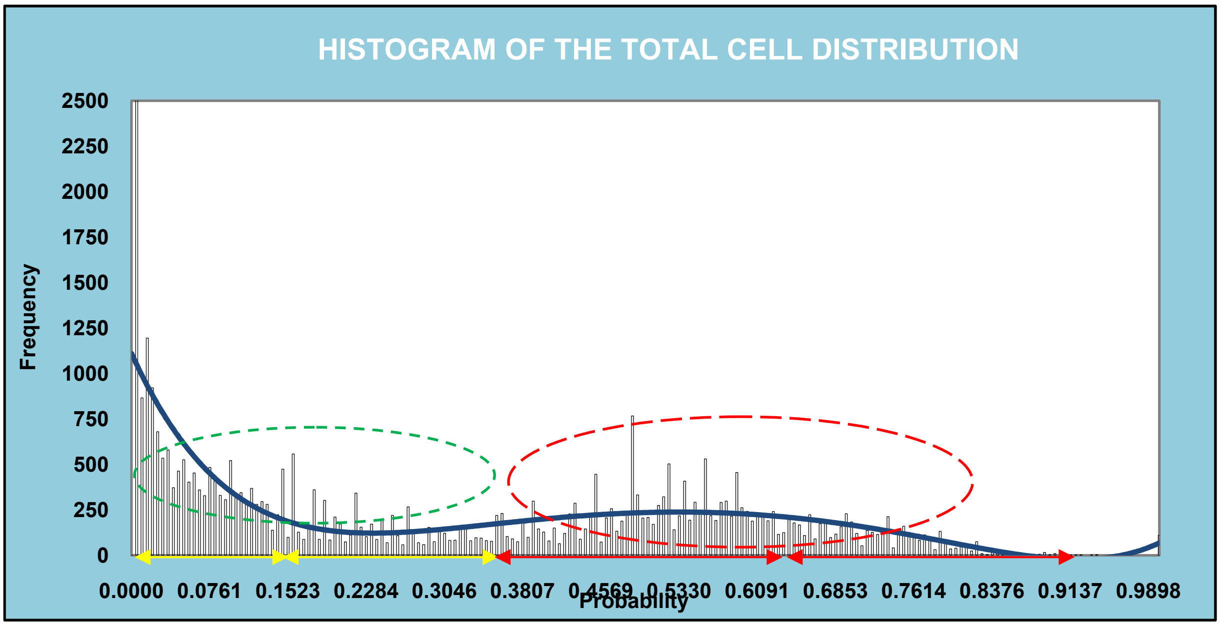

Figure 7-5: Histogram shows the frequency distribution of the total cell probability

According to the above histogram, it was decided that four classes have been derived through the standard deviation method. Because, the frequency was high for the probability values from 0.15 to 0.38 and 0.38 to 0.68. Therefore, the probability map was dived into four susceptibility classes: Very low, low, medium and high susceptible class. Finally, a susceptibility map was prepared according to the classes, which are shown below.

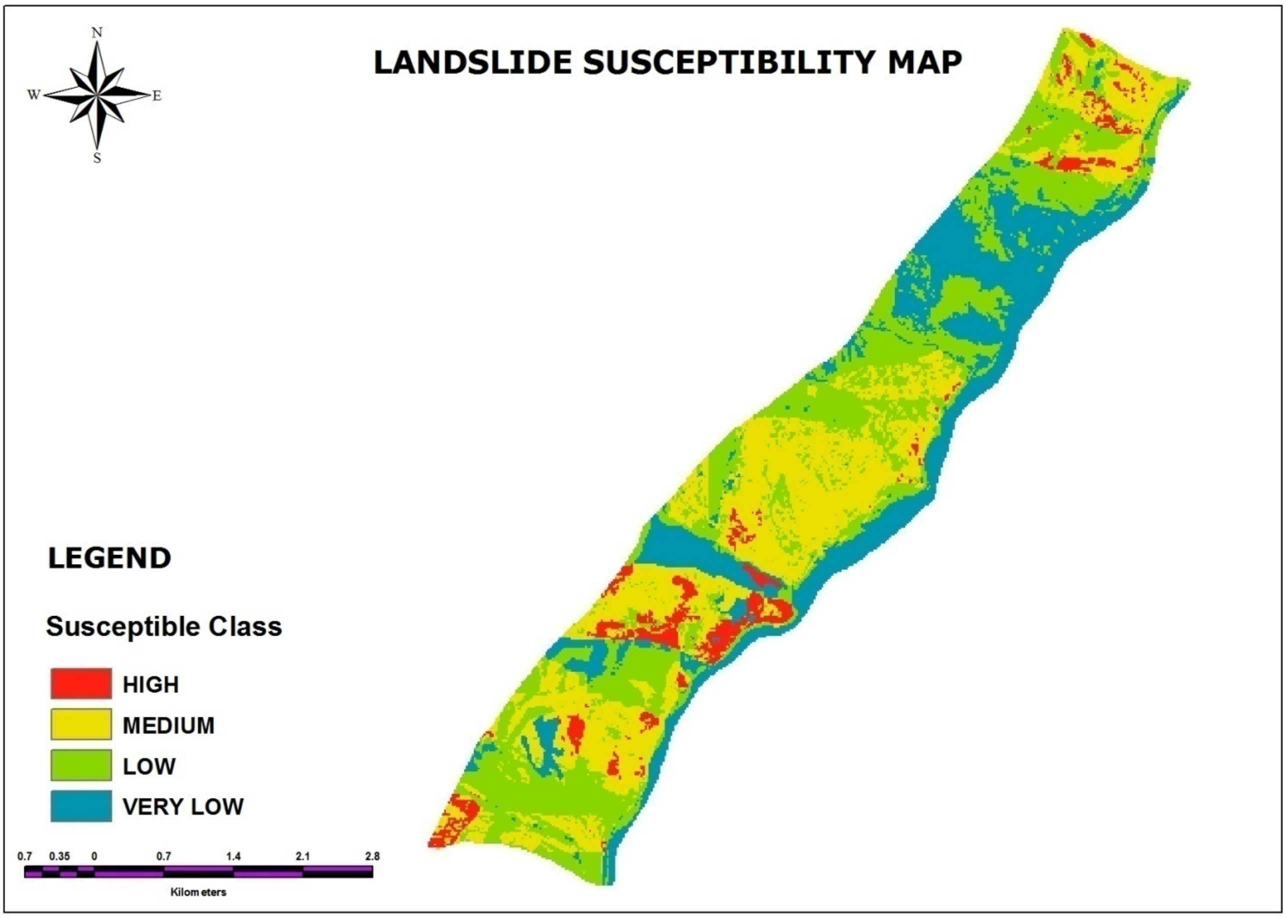

Figure 7-6: Landslide susceptibility map produced using the logistic regression model

The above figure shows the landslide susceptibility map derived through the probability map. According to the susceptibility map, the area of each susceptible class or zone was calculated below.

Table 7-5: Shows the area distribution of each susceptible class in the study area

Probability value range	Class Name	Area (%)
0 - 0.1523	Very low susceptible	**24.19**
0.1524 – 0.3807	Low susceptible	**36.52**
0.3808 – 0.6853	Medium susceptible	**33.51**
0.6854 – 0.9897	High susceptible	**5.78**

As shown in the output susceptibility map, 24.19% of the study area is designated to be very low susceptible zone. Low and medium susceptible zones make up 36.52% and 33.51% respectively. The zone corresponding to the high susceptibility constitutes 5.78% and it is slightly more than the total coverage of the mapped landslides (4.26%), which also shows the validity of the system adopted to divide the probability map. According to the above classification, most parts of the study area are found in very low to low susceptible zones. But, some parts of the central part of the study area shows the medium susceptible zones and high susceptible zones are very less but it also considerable with nature.

In the study area, the susceptibility shows medium to high for relatively weaker strength of rock types like Biotite gneiss, quartz-mica-schist, and Migmatite gneiss. High to moderately susceptible zones has been observed in 25 to 55 degree of slopes and mostly in south-east aspect. In addition, road or slope cut portion shows the little percentage of the high susceptible zone. Generally, the landslide inventory map and the statistical approach used as depending upon the considerable independent parameters. Therefore, the best predictor parameters and the predicted probability map of a logistic regression can vary with each other. But, it is always required to check the accuracy and validation of the susceptibility map.

7.7. Accuracy Assessment

Generally, many predictive modelling techniques such as logistic regression give predictions of landslide probability instead of directly predicting the presence or absence of landslide (Brenning, 2005). The evaluation of a model can be done with respect to another dataset in same area or framework or could be tested in an adjacent area of similar geo-environmental conditions to find out the reliability. However, the present study area has only 1668 cells which is quite less for accuracy assessment. Therefore, it has been decided to carry out the accuracy assessment of the logistic regression model result using ROC curve analysis. The input for the ROC curve analysis is a table which contains the predicted probabilities of the samples chosen for the purpose of accuracy assessment and their actual state of the dependent variable represented as 1 (present) and 0 (absent). In this present study, the predicted probabilities for the whole cells have been extracted and filled in the input table for the ROC curve analysis. After the extraction process, a new input table has been created which contains the status of the dependent variable represented by 1 in the first column and their corresponding probability values in the second column. Thus, the input table was used for the ROC curve analysis. The ROC curve shows the success rate of the model through the area under the curve plotted between sensitivity and 1-specificity. Sensitivity means the cumulative percentage of the area of the study area and specificity means the cumulative percentage of the probability. The processed ROC curve has shown below.

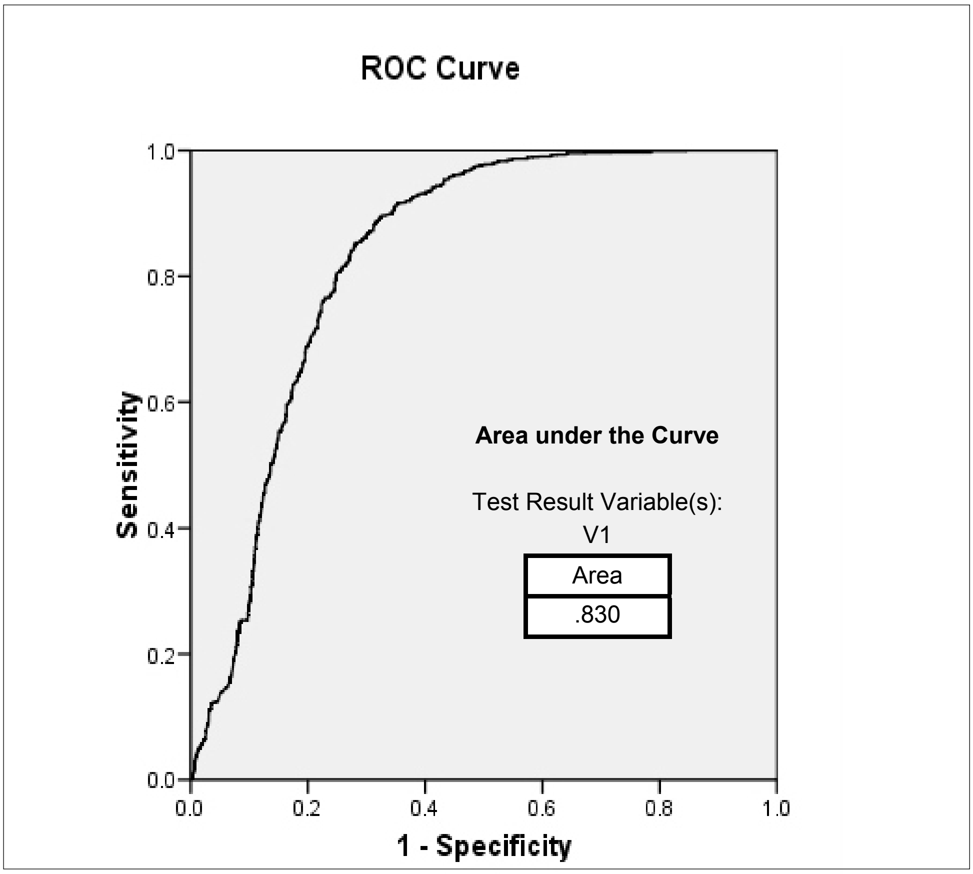

Figure 7-7: ROC curve for Logistic regression model

The above ROC curve shows the area under the curve is .830, which gives an accuracy of 83% for the model developed using logistic regression model. The standard error in the ROC curve is 0.005 and asymptotic signature value is less than 0.05, which shows precision of the accuracy result. From the above graph, it can be easily observed that, when cumulative percentage of the area gradually increases with the increase of the probability of occurrence. The shape of graph shows the accuracy of the model, which is quite acceptable.

7.8. Validation of the Results

In this present study, the output of the susceptibility map can be validated with the slope stability map, which is a pure field based approach. As discussed above in chapter-6, Slope stability assessment for the road corridor has been done with SSPC system, which is already validated in the field itself. So it is a better approach for the validation of the susceptibility map. According to Slope stability assessment result, total road corridor has divided into 32 homogenous sections and the slope independent stability has been calculated for each section. The output-classified map of the slope stability can be cross verified with the landslide susceptibility map of the whole region. After cross verification of both maps, it can easily calculates the common areas in different susceptible zones for both maps. Thus, it was observed that, about 72% of the area under medium to high susceptible class has purely classified in both the maps, which shows a quite good relation of slope stability towards the susceptibility assessment. Slope stability assessment has done only along the road corridor. That is why, the overall classification is not so high accuracy but it may be considered as one of the constraints. But, as the result shows, the slope stability map is very much useful for the susceptibility of the road corridor.

8. Conclusion and Recommendations

The present chapter discusses in detail conclusion arrived after examining the different methods and approached adopted in the study for their utility to assess the landslide susceptibility in the study area. This chapter ends with a brief note about the limitation of the research and recommendation for future studies in this topic.

8.1. Conclusion

The preparation of landslide susceptibility map is a major step for attempting comprehensive hazard management. In recent years, such type of maps can be prepared by GIS-based qualitative and quantitative techniques. This research used two different approaches like logistic regression for preparing the landslide susceptibility map for the whole study area and SSPC system for assessing the slope stability assessment along the road corridor. The second approach was also used for the validating the resultant susceptibility map from logistic regression model because SSPC system is a purely field based approach and slope stability was assessed for all exposures according to their slope orientation as well as all the required rock mass parameters. The slope stability was assessed for a total no. of 32 exposures selected along the national highway. After calculating the slope independent orientation stability for all slope exposures, it was found that eight exposures out of 32 are having the slope instability probability above 0.6. However, 40 % area of the total road corridor shows high to moderate slope instability, which was already verified by field survey. Most of the slope exposures showed high probability of failure towards south-east slope orientation. This result shows that the slope stability along the road is quite acceptable with the natural conditions. But, for susceptibility assessment for whole of the study area, a total of 41 landslides were mapped using aerial photographs and image interpretation with field check. The influencing parameters considered for the logistic regression model include lithology, slope angle, aspect, geomorphology, landuse or land cover, drainage density, soil depth, geological structure like lineament density, weathering, proximity to road (road buffer) and anthropogenic (Road / slope cut) etc. Landslide densities were also determined using density analysis to know which parameters have more influencing character towards the slope failure. In chapter-7, it was clearly described the results and analysis of the logistic regression model.

First, the initial results of the logistic regression model were the model statistics and coefficients, which were useful to access the accuracy of the regression function and the role of parameters corresponding to the presence or absence of landslides. It was found that, slope from 25 to 55 degree as well as NE to SE aspect has strong relation with the slope failure. It means, the logistic result is quite acceptable with relation to the slope stability assessment using SSPC system. Because, according to SSPC, slope stability probability is high towards the SE slope orientation. It was also noticed that, shallow soil depth, high lineament density and high drainage density as well as litho types like Gneiss and Schist have the positive influence towards the slope failure. However, most of the geomorphological units except Cuesta type dissected type hill and land cover having negative relation towards landslide occurrence. Road cut or slope cut parameters shows a little role for slope failure activities.

For this present research, three training datasets were used for the logistic regression model. But according to their classification accuracy, the third training dataset was used for final susceptibility analysis. The output probability map from the logistic regression analysis showed that the majority of probability values vary between the ranges from 0.15 to 0.68. But the map also showed a significant number of pixels above a threshold probability value of 0.5. Using the standard deviation corresponding to histogram, the output probability map was classified into four zones or classes of landslide susceptibility, namely very low, low, medium and high susceptible class. The proportion of high susceptible class was far smaller (5%) than the other three classes, but the moderate and low susceptible class having high percentage of area. The accuracy of the output susceptibility map using logistic regression model has been assed with the help of ROC curve analysis, which shows 83% of the area under curve is purely classified for whole region. The result was also validated with cross verification by the present landslide information and the slope stability map. After validation, it was finally observed that 68% of the high to moderate class in susceptibility map was properly matched with the same class in slope stability map. This means, the susceptibility map for the whole area having good accuracy because the slope stability was assessed only along the road corridor and the susceptibility map was validated with only road corridor part. If it is possible for assessment of the slope stability for whole the study area, then the accuracy of the map should increase higher. At last, the resulting map supported the observation to conclude that the logistic regression is very useful multivariate statistical procedure to model the probability of occurrence of a dichotomous dependent variable like landslide.

8.2. Limitations of the study

The most significant limitation of this study has noticed as follows:

- More the number of input factors, better the output result. In this present study, geotechnical factors like rock mass strength, orientation and condition of discontinuity were not considered for the whole region, which could have been helpful to improve the susceptibility map. This is because of the inaccessible nature of the terrain.

- Though historical landslide records are available for the road corridor, the same was not available for the whole study area. This could have improved the quality of the output map.

- The expert opinion could have been incorporated as the prior information to quantify the susceptibility in a better way.

8.3. Recommendation for further study

As observed during the field survey, rainfall plays an important role in this area for landslides to occur. Analysis of historical records of landslide data with reference to rainfall can bring out the temporal probability of landslide occurrence leading to hazard scenario in the area. Also vulnerability assessment can be carried out by considering the damage scenario in the area. It is also recommended that a rock mass rating system can be incorporated for whole the study area to establish a proper relationship with slope failure mechanism.

9. Bibliography

Agrwal, N.C. and Kumar, G., 1973. Geology of the Upper Bhagirathi and Yamuna Valleys, Uttarkashi District, Kumaun Himalaya. Himalayan Geology, 3: 2-23.

Akgun, A. and Bulut, F., 2007. GIS-based landslide susceptibility for Arsin-Yomra (Trabzon, North Turkey) region. Environmental Geology, 51: 1377-1387.

Atkinson, P.M. and Massari, R., 1998. Generalised Linear Modelling of Susceptibility to Landsliding in the Central Apennines, Italy. Computers & Geosciences, 24(4): 373 - 385.

Ayalew, L. and Yamagishi, H., 2005. The application of GIS-based logistic regression for landslide susceptibility mapping in the Kakuda-Yahiko Mountains, Central Japan. Geomorphology, 65(1-2): 15-31.

Baeza, C. and Corominas, J., 2001. Assessment of hallow landslide susceptibility by means of multivariate statistical techniques. Earth Surface Processes and Landforms, 26: 1251–1263.

Barlow, J., Franklin, S.E. and Martin, Y., 2006. High Spatial Resolution Satellite Imagery, DEM Derivatives, and Image Segmentation for the Detection of Mass Wasting Processes. Photogrammetric Engineering and Remote Sensing, 72(6): 687-692.

Barton, N.R., 1976. Recent experiences with the Qsystem of tunnel support design. Pro. Symp. on Exploration for Rock Engineering. Johannesburg. ed. Bieniawski. publ. Balkema, Rotterdam. 107-117.

Bieniawski, Z., 1979. The geomechanics classification in rock engineering applications. In: Proceedings of the 4th international congress on rock mechanics, Montreux: 41–48.

Bieniawski, Z.T., 1989. Engineering Rock Mass Classifications. publ. Wiley, New York. 251 p.

Brabb, E.E., 1984. Innovative approaches to landslide hazard and risk mapping. In: Proc., Fourth International Symposium on Landslides, Canadian Geotechnical Society, Toronto, Canada, 1(307-324).

Brardinoni, F., Slaymaker, O. and Hassan, M.A., 2003. Landslide inventory in a rugged forested watershed: a comparison between air-photo and field survey data. Geomorphology, 54: 179-196.

Brenning, A., 2005. Spatial prediction models for landslide hazards: review, comparison and evaluation. Natural Hazards and Earth System Sciences, 5: 853-862.

BRO, 2007. Boarder Roads Organization : Official website. Accessed on 27 November, 2008, http//bro.nic.in.

BS5930, 1981. Code of practice for site investigations. British Standards Institution, London.

Carrara, A., Cardinali, M., Guzzetti, F. and Reichenbach, P., 1995. GIS technology in mapping landslide hazard. In: Carrara, A., Guzzetti,F. (Eds.), Geographical Information Systems in Assessing Natural Hazards. Kluwer Acad. Publ, Dordrecht: 135–176.

Carrara, A., Crosta, G.B. and Frattini, P., 2003. Geomorphological and historical data in assessing landslide hazard. Earth Surface Processes and Landforms, 28(10): 1125-1142.

Chakraborty, D. and Anbalagan, R., 2008. Landslide Hazard Evaluation of Road Cut Slopes Along Uttarkashi-Bhatwari Road, Uttaranchal Himalaya. Journal of Geological Society of India, 71: 115-124.

Chakraborty, S., 2008. Spatio-temporal landslide hazard analysis along a road corridor based on historical information: A case study from Uttarakhand India. (M.Sc. Thesis).ITC, Enschede,2008: 72p.

Chung, C.J. and Fabbri, A.G., 1999. Probabilistic prediction models for landslide hazard mapping. Photogrammetric Engineering and Remote Sensing, 65(12): 1389-1399.

Clark, W.A. and Hosking, P.L., 1986. Statistical Methods for Geographers.John Wiley and Sons, New York. 518 pp.

Crozier, M.J., 1986. Landslides: Causes, Consequences and Environment. Croom Helm, London: 245p.

Cruden, D.M. and Varnes, D.J., 1996. Landslide types and processes. In: Turner, A.K., Schuster, R.L. (Eds.), Landslides: investigation and mitigation. National Academy Press,Washington, D.C: 36–75.

Dai, F.C. and Lee, C.F., 2002. Landslide characteristics and slope instability modeling using GIS, Lantau Island, Hong Kong. Geomorphology, 42(3-4): 213-228.

Dai, X.L. and Khorram, S., 1998. The effects of image misregistration on the accuracy of remotely sensed change detection. IEEE Transactions on Geoscience and Remote Sensing, 36(5): 1566-1577.

Devoli, G., Morales, A. and Hoeg, A., 2006. Historical landslides in Nicaragua- collection and analysis of data. Landslides (accepted on 2008).

EM-DAT, 2008. List of Landslides in India. Excel Sheet. www.em-dat.net. Accessed on: 2008-09-11. EM-DAT: The OFDA/CRED International Disaster Database, Université Catholique deLouvain, Belgium. Brussels.

Ercanoglu, M. and Gokceoglu, C., 2004. Use of fuzzy relations to produce landslide susceptibility map of a landslide prone area (West Black Sea Region, Turkey). Engineering Geology, 75(3-4): 229-250.

Ferretti, A., 2000. Non-Linear subsidence rate estimation using Permanent Scatterers in Differential SAR Interferometry. IEEE Trans. Geosci. Remote Sensing, 38(5): 2202-2212.

Finlay, P.J., Fell, R. and Maguire, P.K., 1997. The relationship between the probability of landslide occurrence and rainfall. Can Geotech J, 34(6): 811–824.

Goodman, R.E., 1989. Introduction to rock mechanics. publ. Wiley, new York. 526pp.

Gorsevski, P.V., Glesser, P.E. and Foltz, R.B., 2000. Spatial prediction of landslide hazard using logistic regression and GIS. In: Proc., 4th International Conference on Integrating GIS and Environmntal Modelling: Problems, Prospects and Research Needs, Banff, Alberta, 2-8 September 2000: 10p.

Guzzetti, F., 2000. Landslide fatalities and the evaluation of landslide risk in Italy. Engineering Geolology, 58(2): 89–107.

Guzzetti, F., 2005. Landslide Hazard and Risk Assessment. PhD Thesis. Mathematics-Scientific Faculty, University of Bonn, Bonn, Germany: 389 pp.

Guzzetti, F., Reichenbach, P., Cardinali, M., Galli, M. and Ardizzone, F., 2005. Probabilistic landslide hazard assessment at the basin scale. Geomorphology, 72: 272–299.

Hack, H.R.G.K., 1998. Slope stability probability classification, SSPC. 2nd edition. publ. ITC, Enschede,The Netherlands. ISBN 90 6164 154 3. 258 p.

Hansen, A., 1984. Landslide Hazard Analysis. In: Slope Instability. D. Brunsden and D.B. Prior (eds), Wiley & Sons, New York. 523-602.

Hoek, E., Practical rock engineering. Available from: http://www.rockscience.com.

Hosmer, D.W. and Lemeshow, S., 2000. Applied Logistic Regression - 2nd edition. John Wiley & Sons, New York, 367 pp.

Hutchinson, J.N., 1988. Morphological and geotechnical parameters of landslides in relation to geology and hydrology. In: Vol 1. 5th International Symposium on Landslides. Balkema,Netherlands.

Kanungo, D.P., Arora, M.K., Sarkar, S. and Gupta, R.P., 2006 A comparative study of conventional, ANN black box, fuzzy and combined neural and fuzzy weighting procedures for landslide susceptibility Zonation in Darjeeling Himalayas. Engineering Geology, 85: 347–366.

Kleinbaum, D.G. (Editor), 1994. Logistic regression: A self-learning text. Springer, New York, 282p.

Kuthari, S., 2007. Establishing precipitation thresholds for landslide initiatiation along with slope characterisation using GIS-based modeling. (M.Sc. Thesis).ITC, Enschede: 63p.

Laubscher, D.H., 1990. A geomechanics classification system for rating of rock mass in mine design. Journal South African Inst. of Mining and Metallurgy, 90(10): 257-273.

Lee, S., 2005. Application of logistic regression model and its validation for landslide suseptibility mapping using GIS and remote sensing data. International Journal of Remote Sensing, 26(7): 1477-1491.

Lee, S., Choi, J. and Min, K., 2002. Landslide susceptibility analysis and verification using the Bayesian probability model. Environmental Geology, 43(12): 120-131.

LPSmanual, 2003. Leica Photogrammetry Suite, OrthoBASE & OrthoBASE Pro User's Guide, Leica Geosystems GIS & Mapping, LLC.

M. Van Den Eeckhaut et al., 2006. Prediction of landslide susceptibility using rare events logistic regression: A case-study in the Flemish Ardennes (Belgium). Geomorphology, 76: 392-410.

Mathew, J., 2007. Statistical spatial modeling for Landslide hazard zonation in Song river basin, Dehradun and Tehri districts; Garwal Himalaya. (Ph.D Thesis). H.N.B. Garhwal University, India.2007: 192p.

Mathew, J., Jha, V.K. and Rawat, G.S., 2007. Weights of evidence modelling for landslide hazard zonation mapping in part of Bhagirathi valley, Uttarakhand. Current Science, 92(5): 628-638.

Metternicht, G., Hurni, L. and Gogu, R., 2005. Remote sensing of landslides: An analysis of the potential contribution to geo-spatial systems for hazard assessment in mountainous environments. Remote Sensing of Environment, 98(2-3): 284-303.

Mila, A., Yang, X. and Carriquiry, A., 2003. Bayesian logistic regression of Soyabean Sclerotinia stem rot prevalence in the U.S. north-central region: Accounting for uncertainty in parameter estimation. Phytopathology, 93: 758-763.

Neuhäuser, B. and Terhorst, B., 2007. Landslide susceptibility assessment using "weights-of-evidence" applied to a study area at the Jurassic escarpment (SW-Germany). Geomorphology, 86(1-2): 12-24.

Ohlmacher, G.C. and Davis, J.C., 2003. Using multiple logistic regression and GIS technology to predict landslide hazard in northeast Kansas, USA. Engineering Geology, 69: 331–343.

Pantelidis, L., 2008. Rock slope stability assessment through rock mass classification systems. International Journal of Rock Mechanics and Mining Sciences, In Press, Corrected Proof.

Popescu, M.E., 1996. From Landslide causes to Landslide remediation. In: Proc., 7th International Symposium on landslides, Trondheim, 1: 75-96.

Purohit, K.K., Islam, R. and Thakur, V.C., 1990. Metamorphism of Psammo-Pellitic Records-Bhagirathi Valley –Garhwal Himalaya. Journal of Himalayan Geology, 1(2): 167-174.

Rao, P.J., 1989. General Report on Landslides. In: Vol 2. Symposium on Preparedness, Mitigation and Management of Natural Disaster. New Delhi.

Saha, A.K., Gupta, R.P., Sarkar, I., Arora, M.K. and Csaplovics, E., 2005. An approach for GIS-based statistical landslide susceptibility zonation - with a case study in the Himalayas. Landslides, 2: 61-69.

Sarkar, S. and Gupta, P.K., 2005. Techniques of landslides zonation- Application to Srinagar-Rudraprayag area of Garhwal Himalaya. Journal of Geological Society of India, 65: 217-230.

Sekhar, L.K., 2006. Effect of vegetation on debris flow initiation : conceptualisation and parameterisation of a dynamic model for debris flow initiation in Tikovil river basin, Kerala, India, using PCRaster. (M.Sc. Thesis).ITC, Enschede,2006: 100p.

Sharma, V.K., 1996. A Probabilistic approach for Landslide Zonation in parts of Garhwal Himalaya. proc. VII Int. Symp. On Landslides: 17-21.

Soeters, R. and Van Westen, C.J., 1996. Slope instability Recognition, analysis and zonation. In: Turner, A.K., Schuster, R.L. (Eds.), Landslide: Investigations and Mitigation. Special Report, vol. 247. Transportation Research Board, National Research Council, National Academy Press, Washington, D.C.: 129–17.

SPSS, 2007. SPSS for Windows, Version 15, 2007, SPSS Inc., Chicago.

Suzen, M.L., 2002. Data driven landslide hazard assessment using geographical information systems and remote sensing. Ph.D Thesis, Middle East Technical University, Turkey: 196p.

Tangestani, M.H., 2004. Landslide susceptibility mapping using the fuzzy gamma approach in GIS, Kakan catchment area, Southwest Iran. Australian Journal of Earth Sciences, 15(3): 439-450.

Terzaghi, K., 1950. Mechanism of Landslides. Engineering Geology, Berkley Volume, The Geological Society of America: 83-123.

USGS, 2004. USGS fact sheet. Accessed at http://pubs.usgs.gov/fs/2004/3072/fs-2004-3072.html on 13 August, 2008.

Valdiya, K.S., 1980. Geology of Kumaun Lesser Himalaya, Wadia Institute of Himalayan Geology, Dehradun, Uttaranchal, India.: 291p.

Van Den Eeckhaut, M. et al., 2006. Prediction of landslide susceptibility using rare events logistic regression: A case-study in the Flemish Ardennes (Belgium). Geomorphology, 76(3-4): 392-410.

Van Westen, C.J., 1993. Application of Geographic Information Systems Landslide hazard Zonation. ITC Publication, 15.

Van Westen, C.J., Van Asch, T.W.J. and Soeters, R., 2006. Landslide hazard and risk zonation-why is it still so difficult? Bull. Engineering Geol. Environment, 65: 167-184.

Varnes, D.J., 1978. Slope movement types and processes, In Schuster, R.L., and Krizek, R.J. Landslides: Analysis and control, Special Report 176, Transportation Research Board, National Academy Press,National Research Council, Washington, D.C.: 11–33.

Wu, S. et al., 2004. Investigations and assessment of the landslide hazards of Fengdu county in the reservoir region of the Three Gorges project on the Yangtze River. Environmental Geology, 45(4): 560-566.

Yesilnacar, E. and Topal, T., 2005. Landslide susceptibility mapping: A comparison of logistic regression and neural networks methods in a medium scale study, Hendek region (Turkey). Engineering Geology, 79(3-4): 251-266.

Yin, K. and Yan, T., 1988. Statistical prediction model for slope instability of metamorphosed rocks. In: Proceedings of 5th Int Symp on Landslides, Lausanne, Switzerland, 2: 1269–1272.

Zhang, J. and Zhang, Y., 2007. Remote sensing research issues of the National Land Use Change Program of China. ISPRS Journal of Photogrammetry & Remote Sensing, 62: 461-472.

Zhou, C., Lee, C., Li, J. and Xu, Z., 2002. On the spatial relationship between landslides and causative factors on Lantau Island, Hong Kong. Geomorphology, 43: 197-207.

10. Appendices

Appendix 1(A): DGPS point processing on both Fore and Aft band of Cartosat-1

Bhatwari Bridge

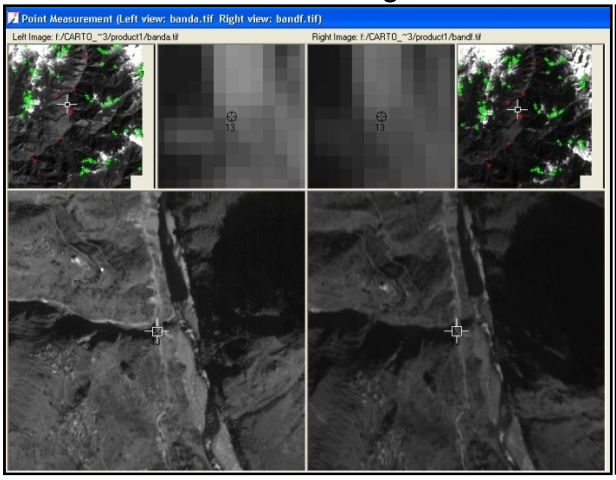

Barsu Pond Corner

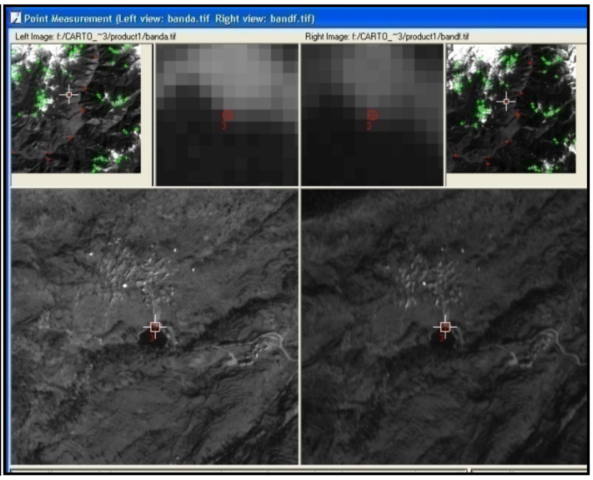

Tin Shed near Thrang Tunnel

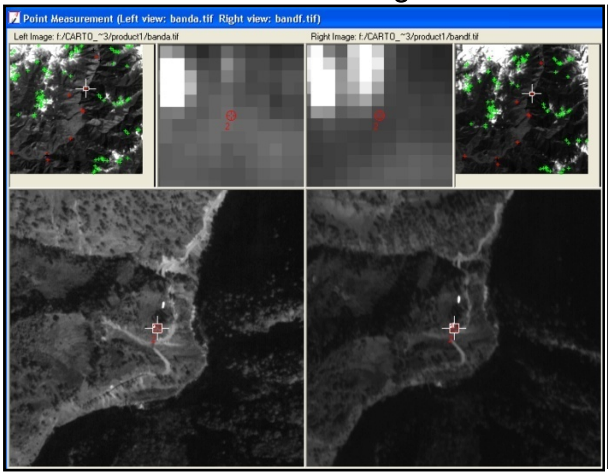

Gangnani Bridge

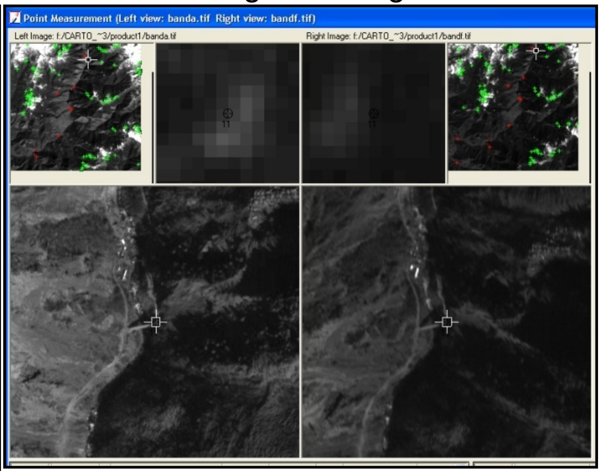

Appendix 1(B): Kilo meter location mark by BRO along National Highway 108

Source: Border Road Organization, India

	NH-108	
143.350	DHARASU-BEND	0.000
149.350	KHATUKHAL	6.000
151.350	DEVIDHAR	8.000
154.350	DUNDA	11.000
162.350	MATLI	19.000
167.350	GYANSU	24.000
170.350	UTTARKASHI	27.000
184.350	MANERI	41.000
199.350	BHATWARI	56.000
206.350	BHUKKI	63.000
214.350	GANGNANI	71.000
221.350	DABRANI	78.000
231.350	SUKHI	84.000
239.350	JHALA	96.000
246.350	HARSIL	103.000
249.350	DHARALI	106.000
252.350	JANGLA	109.000
257.350	LANKA	114.000
259.350	BHAIRONGHATI	116.000
267.350	GANGOTRI	124.000

Appendix 2: Processes data for DEM after DGPS survey

LOCATION	HEIGHT (m)	EASTING	NORTHING	S lat (m)	S lon (m)	S ht (m)	Psn qlty (m)
GMVN_guest_Base	1535.5977	272298.0891	3411109.355	0.0328	0.0290	0.0889	0.0438
Bhatwari_College	1553.5394	272509.6252	3410883.872	0.0003	0.0003	0.0009	0.0004
HMW_Road cross	1360.1379	268710.2096	3405755.162	0.0003	0.0003	0.0011	0.0004
Bhangeli_Temple corner	2361.4306	277207.2493	3422827.041	0.0006	0.0006	0.0019	0.0009
Gonargu_house corner	2135.9295	277571.7479	3421411.251	0.0003	0.0002	0.0010	0.0004
Bhonkoli_Vetenary hospital	2025.6484	257381.2145	3415073.815	0.0005	0.0004	0.0015	0.0006
Tala_House_Below Jamak	1228.9824	262538.4185	3402812.077	0.0009	0.0007	0.0022	0.0012
Maneri_Quaters	1318.0861	263639.9465	3403600.131	0.0006	0.0005	0.0018	0.0008
Bonga_House corner	1207.3761	255914.7083	3400564.512	0.0006	0.0005	0.0013	0.0008
Gangori_Fish pond	1138.6118	257245.3296	3405378.502	0.0007	0.0005	0.0020	0.0009
Barsu_Pond Corner	2198.2560	270601.6579	3414667.653	0.0004	0.0002	0.0011	0.0004
Thrang_Patel Tin Shed	1700.5630	274071.998	3415318.285	0.0006	0.0006	0.0021	0.0008
Maneri_Tinshed	1268.1726	263567.2428	3403309.228	0.0007	0.0007	0.0019	0.0010
Netala_Building Corner	1177.6038	259306.939	3403761.145	0.0009	0.0006	0.0019	0.0011
Kumalti_Bridge	1403.9203	269497.6904	3406200.396	0.0002	0.0002	0.0006	0.0003
Limchigad_Bridge	2038.8916	278689.3825	3423187.052	0.0006	0.0005	0.0017	0.0008
NTPC_Tin shed	1973.2448	277937.4628	3421712.335	0.0008	0.0012	0.0028	0.0014
Gangnani_Bridge	1816.4488	278090.0548	3420450.492	0.0006	0.0006	0.0017	0.0009
IndravatiGad_Temple	1573.9554	259558.2245	3398388.098	0.0004	0.0006	0.0015	0.0007
Sangramchatti_Bridge	1548.7569	256174.9209	3414273.365	0.0005	0.0005	0.0014	0.0007
Doordarshan_Building Corner	1642.4853	272218.2025	3411447.356	0.0003	0.0004	0.0009	0.0005
Bhatwari_Bridge	1573.6271	272175.9947	3412488.632	0.0003	0.0003	0.0007	0.0004
Helgugad_Bridge	1750.4675	275983.9034	3417593.051	0.0007	0.0009	0.0030	0.0011

Appendix 3: Field data collection form for landslide mapping

1. LOCATION [ ]

Latitude [ ] [ ] [ ] N Longitude [ ] [ ] [ ] E

Altitude [ ] m above M.S.L Toposheet No [ ] [ ] [ ]

2. SLIDE DATA

	Length	Width	Depth	Crown Height	
A. Geometry:					in m. (Approx.)

B. Volume of Material (V): [ ] Cubic mt. (m^3)

C. *Whether Slide is:* *FRESH* *REACTIVATED* **D M Y**

D. If *Fresh,* Date of Occurrence [ ] [ ] [ ] **If *Reactivated,* Date of Event** [ ] [ ] [ ]

E. *Activity of Slide:* *ACTIVE* *DORMANT* *STABILIZED*

F. Rapidity of movement: *SLOW* *MODERATE* *RAPID* *ABRUPT*

G. Type of Slide: *DEBRIS SLIDE* *ROCK SLIDE* *ROCK FALL* *TOPPLE*
SLUMP (Subsidence followed by Debris Slide) *FLOWS*

H. Run out distance [ ] in m

3. CONTRIBUTING FACTORS

[i] Rock *Weathered* *Fresh*

[ii] Saturation Condition *SATURATED* *WET* *DRY*

[iii] Vegetation Cover *BARREN* *BUSHY*

[iv] Erosion by water *TOE* *HEADWORD* *CLAYEY*

4. DAMAGES [ ]

Appendix 4: Landslide database prepared during July 2007 to August 2008 (According to BRO)

Attributes of LANDSLIDE

OBJECTID *	Shape *	LOCATION	ACTIVITY	SLIDE_TYPE	code	Shape_Area	PT_LOCTION	DATE_ACTIV
1	Polygon	NON LANDSLIDE AREA	NO SLIDE	NO SLIDE	0	15993785.151088		
2	Polygon	NEAR BHATWARI TEHSIL	ACTIVE SLIDE	TOE CUTTING	1	938.744101	55.85	18/04/2008
3	Polygon	BHTWARI BRIDGE(1ST)	ACTIVE SLIDE	ROCK SLIDE	1	796.019743	56.05	25/07/2008
4	Polygon	AFTER BHATWARI BRIDGE	ACTIVE SLIDE	DEBRIS SLIDE	1	2077.435173	56.35	13/08/2008
5	Polygon	BARSU CROSS	ACTIVE SLIDE	DEBRIS SLIDE	1	2759.496385	58.35	14/06/2008
6	Polygon	NEAR BARSU CHAWK	ACTIVE SLIDE	DEBRIS SLIDE	1	1882.638856	58.25	23/06/2008
7	Polygon	AFTER BARSU	ACTIVE SLIDE	DEBRIS SLIDE	1	3233.288274	58.45	11/08/2008
8	Polygon	THRANG	ACTIVE SLIDE	ROCK SLIDE	1	4400.269989	60.0	26/07/2008
9	Polygon	BEFORE BARSU CHAWK	ACTIVE SLIDE	ROCK FALL	1	1285.668661	57.25	18/06/2008
10	Polygon	MARARI	ACTIVE SLIDE	DEBRIS SLIDE	1	2218.541163	59.25	25/11/07, 17/07/08
11	Polygon	AFTER MARARI	ACTIVE SLIDE	DEBRIS SLIDE	1	3666.231116	59.5	14/07/07, 27/07/08
12	Polygon	SANGLAI	ACTIVE SLIDE	ROCK FALL	1	6950.393252	62.9	12/07/2008, 30/08/08
13	Polygon	AGRA	ACTIVE SLIDE	ROCK FALL	1	4731.196894	63.8	10/9/07,12/7,21/7/08
14	Polygon	SOHAN NAGAR	ACTIVE SLIDE	DEBRIS SLIDE	1	50856.997119	68.25	25/07/2008
15	Polygon	TIBRU	ACTIVE SLIDE	ROCK SLIDE	1	40881.011778	68.65	28/06/2008
16	Polygon	NEAR GANGNANI BRIDGE	ACTIVE SLIDE	DEBRIS SLIDE	1	6634.58714	68.85	02/07/2008, 28/07/08
17	Polygon	SCHOOL	ACTIVE SLIDE	DEBRIS SLIDE	1	8870.599437	68.55	22/07/08,04/08/08
18	Polygon	MAMLAPANI GAD	ACTIVE SLIDE	ROCK SLIDE	1	1481.012862	68.05	18/07/2007
19	Polygon	HELGU GAD	ACTIVE SLIDE	DEBRIS SLIDE	1	13175.800672	65.95	01/08/07, 20/08/07
20	Polygon	AFTER HELGU GAD	ACTIVE SLIDE	SLUMP	1	6675.432955	66.1	21/7,22/7, 30/7/08
21	Polygon	BHUKHI	ACTIVE SLIDE	BIG DEBRIS SLIDE	1	15199.578532	65.1	12/07/2008, 03/07/20
22	Polygon	AFTER BHUKHI BRIDGE	ACTIVE SLIDE	DEBRIS SLIDE	1	14304.117468	65.8	09/11/07,11/011/08
23	Polygon	TIARA	ACTIVE SLIDE	ROCK SLIDE	1	17902.42772	64.15	26/07, 28/09/2008
24	Polygon	NEAR SPRING	ACTIVE SLIDE	DEBRIS SLIDE	1	23113.839345	64.0	06/04/2008
25	Polygon	NTPC CONSTRUCTION ALONG ROAD	ACTIVE SLIDE	ROCK SLIDE DUE TO ROAD CUT	1	5751.81987	61.55	18/8/07, 27/7/08
26	Polygon	NTPC CONSTRUCTION(SARCHNALA)	ACTIVE SLIDE	ROCK SLIDE DUE TO ROAD CUT	1	5000.46513	61.6	19/06/08
27	Polygon	SARCHNALA	ACTIVE SLIDE	MAJOR ROCK SLIDE	1	18150.107073	61.5	12/7,21/7, 30/7/08
28	Polygon	SOUNDAR GAD	ACTIVE SLIDE	DEBRIS SLIDE	1	456.443517	58.85	02/07/2008
29	Polygon	PALA	ACTIVE SLIDE	ROCK SLIDE	1	695.003374	58.65	29/06/2008
30	Polygon	SIRI	ACTIVE SLIDE	DEBRIS SLIDE	1	1488.843527	55.1	18/08, 31/07/08
31	Polygon	NEAR TO SIRI	ACTIVE SLIDE	DEBRIS SLIDE	1	2401.83986	55.05	25/08/2007
32	Polygon	UPPER NALA	ACTIVE SLIDE	DEBRIS SLIDE	1	1639.064862	55.0	24/09/2008
33	Polygon	AFTER BHATWARI BRIDGE	ACTIVE SLIDE	ROCK SLIDE	1	2364.193602	56.95	19/06/2008
34	Polygon	BARSU (UPPER PART)	ACTIVE SLIDE	ROCK SLIDE	1	1494.035554	58.75	27/11/2006, 18/9/08
35	Polygon	UPPER THRANG	ACTIVE SLIDE	DEBRIS SLIDE	1	3789.790476	61.35	28/07/2007
36	Polygon	SURANAGAR	OLD SLIDE	DEBRIS SLIDE	1	210335.500992	67.8	24/08/06, 11/11/06
37	Polygon	SOUNDAR GAD	OLD SLIDE	ROCK SLIDE	1	37864.439541	58.8	28/07/2006
38	Polygon	BHATWARI NALA	ACTIVE SLIDE	DEBRIS SLIDE	1	1088.610382	55.15	14/07/2008
39	Polygon	SALANG	ACTIVE SLIDE	DEBRIS SLIDE	1	26641.913252	59.0	18/06/2008
40	Polygon	NEAR NTPC TUNNEL	ACTIVE SLIDE	ROCK SLIDE	1	2543.803204	60.15	29/06/2008
41	Polygon	UPPER SOUNDAR GAD	OLD SLIDE	DEBRIS SLIDE	1	49207.327514	58.95	11/08/2007
42	Polygon	UPPER THRANG	OLD SLIDE	ROCK SLIDE	1	66745.95578	59.1	05/07/2006

Appendix 5: Description about each class of Dependent and Independent Parameters

Factor or Parameters	Class Code	Class Name	Number of Pixels	No of Pixels showing Landslide	Percentage of Landslide
LANDSLDE	1	Slide	1668		
	2	No Slide	37451		
SLOPE	1	0-15	1659	67	4.02
	2	15-25	4889	142	8.51
	3	25-35	10791	422	25.30
	4	35-45	12831	583	34.95
	5	45-60	8313	438	26.26
	6	>60	636	16	0.96
ASPECT	1	N Facing	3706	89	5.34
	2	NE Facing	6148	359	21.52
	3	E Facing	7460	475	28.48
	4	SE Facing	10396	401	24.04
	5	S Facing	5636	233	13.97
	6	SW Facing	981	19	1.14
	7	W Facing	2470	56	3.36
	8	NW Facing	2322	36	2.16
LITHOLOGY	1	Chlorite-Schist	1109	1	0.06
	2	Quartz-Mica-Schist	3895	684	41.01
	3	Calc-Silicate-Gneiss	588	112	6.71
	4	Biotite-Gneiss	17397	345	20.68
	5	Migmatite-Gneiss	10859	140	8.39
	6	Augen Gneiss	3195	368	22.06
	7	Schistose-Quartzite	1073	1	0.06
	8	Quartzite	1003	17	1.02
GEOMORPHOLOGY	1	Channel Bar	2	0	
	2	River Terraces Younger	0	0	
	3	Ridge High Dissected Hill	6641	635	38.07
	4	Cuesta Moderate Dissected Hill	19931	491	29.44
	5	Hogback high Dissected Hill	8997	523	31.35
	6	Hogback Moderate Dissected Hill	319	0	0.00

	7	Poor Dissected Denu Hill	43	0	0.00
	8	Moderate Dissected Denu Hill	1858	0	0.00
	9	Large Intermonatane Valley	1045	13	0.78
	10	Small Intermonatane Valley	283	6	0.36
Landuse Land cover	1	River Channel	696	6	0.36
	2	Barren Land	21126	1172	70.26
	3	Sand Area	61	3	0.18
	4	Open Forest	413	0	0.00
	5	Degraded Forest	110	28	1.68
	6	Scrub Land	5295	133	7.97
	7	Agricultural Land	3231	255	15.29
	8	Dense Forest	8088	57	3.42
	9	Built-up Land	99	14	0.84
SOIL	1	Very Shallow	1423	127	7.61
	2	Shallow	9820	497	29.80
	3	Moderate	10036	279	16.73
	4	Deep	17840	765	45.86
DARINAGE DENSITY	1	Very High	24990	1176	70.50
	2	High	8985	72	4.32
	3	Moderate	440	0	0.00
	4	Low	4545	377	22.60
	5	Very Low	159	43	2.58
LINEAMENT DENSITY	1	Very High	379	10	0.60
	2	High	19882	988	59.23
	3	Moderate	16666	638	38.25
	4	Low	2192	32	1.92
WEATHERING	1	Very High	22918	1327	79.56
	2	High	13856	313	18.76
	3	Moderate	2193	28	1.68
	4	Low	152	0	
ANTHROPOGENIC	0	No Cutting	38849	1586	95.08
	1	Road/Slope Cutting	270	82	4.92
ROAD BUFFER	1	Buffer	10131	581	34.83
	2	Without Buffer	28988	1087	65.17

Appendix 6: Slope Stability Probability Classification (SSPC) calculation form (Source: Dr. Robert Hack, ITC)

ITC	ITC GEO-ENGINEERING	exposure characterization			SSPC - SYSTEM
	LOGGED BY: SASHIKANT , M.Sc., IIRS-ITC JEP COURSE	DATE: 30/09/2008	TIME:	10:30hr	exposure no: 1

WEATHER CONDITIONS			LOCATION BHATWARI NALLA	map no:	53J/9
Sun:	cloudy/fair/bright	FAIR	Map coordinates:	northing:	30° 51′ 00″N
Rain:	dry/drizzle/slight/heavy	DRY		easting:	78° 38′ 16″

METHOD OF EXCAVATION (ME)		DIMENSIONS/ACCESSIBILITY							
(tick)		Size total exposure:	(m)	l:	40	h:	20	d:	10
natural/hand-made	1.OO 1.00	mapped on this form	(m)	l:		h:		d:	
pneumatic hammer excavation	0.76	Accessibility:	poor/fair/good GOOD						
pre-splitting/smooth wall blasting	0.99								
conventional blasting with result:									
good	0.77								
open discontinuities	0.75								
dislodged blocks	0.72								
fractured intact rock	0.67								
crushed intact rock	0.62								

FORMATION NAME: GNEISS

DESCRIPTION (BS 5930: 1981)				
colour	grain size	structure & texture	weathering	NAME
BLACK AND WHITE ALTERNATE BAND	COARSE	FOLIATED WITH SCHISTOSE BAND	SLIGHTLY	MIGMATITIC GNEISS

INTACT ROCK STRENGTH (IRS) (tick)		sample number(s):	WEATHERING (WE)	
			(tick)	
< 1.25 MPa	Crumbles in hand		unweathered	1.00
1.25 - 5 MPa	Thin slabs break easily in hand		slightly	0.95
5 - 12.5 MPa	Thin slabs broken by heavy hand pressure		moderately	0.90
12.5 - 50 MPa	Lumps broken by light hammer blows		highly	0.62
50 - 100 MPa	Lumps broken by heavy hammer blows → 50 MPa (Lumps broken by hammer blows)		completely	0.35
100 - 200 MPa	Lumps only chip by heavy hammer blows (Dull ringing sound)			
> 200 MPa	Rocks ring on hammer blows. Sparks fly			

DISCONTINUITIES B=bedding C=Cleavage J=joint			1 (S1)	2 (J2)	3 (J3)	4 (J4)	5	EXISTING SLOPE?	
Dip direction		(degrees)	050	120	202	310		dip-direction/dip	
Dip		(degrees	42	45	68	80		212/70	
Spacing (DS)		(m)	0.400	1.000	3.000	1.000			
Persistence	along strike	(m)	>5	5	3	5		height:	20 m
	along dip	(m)	>3	2	3	1		Stability (tick) SMALL PROBLEMS	

CONDITION OF DISCONTINUITIES										
Roughness large scale (Rl) (on an area between 0.2 x 0.2 and 1 x 1 m2)	wavy: slightly wavy: curved: slightly curved straight		1.00 0.95 0.85 0.80 0.75	1.00	0.75	0.85	0.75			
Roughness small scale (Rs) (on an area of 0.2 x 0.2 m2)	rough stepped smooth stepped polished stepped rough undulating smooth undulating polished undulating rough planar smooth planar polished planar		0.95 0.90 0.85 0.80 0.75 0.70 0.65 0.60 0.55	0.80	0.80	0.75	0.80		notes: 1) For infill 'gouge > irregularities' and 'flowing material' small scale roughness = 0.55. 2) If roughness is anisotropic (e.g. ripple marks, striation, etc.) roughness should be assessed perpendicular and parallel to the roughness and directions noted on this form. 3) Non-fitting of discontinuities should be marked in roughness columns.	
Infill material (Im)	cemented/cemented infill no infill - surface staining		1.07 1.00	0.95	1.00	1.00	1.00			
	non softening & sheared material, e.g. free of clay, talc, etc.	coarse medium fine	0.95 0.90 0.85							
	soft sheared material, e.g. clay, talc, etc.	coarse medium fine	0.75 0.65 0.55							
	gouge < irregularities gouge > irregularities flowing material		0.42 0.17 0.05							
Karst (Ka)	none karst		1.00 0.92	1.00	1.00	1.00	1.00			

SUSCEPTIBILITY TO WEATHERING (SW)			remarks:
degree of weathering:	date excavation:	remarks:	*IT WAS VISUALLY ASSESSED THAT THE SLOPE EXPOSURE HAS SMALL PROBLEMS OF SLOPE FAILURE, MAY AFTER A LONG DURATION OF TIME (FUTURE)*

Appendix 7: Field location points for slope stability assessment along the National Highway – 108, Uttarakhand, India

EXPOSURE NO.	LONGITUDE	LATTITUTE	ALTITUTE
1	78° 37′ 05″ E	30° 49′ 23″ N	1613
2	78° 37′ 06″ E	30° 49′ 32″ N	1628
3	78° 37′ 16″ E	30° 49′ 44″ N	1634
4	78° 37′ 21″ E	30° 49′ 53″ N	1642
5	78° 37′ 21″ E	30° 50′ 01″ N	1649
6	78° 37′ 28″ E	30° 50′ 14″ N	1656
7	78° 37′ 36″ E	30° 50′ 23″ N	1664
8	78° 37′ 46″ E	30° 50′ 33″ N	1671
9	78° 37′ 55″ E	30° 50′ 42″ N	1678
10	78° 38′ 06″ E	30° 50′ 47″ N	1685
11	78° 38′ 11″ E	30° 50′ 48″ N	1689
12	78° 38′ 12″ E	30° 50′ 51″ N	1701
13	78° 38′ 14″ E	30° 50′ 53″ N	1707
14	78° 38′ 16″ E	30° 51′ 00″ N	1714
15	78° 38′ 25″ E	30° 51′ 08″ N	1724
16	78° 38′ 34″ E	30° 51′ 14″ N	1735
17	78° 38′ 45″ E	30° 51′ 25″ N	1741
18	78° 38′ 56″ E	30° 51′ 33″ N	1749
19	78° 39′ 03″ E	30° 51′ 47″ N	1754
20	78° 39′ 18″ E	30° 52′ 06″ N	1760
21	78° 39′ 31″ E	30° 52′ 13″ N	1765
22	78° 39′ 44″ E	30° 52′ 34″ N	1772
23	78° 39′ 48″ E	30° 52′ 43″ N	1778
24	78° 39′ 53″ E	30° 52′ 49″ N	1782
25	78° 40′ 03″ E	30° 52′ 58″ N	1793
26	78° 40′ 09″ E	30° 53′ 02″ N	1796
27	78° 40′ 15″ E	30° 53′ 08″ N	1801
28	78° 40′ 20″ E	30° 53′ 11″ N	1818
29	78° 40′ 22″ E	30° 53′ 19″ N	1832
30	78° 40′ 21″ E	30° 53′ 29″ N	1840
31	78° 40′ 27″ E	30° 53′ 33″ N	1857
32	78° 40′ 36″ E	30° 53′ 41″ N	1868

Appendix 8: Slope Stability Probability for each exposures along the road corridor

Exposure No	Slope Intact Rock Strength (MPa)	Spacing Factor	Condition of Discontinuities	Rock mass Friction (Degree)	Rock mass Cohesion (MPa)	Stability Probability
1 (Zone-A)	100	0.314	0.347	43	19.668	**0.65**
1 (Zone-B)	9	0.298	0.29	19	10.421	**0.97**
2	200	0.31	0.407	67	29.176	**0.3**
3	100	0.393	0.477	47	22.405	**0.02**
4	100	0.245	0.436	39	18.01	**0.05**
5	100	0.394	0.487	48	22.448	**0.96**
6	150	0.305	0.307	54	23.972	**0.5**
7 (Zone-A)	100	0.31	0.401	43	19.73	**0.1**
7 (Zone-B)	50	0.205	0.376	25	11.923	**0.85**
8	150	0.31	0.532	55	24.912	**0.7**
9	100	0.31	0.423	43	19.808	**0.3**
10	150	0.001	0.522	39	16.049	**0.5**
11	75	0.301	0.332	36	16.875	**0.55**
12	100	0.397	0.551	48	22.78	**0.5**
13	100	0.383	0.508	47	22.208	**0.05**
14	50	0.414	0.611	37	18.771	**0.85**
15	100	0.393	0.427	47	22.226	**0.5**
16	111	0.327	0.428	46	21.382	**0.3**
17	105	0.341	0.642	47	21.992	**0.25**
18	150	0.003	0.505	39	16.03	**0.06**
19	100	0.274	0.324	40	18.442	**0.98**
20	150	0.274	0.479	53	23.711	**0.05**
21	105	0.342	0.643	46	21.202	**0.15**
22	93	0.002	0.282	24	9.826	**0.4**
23	100	0.31	0.453	43	19.915	**0.25**
24	150	0.393	0.546	60	27.365	**0.002**
25	100	0.356	0.471	45	21.302	**0.95**
26	150	0.376	0.4	58	26.343	**0.4**
27	100	0.387	0.333	46	21.716	**0.89**
28 (Zone-A)	100	0.347	0.516	45	21.217	**0.2**
28 (Zone-B)	50	0.292	0.583	31	15.155	**0.9**
29	150	0.399	0.472	60	27.256	**0.034**
30	100	0.292	0.463	42	19.438	**0.96**
31	150	0.367	0.535	58	26.555	**0.05**
32	50	0.405	0.562	36	18.318	**0.15**

Appendix 9: Format of the input table for Logistic Regression Model (some random cells from whole cells of study area)

Slide Code	Slope Code	Aspect Code	Lithology Code	Geomorphology Code	Land Cover Code	Drainage Density Code	Lineament Density Code	Soil Code	Weathering Code	Anthropogenic Code	Road Buffer Code
1	4	2	8	3	2	4	3	3	1	0	0
1	4	2	8	3	2	4	3	3	1	0	0
1	3	3	8	3	2	4	3	3	1	0	0
1	3	3	8	3	2	4	3	3	1	0	0
1	3	4	8	3	2	4	3	3	1	0	0
0	4	4	8	3	2	4	3	3	1	0	0
0	4	4	8	3	2	4	3	4	1	0	0
0	5	3	8	3	2	4	3	4	1	0	0
0	3	3	8	3	2	4	2	4	1	0	1
0	2	3	8	3	2	4	2	4	1	0	1
1	1	2	8	3	2	4	2	4	1	0	1
1	3	7	8	3	2	4	2	4	1	0	1
1	5	7	8	3	2	4	2	4	1	0	1
1	5	7	8	3	2	4	2	4	1	0	1
0	3	7	8	3	2	4	2	4	1	0	1
0	2	7	1	9	1	4	2	4	1	0	1
0	4	5	8	3	2	4	3	3	2	0	0
0	4	5	8	3	2	4	3	3	2	0	0
0	3	4	8	3	2	4	3	3	2	0	0
1	3	3	8	3	2	4	3	3	2	0	0
1	4	2	8	3	2	4	3	3	2	0	0
1	3	2	8	3	2	4	3	3	1	0	0
1	4	2	8	3	2	4	3	3	1	0	0
1	3	2	8	3	2	4	3	3	1	0	0
0	2	3	8	3	2	4	3	3	1	0	0
0	4	3	8	3	2	4	3	3	1	0	0
0	1	3	8	3	2	4	2	4	1	0	1
0	1	7	8	3	2	4	2	4	1	0	1
1	5	7	8	3	2	4	2	4	1	0	1
1	5	7	8	3	2	4	2	4	1	0	1

Appendix 10: Probability estimation after logistic regression analysis

Probability Estimate	Landslide Status	Probability Estimate	Landslide Status	Probability Estimate	Landslide Status
0.832576698	1	0.378524663	0	0.79721854	1
0.852204883	1	0.323319308	0	0.861284523	1
0.852204883	1	0.823319308	1	0.361284523	0
0.832576698	1	0.39721854	0	0.347712655	0
0.832576698	1	0.31920936	0	0.314673451	0
0.470121963	0	0.832576698	1	0.662174584	1
0.470121963	0	0.832576698	1	0.641987286	1
0.307038776	0	0.843433471	1	0.703495691	1
0.707038776	1	0.832576698	1	0.303495691	0
0.769584436	1	0.432576698	0	0.448193368	0
0.369584436	0	0.332576698	0	0.748193368	1
0.323319308	0	0.338049152	0	0.73633387	1
0.835895475	1	0.707038776	1	0.553246004	0
0.489846432	0	0.614673451	1	0.597864416	0
0.432576698	0	0.678524663	0	0.854457671	1
0.852204883	1	0.110465012	0	0.61787258	0
0.832576698	1	0.342538984	0	0.849795751	1
0.811838379	1	0.731058579	1	0.621283595	0
0.443433471	0	0.782449776	1	0.641987286	1
0.407038776	0	0.697622102	1	0.662174584	1
0.407038776	1	0.17399355	0	0.662174584	0
0.514745723	1	0.254457671	0	0.71320475	0
0.479261904	1	0.854457671	1	0.766919866	1
0.567829252	0	0.21920936	0	0.653246004	0
0.532703245	0	0.29721854	0	0.77399355	1
0.707038776	1	0.811838379	1	0.77399355	1
0.369584436	0	0.797864416	1	0.554457671	0
0.32278551	0	0.832576698	1	0.597864416	0
0.71320475	1	0.261284523	0	0.658046652	0
0.766919866	1	0.314673451	0	0.839296097	1

Appendix 11: Structure of the input table for ROC curve analysis (For Accuracy Assessment)

Probability Estimate	Landslide Status	Probability Estimate	Landslide Status	Probability Estimate	Landslide Status	Probability Estimate	Landslide Status
0.494872786	0	0.224784307	0	0.444726821	1	0.844092605	1
0.535689203	0	0.188467325	0	0.757679639	1	0.798669599	1
0.462240053	0	0.209656033	0	0.409991625	1	0.742308157	1
0.292349567	0	0.224784307	0	0.603722516	1	0.787345772	1
0.292349567	0	0.510949503	0	0.757679639	1	0.861880812	1
0.292349567	0	0.510949503	0	0.757679639	1	0.861880812	1
0.274282943	0	0.573047279	0	0.730665173	1	0.861880812	1
0.21738005	0	0.507499438	0	0.261922534	1	0.844092605	1
0.292349567	0	0.507499438	0	0.261922534	1	0.844092605	1
0.292349567	0	0.622459331	0	0.290285058	1	0.683088095	1
0.21738005	0	0.622459331	0	0.261922534	1	0.757863193	1
0.292349567	0	0.643135666	0	0.66418493	1	0.811685575	1
0.292349567	0	0.554779235	0	0.72352206	1	0.843301372	1
0.202619846	0	0.097088641	0	0.610876967	1	0.844092605	1
0.274282943	0	0.554779235	0	0.631812418	1	0.844092605	1
0.21738005	0	0.219942755	0	0.72352206	1	0.861880812	1
0.365632432	0	0.250490124	0	0.739235723	1	0.861880812	1
0.232901428	0	0.250490124	0	0.675024677	1	0.811685575	1
0.259225101	0	0.173790187	0	0.69423634	1	0.811685575	1
0.232901428	0	0.173790187	0	0.692961224	1	0.789015284	1
0.399151927	0	0.661055181	0	0.765666252	1	0.798669599	1
0.284957894	0	0.692109504	0	0.739235723	1	0.812600973	1
0.259225101	0	0.692109504	0	0.721718102	1	0.861880812	1
0.259225101	0	0.173790187	0	0.739235723	1	0.812600973	1
0.365632432	0	0.620106432	0	0.771005938	1	0.738657009	1

Appendix 12: Field photographs (for slope stability assessment)

Exposure No-1 near Bhatwari Bridge

Exposure No-2 near Thrang Tunnel

Structural mapping of the expoure with Dr. Robert Hack